AD NUMBER

ADB004396

LIMITATION CHANGES

TO:

Approved for public release; distribution is unlimited.

FROM:

Distribution authorized to U.S. Gov't. agencies only; Test and Evaluation; OCT 1973. Other requests shall be referred to Air Force Aero Propulsion Lab., Wright-Patterson AFB, OH 45433.

AUTHORITY

AFAL ltr 7 Nov 1978

AFAPL-TR-73-99

SHORT PULSE SWITCHES FOR AIRBORNE HIGH POWER SUPPLIES

MICHAEL A. LUTZ

HUGHES RESEARCH LABORATORIES

TECHNICAL REPORT AFAPL–TR–73–99

OCTOBER 1973

FINAL REPORT FOR PERIOD JUNE 1972 – FEBRUARY 1973

AIR FORCE AERO PROPULSION LABORATORY
AIR FORCE SYSTEMS COMMAND
WRIGHT–PATTERSON AIR FORCE BASE, OHIO 45433

NOTICE

When Government drawings, specifications, or other data are used for any purpose other than in connection with a definitely related Government procurement operation, the United States Government thereby incurs no responsibility nor any obligation whatsoever; and the fact that the government may have formulated, furnished, or in any way supplied the said drawings, specifications, or other data, is not to be regarded by implication or otherwise as in any manner licensing the holder or any other person or corporation, or conveying any rights or permission to manufacture, use, or sell any patented invention that may in any way be related thereto.

This report contains the results of an effort to develop a switch to be used with the inductive energy storage. The work was performed in the Aerospace Power Division of the Air Force Aero-Propulsion Laboratory, Air Force Systems Command, Wright-Patterson AFB, Ohio, under Project 3145, Task 314532, and Work Unit 31453203. The effort was conducted by Mr. Richard L. Verga (AFAPL/POD-1) during the period of 1 June 1972 28 February 1973.

Distribution limited to U.S. Government Agencies only; Test and Evaluation, October 1973. Other requests for this document must be referred to the Air Force Aero-Propulsion Laboratory, Wright-Patterson AFB OH 45433.

This technical report has been reviewed and is approved for publication.

Richard L. Verga

RICHARD L. VERGA
Project Engineer

FOR THE COMMANDER

Philip E. Stover

PHILIP E. STOVER
Chief
Power Distribution Branch

Copies of this report should not be returned unless return is required by security considerations, contractual obligations, or notice on a specific document.

AIR FORCE/56780/20 May 1975 — 100

UNCLASSIFIED

SECURITY CLASSIFICATION OF THIS PAGE *(When Data Entered)*

REPORT DOCUMENTATION PAGE		READ INSTRUCTIONS BEFORE COMPLETING FORM
1. REPORT NUMBER AFAPL TR 73-99	2. GOVT ACCESSION NO.	3. RECIPIENT'S CATALOG NUMBER
4. TITLE *(and Subtitle)* Short Pulse Switches for Airborne High Power Supplies		5. TYPE OF REPORT & PERIOD COVERED Technical 1 Jun 72 - 28 Feb 73 6. PERFORMING ORG. REPORT NUMBER
7. AUTHOR(s) Michael A. Lutz		8. CONTRACT OR GRANT NUMBER(s) F33615-72-C-1688
9. PERFORMING ORGANIZATION NAME AND ADDRESS Hughes Research Laboratories Malibu, California		10. PROGRAM ELEMENT, PROJECT, TASK AREA & WORK UNIT NUMBERS 3145, 314532, 31453203
11. CONTROLLING OFFICE NAME AND ADDRESS AF Aero Propulsion Laboratory AFAPL/POD		12. REPORT DATE Oct 1973 13. NUMBER OF PAGES 159
14. MONITORING AGENCY NAME & ADDRESS *(if different from Controlling Office)*		15. SECURITY CLASS. *(of this report)* Unclassified 15a. DECLASSIFICATION/DOWNGRADING SCHEDULE

16. DISTRIBUTION STATEMENT *(of this Report)*

Distribution limited to US Government Agencies Only; Test and Evaluation, Oct 1973. Other requests for this document must be referred to AF Aero Propulsion Laboratory, Wright Patterson AFB OH 45433.

17. DISTRIBUTION STATEMENT *(of the abstract entered in Block 20, if different from Report)*

18. SUPPLEMENTARY NOTES

19. KEY WORDS *(Continue on reverse side if necessary and identify by block number)*

20. ABSTRACT *(Continue on reverse side if necessary and identify by block number)*

The general objective of this program has been to design a switch suitable for use in inductive energy storage power supplies. This switch consists of two major components, one for inductor charging (bypass switch) and one for high voltage direct current interruption (interrupter tube). Within the general objective of this program, there are six primary tasks: (1) evaluate the various bypass switch candidates and make a selection, (2) design the selected bypass switch, (3) design the interrupter tube for operation at the 100 KV, 20 KA, 5 Hz level, (4) perform a thermal analysis for the complete switch system, (5)

DD FORM 1 JAN 73 1473 EDITION OF 1 NOV 65 IS OBSOLETE

UNCLASSIFIED

SECURITY CLASSIFICATION OF THIS PAGE *(When Data Entered)*

determine the range of operating parameters (scaling study), and (6) perform a systems study to determine the various means of interconnecting switch modules. Task (6) was expanded to include an evaluation of the relative merits of inductive versus capacitive storage.

The three kinds of mechanical switch mechanisms evaluated were rotary, reciprocating, and torsional. The torsional mechanism was chosen primarily because of its potential ability to operate at repetition rates >5Hz. A switch based on this principle along with an interrupter tube have been designed for operation at the required levels.

A thermal analysis of the complete switch system has been performed. Thermal inertia of the components is used to absorb the 88 KW dissipation during one minute of operation at the 100 KV, 20 KA, 5 Hz level, during which time a modulator efficiency of 95% is achieved. Cooldown by circulating fluid takes place during a 10 min off-period. The range of operating parameters of the switch is quite broad with respect to current and voltage, extending essentially over the full range from zero to the peak design valves. The upper limit on repetition rate is set by the torsion bar switch, not by an inherent inability to operate at higher repetition rates, but by the increased dissipation which limits the continuous operating time and reduces the time between maintenance to unacceptably low values.

TABLE OF CONTENTS

LIST OF ILLUSTRATIONS

I. INTRODUCTION AND SUMMARY

A. Program Objectives

The general objective of this program has been to design a switch suitable for use in inductive energy storage (IES) power supplies. Within this general objective, there are six primary tasks. These tasks are described in detail in the Statement of Work and in Hughes Proposal 72M-2079/C6337 and are directed toward the design of an IES switch for operation at the following performance levels:

100 kV	Peak voltage
20 kA	Peak current
5 Hz	PRF

The six tasks are listed below for reference.

Task 1. Evaluate various bypass switch mechanisms, taking into consideration size and weight, probability of successful operation at the required performance levels, and flexibility with respect to higher PRF operation.

Task 2. Design the selected bypass switch for operation at the above levels. Determine its size, weight, dissipation, and auxiliary power requirements.

Task 3. Design an interrupter tube for operation at the above levels. Determine its size, weight, dissipation, and auxiliary power requirements.

Task 4. Perform a thermal analysis of the complete switch system to ascertain the cooling system size, weight, and auxiliary power requirements.

Task 5. Determine the range of operating parameters for the complete switch.

Task 6. Study the various ways in which modules can be interconnected to achieve still higher total system power levels. Investigate the tradeoffs between capacitive and inductive systems.

Table I-1 lists the location of each of these tasks in this report.

TABLE I-1

Location of Tasks Within Report

Task	Subject	Section	Subsection	Page
1	Bypass Switch Evaluation and Selection	II	A & B	10-23
2	Bypass Switch Design	II	C	23-32
		II	E & F	48-68
3	Interrupter Tube Design	III	B	90-103
4	Thermal Analysis	II	C	23-32
		II	E & F	48-68
		III	B	90-103
		IV	A	108
5	Scaling Studies	II	E & F	48-68
		III	B	90-103
6	System Concepts and Specifications	V	A & B	115-123
		VI	A - D	123-133

B. Technical Approach

The Hughes approach to IES switching is based on the parallel connection of a low dissipation bypass switch for inductor charging and the Hughes interrupter tube for forced current interruption. The circuit arrangement is shown in Fig. I-1 where V represents the high current, low voltage power supply, L is the energy storage inductor, B is the bypass switch, and I is the interrupter tube. The reason for the two-component switch approach is because it is considered highly unlikely that a single component can be developed which satisfies the dual requirements of low dissipation inductor charging and high recovery rate forced current interruption.

The bypass switch consists of two discrete components. The first (and major) component is the mechanical switch which allows the

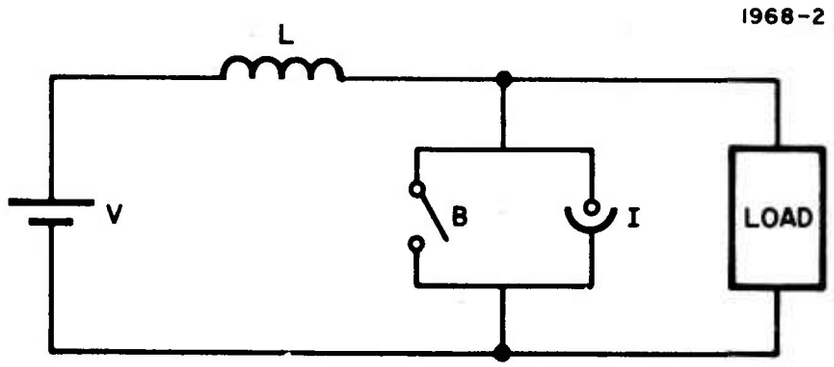

Fig. 1. Basic Inductive Energy Storage Circuit Showing Two Component Switch. B Represents the Bypass (Inductor Charging) Component and I Represents the Interrupter Tube.

inductor to charge during the interpulse period. The second is an electronic switch which closes at the end of the load pulse (after the inductor has delivered a portion of its energy) and conducts current until the contacts of the mechanical switch reclose (typically 750 μsec) (thereby saving the residual energy in the inductor). The latter electronic switch (hereafter called the recloser) is desirable with an IES system because only a fraction of the stored energy can be delivered to the load with acceptable current droop.

The high voltage direct current interrupter tube is patterned after interrupters built by Hughes for HVDC circuit breaker service. These tubes have been tested at the 100 kV, 2 kA, 2 kV/μsec level. This tube is the only known component inherently capable of HVDC interruption (i. e., without the use of commutation circuitry).

Figure I-2 shows the sequence of switching operations. At time zero, full circuit current I_o is flowing in the mechanical switch and the contacts part. It takes about 900 μsec for the contacts to open fully, during which time the full current is carried in the arc mode. After 900 μsec, the generated arc voltage is sufficient to transfer current into the shunt interrupter tube and the contact spacing is sufficient to hold off the full load voltage. Current flow in the mechanical switch then ceases and deionization occurs during the 100 μsec when the interrupter tube is conducting. The interrupter tube then switches off and the current flows into the load. After the required load pulse period of 250 μsec, the recloser is triggered which crowbars the load and conducts the circuit current for 750 μsec until the mechanical switch contacts close. The coil is then recharged during the interpulse period of 200 msec and the cycle is repeated.

C. Output Pulse Waveform

When a current-carrying inductor is connected to a constant voltage load, current decreases at a constant rate equal to the load voltage divided by the inductance. The Statement of Work does not

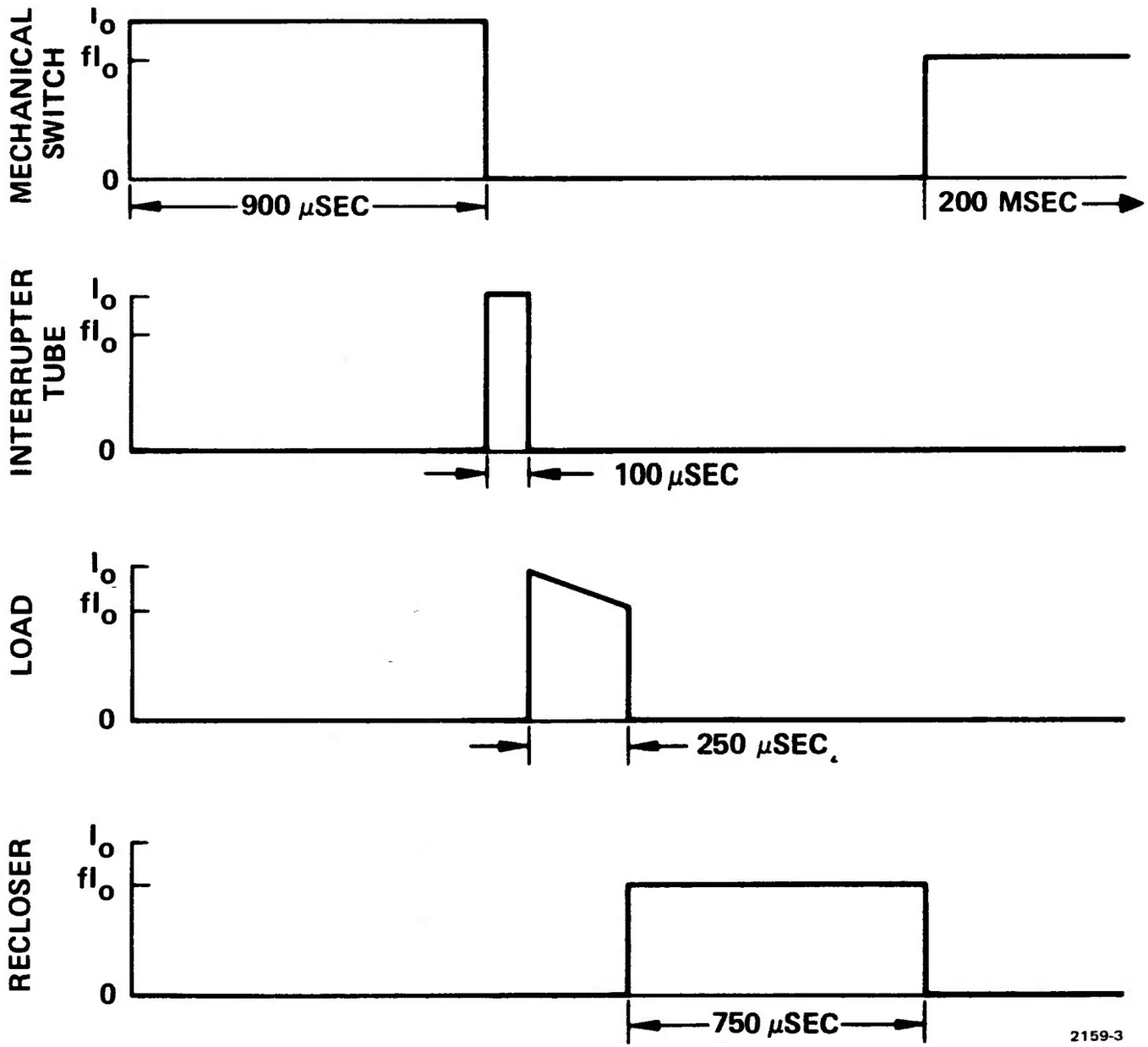

Fig. 2. Current Waveforms in Switch Components and Load. I_o is the Peak Current and f is the Droop Factor.

specify the maximum allowable current droop at the end of the 250 μsec pulse, but implies that the current droops to zero, because it is stated that the inductor is recharged from zero current in 200 msec. This does not appear to be an attractive mode of operation because the load may not operate below a critical current level. If this is so, the energy remaining in the inductor when this critical current is reached will only produce heat in the load and the prime power supply will have to make up these losses every cycle, calling for a higher average power supply.

We have therefore assumed a maximum allowable current droop of 30% (14 kA after 250 μsec). This means that the inductor will still contain 50% of its energy after every pulse. This reduces the prime power by 50% but increases the stored energy in the inductor by a factor of two. It also requires use of the recloser which crowbars the load after 250 μsec, which would otherwise be unnecessary. Nevertheless, the advantages were deemed to outweigh the disadvantages, and this mode of operation has been assumed throughout this report. Based on this mode of operation, it is shown in Section V that the inductor stores 850 kJ (Statement of Work specifies 1 MJ), each load pulse delivers 425 kJ, and the average system power at 5 Hz is 2.125 MW.

D. Summary

We will now summarize the results of the design study of this Phase I program and relate them to the goals listed in the Statement of Work. This is best accomplished with reference to Table I-2. Those items at variance with one another are discussed below.

At the request of the Air Force, every attempt has been made to develop a switch which has the capability of PRF's in excess of 5 Hz. This has been accomplished. However, every operation produces dissipation, requires auxiliary drive energy, and causes erosion of the mechanical switch contacts. Because this dissipated power is not removed on a continuous basis, it must be expected that high PRF operation will allow correspondingly shorter operating periods.

TABLE I-2

Statement of Work Goals and Phase I Design Results

Item	Statement of Work	Phase I Design	Comment
Peak voltage	100 kV	100 kV	
Peak current	20 kA	20 kA	
PRF	≤5 Hz	< 50 Hz	
Dissipation/shot	≤5 kJ	16.6 kJ	
On time at 5 Hz 100 kV, 20 kA	1 min	1 min	
Life (number of operations)	50,000	50,000	With maintenance
Weight	70 lbs	487 lbs	Excluding cooling, auxiliary power supplies, controls, and cables
High altitude operation	required	OK	
Recovery time	< 40 μsec	5 μsec	

A calculation of the energy dissipated per shot has yielded a number larger than the Statement of Work goal. It does not appear feasible to significantly reduce this dissipation level. At a system power level of 2.1 MW, however, a system efficiency of > 95% is still attained at 5 Hz.

The switch weight of 487 lb is considerably higher than the Statement of Work goal of 70 lb. It must be emphasized, however, that the weight of the other components of this system will not include high voltage commutation capacitors. Systems utilizing the forced commutation principle will be much heavier on an overall basis when the

weight of the commutation capacitors are included. This program has resulted in a complete switch system design weighing 1000 lb, with components occupying 40 ft^3, and requiring 7 kW of auxiliary power.

E. Report Organization

Sections II through V are devoted to an IES switch and system operating at the conditions previously described. Sections II and III treat the design of the bypass switch and interrupter tube respectively. Section IV considers the switch as a complete system, including heat exchanger, auxiliary power supplies and controls. Section V contains an analysis of the IES modulator along with size and weight estimates. Section VI looks at the tradeoffs between IES and capacitive energy storage (CES) at both 5 and 50 Hz, and Section VII contains the conclusions and recommendations for future work.

II. BYPASS SWITCH

The bypass switch serves the inductor charging function and consists of two discrete components. The first (and major) component is the mechanical switch whereas the second is electronic (called the recloser). The recloser is a commercially available triggered vacuum gap which shorts the load at the end of the pulse to allow the inductor to recharge from a nonzero initial current. It also serves as a protective crowbar in case of a load fault. The recloser is discussed in detail in Section II-F. The discussion that follows, as well as Sections II-A through II-E are concerned exclusively with the mechanical switch.

During the charging period, when energy is stored in the inductor, the mechanical switch is closed and must be able to carry the full inductor current without excessive heat generation. At the beginning of the energy delivery period the mechanical switch is opened. The contact separating time must be very short (< msec) so that arcing, which produces heat and which leads to contact erosion, is minimized. Once the contacts have fully separated, the current is transferred to the parallel connected interrupter tube. This tube conducts the full current for about 100 μsec, allowing the mechanical switch to deionize. Thereafter, it is turned off so that the current transfers into the load. Accordingly, the mechanical switch must be able to withstand the full voltage generated across the load after this recovery period. Finally, after the energy has been delivered to the load and the recloser triggered, the mechanical switch closes again. This also must be accomplished as quickly as possible so that arc heating and erosion in the electronic recloser is minimized.

It is evident that the performance required of the mechanical switch is very demanding and that a careful choice of a suitable configuration must be made. In Sections II-A and II-B, a description of several alternative approaches will be given and reasons will be presented for the selection of one specific configuration. Once these

reasons have been discussed, we turn to a conceptual design of the mechanical switch in Section II-C, to provide an overview of its basic features and explain its operating principles. Some key facts relating to the drive mechanism and arc chute were unknown about the design and unavailable from the published literature. This prompted two experiments which are described in Section II-D. A detailed design of the mechanical switch, based on both analysis and the results of these experiments is given in Section II-E, and a complete set of specifications for the bypass switch (mechanical switch and electronic recloser) is given in Section II-G.

A. Contact Environment

Among the desirable characteristics of the gaseous insulating medium is a high voltage withstand capability. This involves an important tradeoff because minimum contact separation lowers the acceleration requirements during contact opening and closing. In millisecond opening and closing times, acceleration forces can easily reach the strength limits of the contact materials. A second essential quality is short recovery time. About 100 μsec after arc extinction, the electrode gap must be able to withstand the full circuit voltage. A third characteristic of importance is low viscosity. For millisecond opening times, the acceleration necessary to overcome viscous forces can add considerably to the stress levels in moving contacts. Also, additional energy is required to open and close the contacts. For these latter reasons, oil was eliminated from consideration as an insulating medium. The choice therefore narrowed down to vacuum and pressurized gas.

1. Vacuum

High vacuum is well known for its high voltage withstand capability and its short recovery time (with suitable contacts). Fig. II-1 shows the dependence of the voltage withstand capability between arced electrodes as a function of gap width. It can be seen that a gap of about

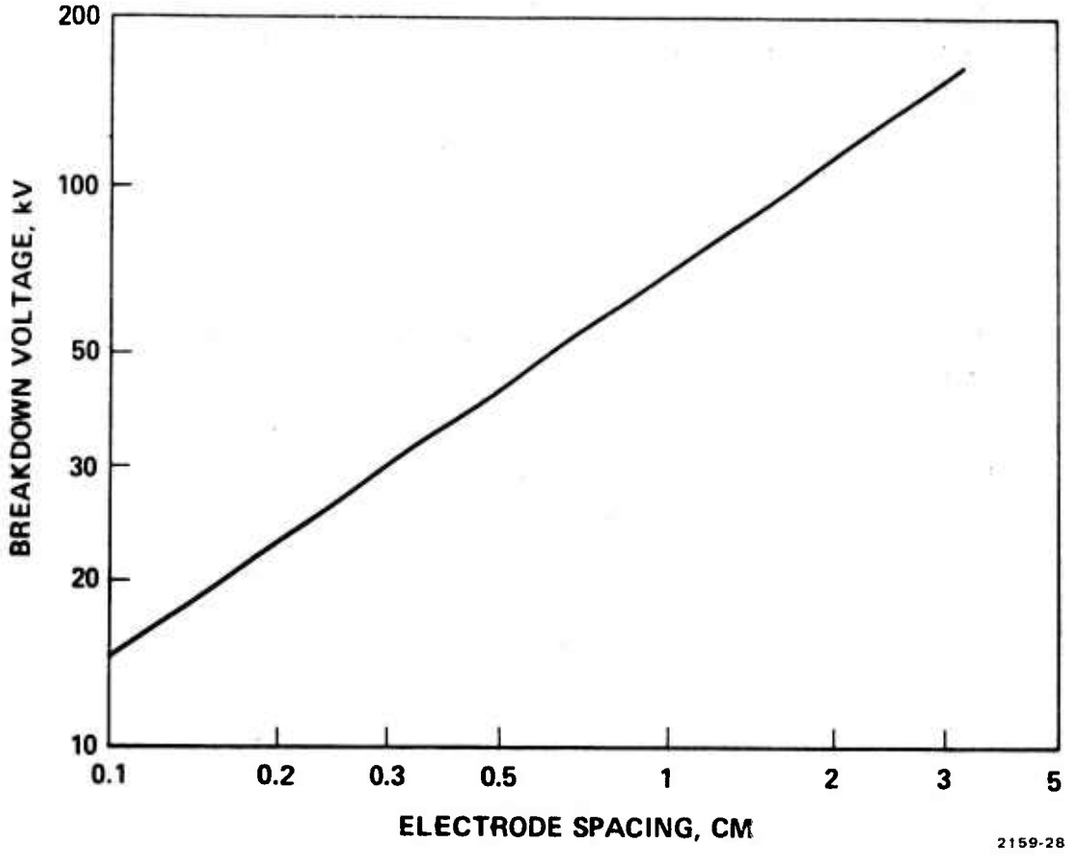

Fig. 3. Vacuum Breakdown Between Arced Copper Electrodes.

2 cm is conservative for a voltage holdoff of 100 kV. The recovery time of a vacuum gap is a somewhat complex matter, depending upon such parameters as gap width d, electrode area A, current change rate dI/dt during commutation and also electrode material. According to Voshall[1] these dependences can be represented by a single, normalized characteristic for each electrode material. In Fig. II-2 the permissible, average rate of voltage application dV/dt (which is directly related to the recovery time τ through the relation

$$\tau = V/dV/dt$$

whereby V is the applied voltage) is represented as a function of the parameter $dI/dt \cdot d^2/A$.

Consider the use of a vacuum interrupter as the mechanical switch. Using the Hughes low voltage commutation technique, the current could be driven to zero with an acceptable $\dot{I}$ of 500 A/μsec. This would require an interrupter tube conduction time of 40 μsec. Using a vacuum interrupter of 200 cm^2 electrode area and 2 cm electrode gap, recovery would take (from Fig. II-2) 50 to 100 μsec (at 1 to 2 kV/μsec). This would require a total conduction time of the interrupter tube of 90 to 140 μsec which is undesirable. (Shorter conduction periods decrease dissipation and increase life. Furthermore, high current density, high recovery rate interrupters can experience transient gas depletion at conduction times in excess of 100 μsec.) Thus, the relatively long recovery rate coupled with the poorer dielectric strength of vacuum relative to high pressure gas (see Section II-A-2 below), rule out the use of vacuum as a contact ambient.

For completeness, consideration was also given to the contact opening mechanism. Basically, there is a choice between mounting the contact drive mechanism inside a rigid vacuum envelope and, on the other hand, using a flexible bellows to actuate the moving contact from the outside. The former approach has been pursued by the Ontario Hydro Research Laboratories (Canada) with the intent of providing an

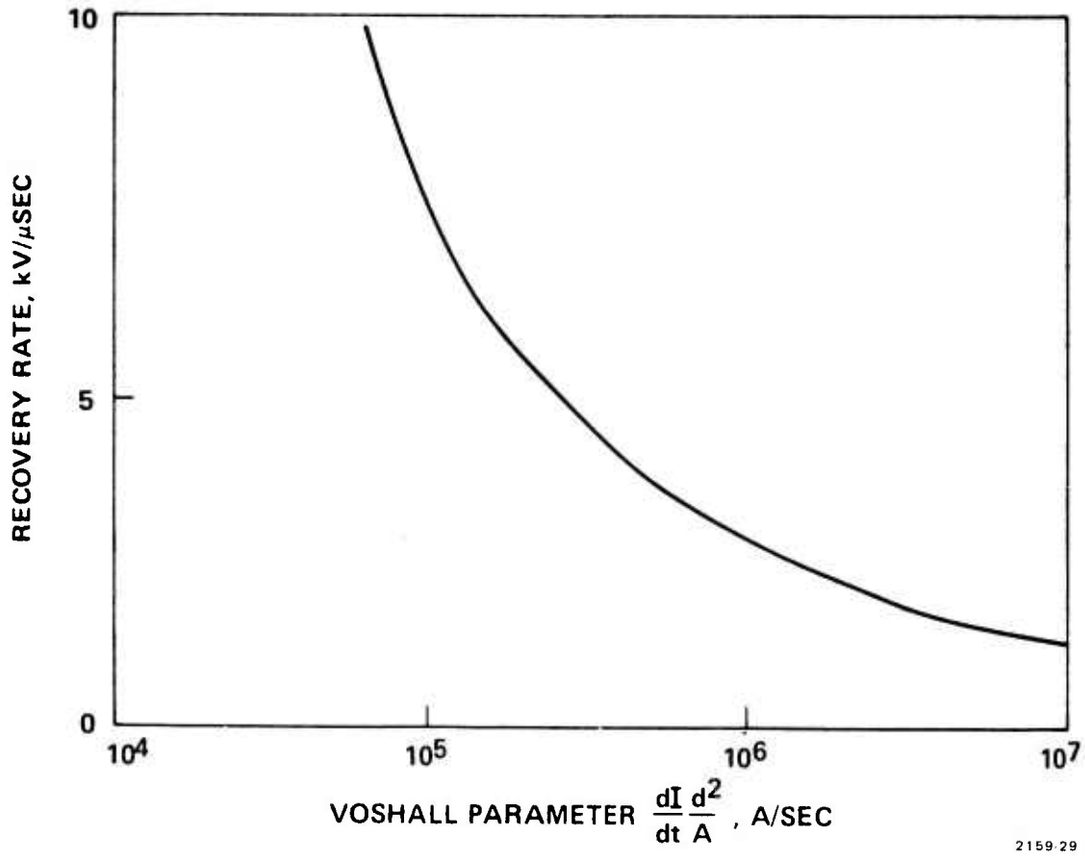

Fig. 4. Recovery Characteristics in Vacuum (Arced Copper Electrodes).

electrodynamically driven, fast opening (1 msec) vacuum interrupter for use as a synchronous circuit breaker in the utility industry. However, this approach has been abandoned recently, presumably because of difficulties in achieving satisfactory high vacuum conditions in the presence of an internal electrodynamic drive coil.

The second approach is utilized in all conventional vacuum interrupters. At present, these devices are limited in their opening times to a minimum of 3 to 5 msec. Such a long arcing period of 20 kA is unlikely to result in a life of 50,000 operations. The question arises whether, through some modifications, vacuum interrupters could be made to open in shorter times. The difficulty in achieving this rests with stress problems in the bellows. As the movable contact is accelerated, a stress wave propagates along the bellows. The stress level S created by this wave is proportional to the speed v_b at which the contact moves. For a welded bellows (Fig. II-3), the relation between S and v_b can be expressed by

$$v_b = \frac{1}{\beta} \left(\frac{\alpha}{\gamma} \frac{1}{3E\rho} \right)^{1/2} S$$

where

$$\alpha = a^2 - b^2 - \frac{4 a^2 b^2}{a^2 - b^2} \left(\log \frac{a}{b} \right)^2$$

$$\beta = 1 - \frac{2 a^2}{a^2 - b^2} \log \left(\frac{a}{b} \right)$$

$$\gamma = a^2 - b^2$$

and a and b are the outer and inner bellows radii, respectively, E is the modulus of elasticity and ρ is the density of the bellows material.

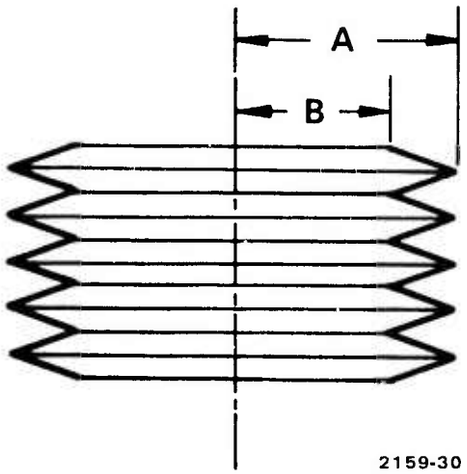

Fig. 5.
Welded Bellows for Vacuum Interrupters.

If we consider a bellows with the dimensions a = 3 cm and b = 2 cm, made of stainless steel ($E = 2.9 \times 10^7$ PSI $= 2 \times 10^{12}$ cgs, $\rho = 7.8$ g/cm^3) and if we assume a peak permissible stress level of $S = 9 \times 10^4$ PSI $= 6.3 \times 10^{10}$ cgs, the maximum permissible contact speed becomes about 7×10^2 cm/sec. Therefore, to separate contacts a distance of 2 cm requires at least 3 msec. If a high strength steel ($S = 1.6 \times 10^5$ PSI $= 11 \times 10^{10}$ cgs) were substituted for stainless steel, the contact opening time could be reduced to about 1.5 ms. An opening time of 1.5 msec is still considered too long for the application under discussion.

2. Pressurized Gas

The above described shortcomings of vacuum insulation suggest that alternative insulating media be considered. Figure II-4 shows the voltage withstand capability of N_2 and of sulfur hexafluoride as a function of gap width for various pressures. It can be seen that for comparable pressures, SF_6 is far superior. Taking into account that the contact surfaces of the mechanical switch are rounded and the holdoff voltage therefore is less than that shown in Fig. II-4, a gap of 1 cm should conservatively withstand 100 kV at a pressure of 2 atm of SF_6.

Sulfur hexafluoride is superior also with respect to recovery times. Figure II-5 shows data collected by J. F. Perkins and L. S. Frost[2] on the recovery of gas blasted arcs in SF_6 and air. It can be seen that SF_6 recovered in about 30 μsec while air required 200 μsec. These times pertain to current levels of 1000 A. However, Perkins found only slight variations with current level. It can be expected, therefore, that even at 20,000 A, the recovery time of a well blasted SF_6 arc remains below 100 μsec. In this connection it is worth noting that vacuum recovery data frequently are compared with data in a stationary gas. The much longer recovery times in the latter case would have one believe that vacuum is vastly superior to SF_6 which definitely is not the case.

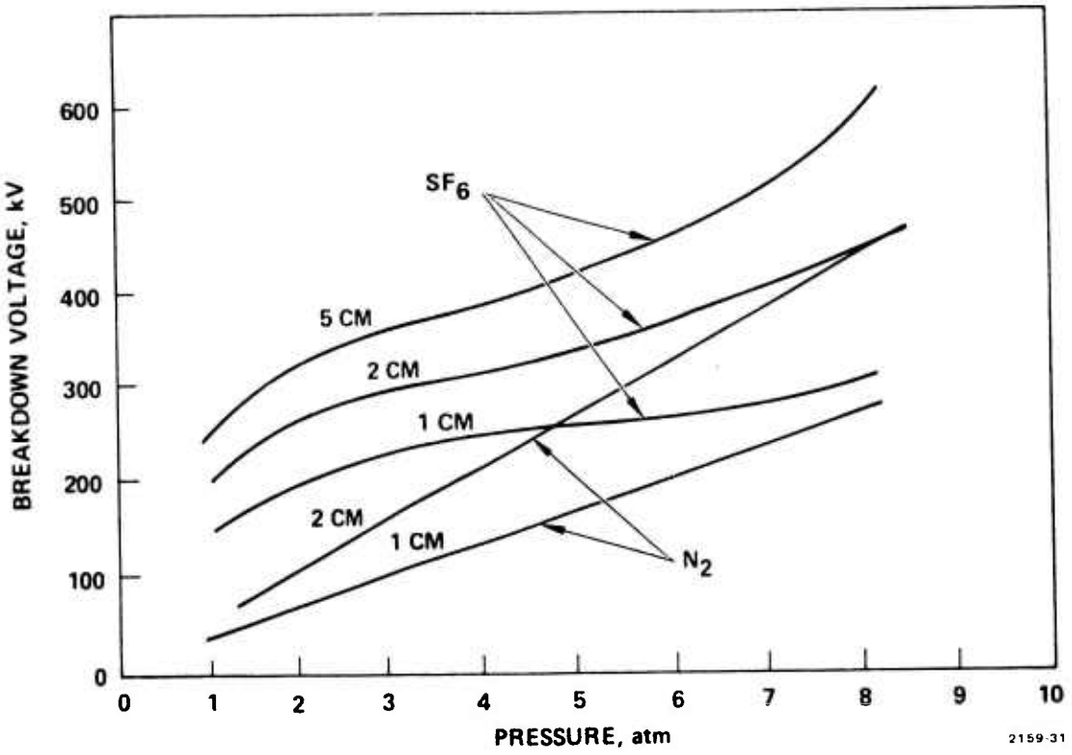

Fig. 6. Breakdown Voltage of SF_6 and N_2 as a Function of Pressure With Gap Width at Parameter.

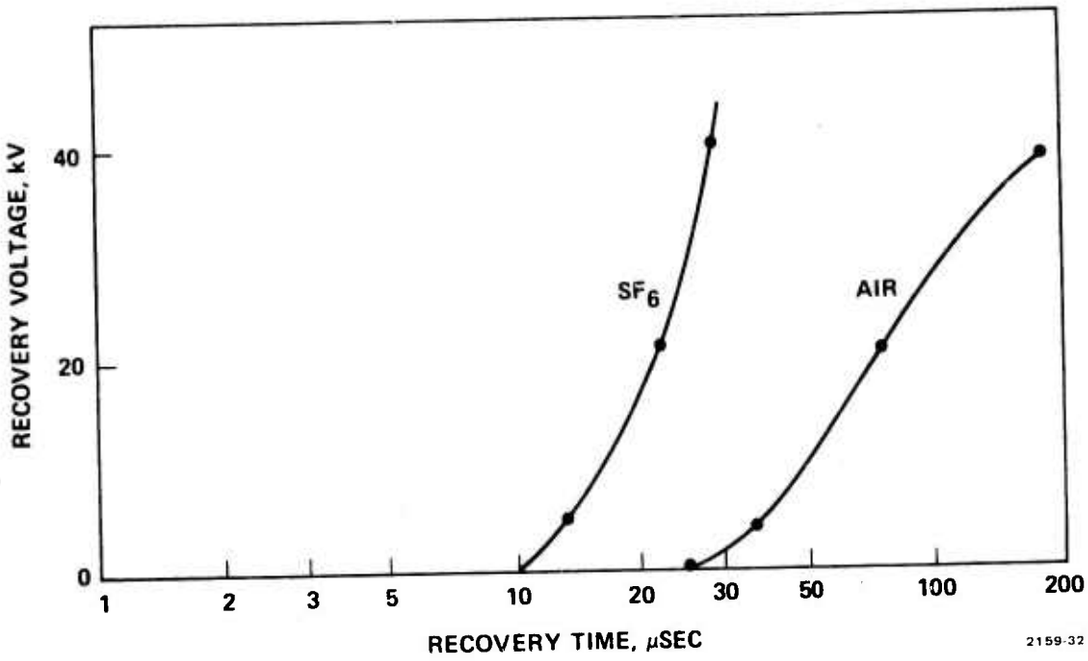

Fig. 7. Recovery Time of SF_6 and Air With Blast Action.

In summary, then, if we consider that SF_6 has, first, a higher voltage withstand capability than vacuum, second, has shorter or at least comparable recovery times and, third, is readily compatible with a built-in electrodynamic drive system (without bellows), the choice of SF_6 as the preferred insulating medium is evident.

B. Drive Mechanism

We now consider the choice of contact opening mechanism. Basically, we require that the contacts open and close as quickly as possible. This motion pattern can be achieved in several ways.

1. Rotary

One approach is to utilize a rotating, slotted cylinder with a set of stationary brushes as shown in Fig. II-6. Whenever the slots pass under the brushes, the circuit opens and closes. Opening and closing times of the order of 1 msec with a gap of 2 cm (two 1 cm gaps in series) can readily be achieved. For example, a cylinder of 12-in. diameter with slots 3 in. wide and rotating at 750 rpm with brushes 2 in. wide would provide the 2 cm series gap with 1 msec opening and closing times at a PRF of 25 Hz.

Acceleration of moving contacts is eliminated in a rotary switch. This appeared sufficiently attractive to warrant a detailed investigation into rotary switch design. This investigation is described in Appendix A. This effort, however, led to the conclusion that the development of such a device would be burdened with considerable uncertainties in the area of brush technology. One basic question was whether brushes could be developed that could maintain good contact with the rotating cylinder at the high current densities required. Removal of large quantities of heat from lightweight, spring mounted brushes posed another problem. Inflexibility with respect to repetition rates and the need for a startup time (order of many seconds) were considered definite disadvantages of this approach. For these reasons consideration was given to switches with reciprocating contact motion which conceptually are closer to existing mechanical switches and therefore can benefit more from existing technologies.

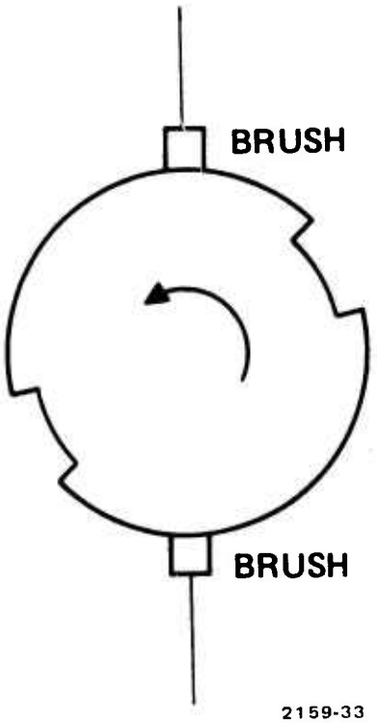

Fig. 8.
Rotary Mechanical Switch.

2. Reciprocating

Most conventional circuit breakers are opened either hydraulically or by solenoids. Both methods, however, are too slow for the present application since they involve too much inertia. Mechanisms which promise millisecond opening and closing times include springs, gas dynamic, and electrodynamic drives. Pure spring action is unsuited for repetitive operations since excessive energy losses will dampen the contact motion very quickly. Also, latch mechanisms would be required. Gas dynamic drives are not readily suited for repetitive operation. This leaves electrodynamic drives and also a combination of electrodynamic drive and spring action as the most promising contenders.

With a purely electrodynamic device, three thrusting periods are required for each contact opening and closing sequence. A first thrust pulse is needed to open the contacts. At the point of full opening a pulse of double intensity is required to reverse the contact motion. Finally, just before the contacts reclose, a third pulse must be applied to prevent the contacts from slamming together at full speed. With a drive mechanism using mixed electrodynamic and spring action, only two thrust periods are required. A first pulse must be applied to open the contacts. As these part, spring tension builds up, slowing down and eventually reversing the contact motion. The second pulse is applied when the contacts are about to slam together. The latter approach has the advantage of requiring less drive energy and simpler circuitry and controls. Accordingly, it was selected for the mechanical switch.

A choice had to be made of whether to incorporate linear or torqued contact motion. Linear motion is simpler to incorporate and, therefore, is used in most conventional circuit breakers. However, the opening speeds required for such breakers are modest. For high speed operation, torqued motion has two distinct advantages. First, a torqued system has a lower inertia and therefore requires less drive energy. The reason for this is that with linearly moving contacts, all

mass elements move the same distance whereas with torqued contacts only the outermost mass element, where the actual contact points are, move the full distance. A comparison of both approaches leads to the conclusion that a torqued system requires less than half the drive energy of a linear contact drive for equal opening times and distances. Second, the coil springs required with a linear drive have an upper speed limit, for much the same reason as the earlier described bellows. For coil springs, the maximum permissible drive speed v_{max} is given by the expression

$$v_{max} = \left(\frac{1}{2G\rho}\right)^{1/2} t_{max}$$

where G is the torsion modulus (= 11.5×10^6 PSI = 8×10^{11} cgs for steel), ρ is the density, and t_{max} is the maximum permissible torsion stress. For regular spring steel, t_{max} is on the order of 11×10^4 PSI = 7×10^9 cgs. This leads to a maximum drive speed of about 2×10^3 cm/sec which would be sufficient for the present application. However, it is generally observed that springs operated near their stress limits take a set. Experiments performed at Hughes Research Laboratories have shown that even with high quality spring steels, contact openings of 2 cm in 2 msec were difficult to achieve in repetitive operation.

Torsion bars, on the other hand, have a much higher speed limit, given by

$$v_{max} = 4\frac{R}{r}\left(\frac{1}{2G\rho}\right)^{1/2} t_{max}$$

whereby R is the contact arm radius and r is the torsion bar radius. With R/r = 5, as adopted for the design presented below, the contact opening speed limit will be 20 times as high as with a coil spring.

Under these circumstances it was clear that a torqued contact arm was the preferred choice for the mechanical switch drive. The conceptual design of such a switch, utilizing a combined torsion bar and electrodynamic drive system to actuate a torqued contact arm with contacts on both ends is described in the following section.

C. Conceptual Design

The utilization of torqued contacts is not entirely new. A configuration, particularly applicable to the mechanical switch, has been discussed by P. Brueckner, et al.[3] Their device was purely torsion bar driven; no earlier work has ever combined a torsion bar with an electrodynamic drive. This necessitated some conceptual design effort prior to the detailed design of the mechanical switch. Below, results of this effort will be described and also some general rules pertaining to the design of torsion bars with attached contact arms will be reviewed. An overall sketch of the switch configuration under discussion is shown in Fig. II-7.

1. Torsion Bar

The torsion bar must fulfill the following three functions: (1) reverse the contact motion when the open position is reached, (2) serve as a support axle for the contact arm, (3) exert a positive force on the contacts while they are closed. This latter force must be sufficiently large to render the contact resistance acceptably small. With a force of approximately 100 lb, the contact impedance can be expected to be about $10^{-5}\,\Omega$. Therefore, with an average current of 17,000 A, about 3000 W of heat are generated.

In order to assess the dynamic behavior of the torsion bar, we assume as an approximation that the electrodynamic drive delivers a very short thrust pulse. The motion of the torsion bar then is simply sinusoidal and the frequency follows directly from the torsion bar oscillation equation

$$f = \frac{1}{8}\left(\frac{d^4 G}{2\pi \ell \theta}\right)^{1/2}$$

2159-23

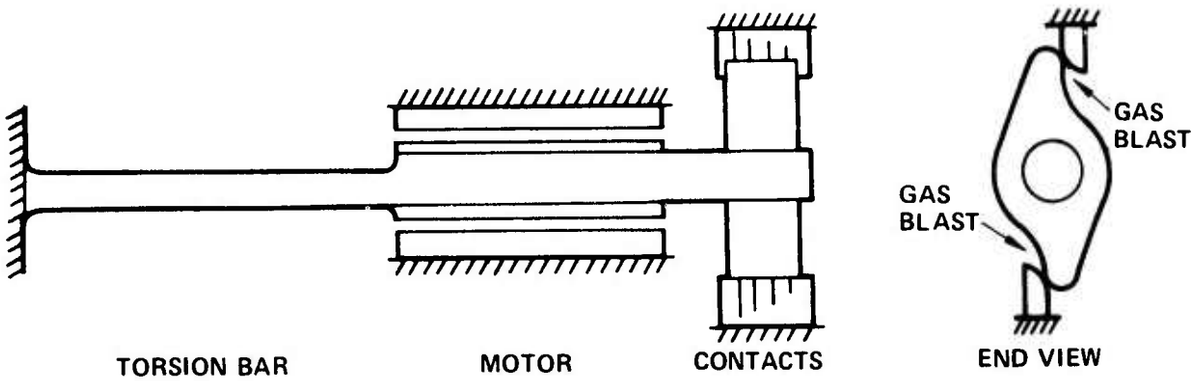

Fig. 9. Mechanical Switch, Essential Elements.

where d is the diameter of the bar, ℓ is its length, G is the torsion modulus, and θ is the moment of inertia of all masses attached to the contact end of the bar. Determination of the torsion bar dimensions d and ℓ for a desired open and close time = $1/(2f)$ necessitates use of a second equation which relates torsion bar stress level t and angular displacement α

$$t = \frac{1}{2} G \frac{d}{\ell} \alpha \quad .$$

For a contact opening and closing time of 2 msec, a moment of inertia of 10,000 g-cm^2 (see below), a maximum contact gap of 1.25 cm at a radius of 5 cm (α = 0.25), and for a peak torsional stress level t of 7×10^9 cgs, these equations lead to a torsion bar configuration of 1.65 cm diameter and 23.5 cm length, which is practical.

2. Contact Arm

The basic considerations which apply to the design of the contact arm include minimum moment of inertia, structural integrity against bending stresses and high electrical conductivity. With respect to the two first named requirements, titanium alloys with their high strength-to-density ratio would be best suited. However, the high electrical resistivity of above 100 $\mu\Omega$-cm precludes their use. In fact, a 10 cm long contact arm with a cross section of 10 cm^2 would be heated at the rate of 70°C/sec if a current of 17,000 A were passed through it. High strength aluminum alloys with an order of magnitude lower resistivity can serve this function much better. It should be added that aluminum, because of its low melting point, is not well suited as a material for contact surfaces. Therefore, W-Cu inserts must be incorporated into the contact bar.

An aluminum contact arm is favorable. The moment of inertia of the arm with approximately eliptical shape can be estimated from

$$\theta_{elip.} = \frac{\pi}{4} ab \, (a^2 + b^2) \, c\rho$$

where a is the major semi-axis, b the minor semi-axis, c the depth, and ρ the density of arm. With a = 5 cm, b = 2 cm, c = 5 cm and $\rho = 2.7\ g/cm^3$, the moment of inertia of the arm becomes approximately 3000 $g\text{-}cm^2$. W-Cu contacts are likely to add another 2000 $g\text{-}cm^2$ so that the total moment of inertia of the contact arm amounts to about 5000 $g\text{-}cm^2$.

During the electrodynamic thrust periods, the contact arm experiences substantial bending stresses across its profile. The strength of the arm determines the maximum intensity of the thrust pulse and therefore also its minimum duration. The torque M exerted on the arm is given by

$$M = \theta\dot{\omega}$$

where $\dot{\omega}$ is the angular acceleration and θ the moment of inertia of the arm. The maximum torque, or bending moment, permitted to act on the arm can be expressed as

$$M_{max} = \frac{1}{6}\, ca^2\, s_{max}$$

where s_{max} is the yield strength of aluminum (= 40,000 PSI = 2.8×10^9 cgs). Numerical evaluation of these equations leads to the conclusion that the angular acceleration cannot exceed 4×10^6/sec. For the case of a contact which is required to open to 1 cm gap in 1 msec, this translates into a minimum electrodynamic drive period of about 100 μsec. There is no difficulty in providing a thrust pulse with this duration.

3. Electrodynamic Drive Motor

Most electrodynamic drives are made to provide linear thrust and they utilize a pancake shaped thrust coil adjacent to a flat thrust plate of high conductivity material. For the present application, this configuration is not suitable. It is preferable to use an arrangement similar to that of an electric motor where the drive coil is

represented by the stator winding and the thrust disc is replaced by the rotor winding. To obtain as much thrust as possible, stator and rotor windings should be as close as possible to each other. This can be achieved with the squirrel cage arrangement shown in Fig. II-8. The force provided by two neighboring current-carrying bars is computed below.

The force k is equal to the change in energy

$$k = dA/ds$$

where

$$dA = \frac{1}{2} I^2 \, dL$$

using I for drive current. The mutual inductance between two parallel bars is approximately equal to

$$L \approx \frac{4\pi}{c^2} \frac{b\ell}{h} \text{ (cgs)}$$

where c is the light velocity = 3×10^{10} cm/sec, h is the height of the current bars, ℓ their length, and b their spacing. With ds = db one obtains

$$k = \frac{2\pi}{c^2} \frac{\ell}{h} I^2 \quad .$$

This relation can be used to determine the currents required to accelerate the contacts to a desired velocity. Now

$$M t_o = \theta\omega$$

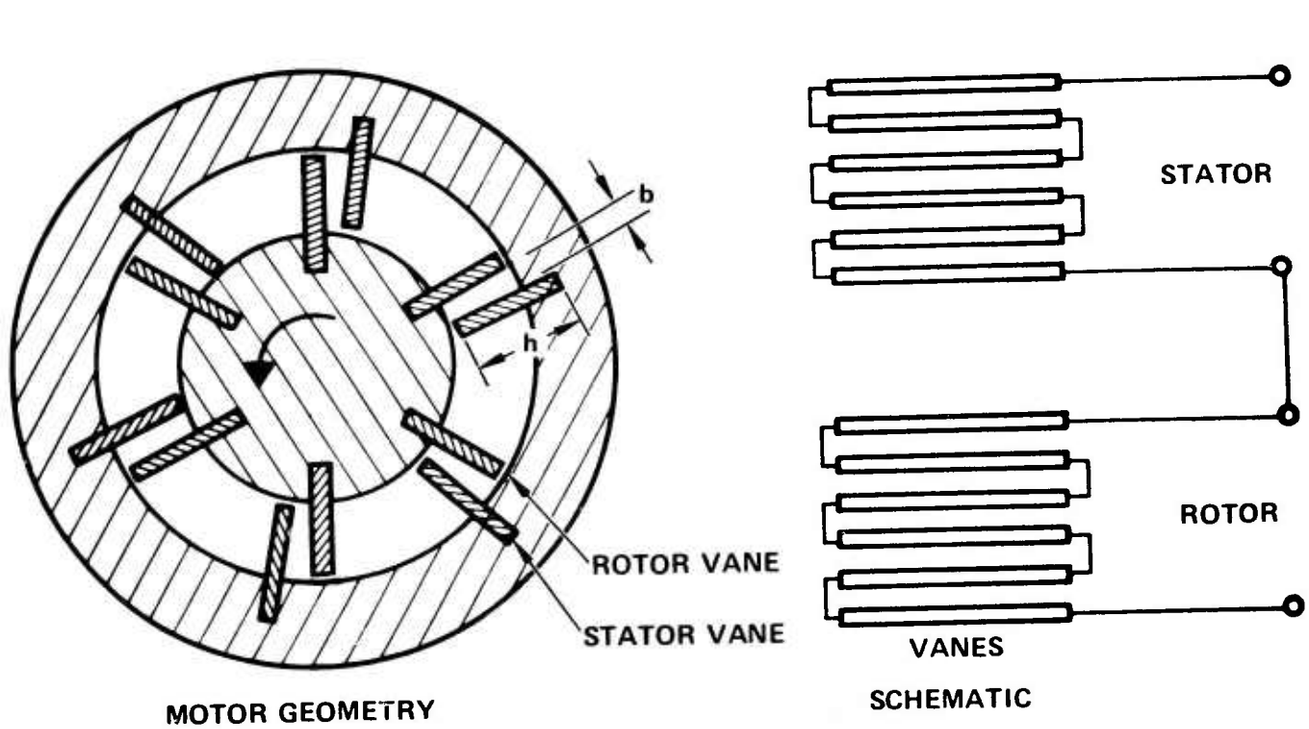

Fig. 19. Motor, Torsion Bar Electrodynamic Drive.

where M is the torque, t_o is the thrust period, θ is the total moment of inertia and ω is the angular velocity of the contact bar. M and k are related by

$$M = NRk$$

where N is the number of rotor and stator vane pairs around the circumference and R is the distance between rotation axis and bars. To obtain an estimate of the current required, we consider the following numerical values: $\omega = 300\ \text{sec}^{-1}$ (for 1 cm contact movement in 1 msec on a 5 cm long contact arm), $\theta = 10,000\ \text{g-cm}^2$, $t_o = 2 \times 10^{-4}$ sec, N = 6, ℓ = 15 cm, h = 1 cm, and R = 3 cm. If these numbers are introduced into the above relations, we obtain a current of $\cong 9 \times 10^{13}$ cgs = 30,000 A. This is a readily manageable current magnitude; switching does not pose problems.

An important factor is the energy consumption of this drive system. If the current bars described above are made of aluminum, the resistance of thrust motor will be on the order of $10^{-3}\ \Omega$. Thus, every opening and closing action will consume a minimum of 400 J. Considering additional losses in leads, etc., one can expect that early operation of the mechanical switch demands between 500 and 1000 J.

The 400 J winding losses will raise the temperature of the aluminum bars. If 200°C is considered an upper temperature limit, the total number of shots during one sequence will be on the order of 100. It should be added that not only the electrodynamic drive motor is heated during operation. While the contacts arc, considerable heat is generated. It can be assumed that on the order of 1000 J are delivered to the contact arm during each shot. With a heat capacity of approximately 600 J/°C and the upper temperature limit set at 200°C, the total number of operations should be on the order of 120, i.e., similar to thermal limit of the motor.

4. Gas Blasting System

As has been mentioned earlier, fast arc recovery in high pressure gas can be achieved only through gas blasting. Conventional breakers utilize such methods as auxiliary pistons to provide the desired gas flow or two-pressure gas systems where the closed contacts provide the seal between the high and low pressure sides. In the present application, one has a choice of blasting continually for the duration of an operational sequence or providing short gas pulses during each contact opening. The former approach would have required a gas reservoir of considerable size (order of 1000 liters), so preference was given to a gas pulsing system. A key element here is the fast acting valve. A search revealed a suitable valve mechanism.* It consists of a lightweight disc serving as the valve and is driven from its seat by electrodynamic forces. A schematic picture of such a valve is shown in Fig. II-9. According to measurements performed by Dr. Hofmann, adequate quantitites of gas (up to 5 liter-atm) should be released by this valve in bursts that can last as long as a millisecond. The electrical driving pulse for the valve can be connected in series with the main electrodynamic drive motor.

5. Summary

The discussion presented in the preceding sections shows clearly that a set of torqued contacts, driven by an electrodynamic thrust motor and operated in an SF_6 atmosphere represent a preferred approach to the mechanical switch. A switch based on this approach can be operated with a minimum of heat generation and arc erosion because of its millisecond opening and closing capability. Its repetition rate can be varied from single shot operation to a maximum ~50 Hz.

*Dr. G.A. Hofmann, Senior Staff Physicist, High Voltage Systems Program, invented this valve mechanism several years ago.

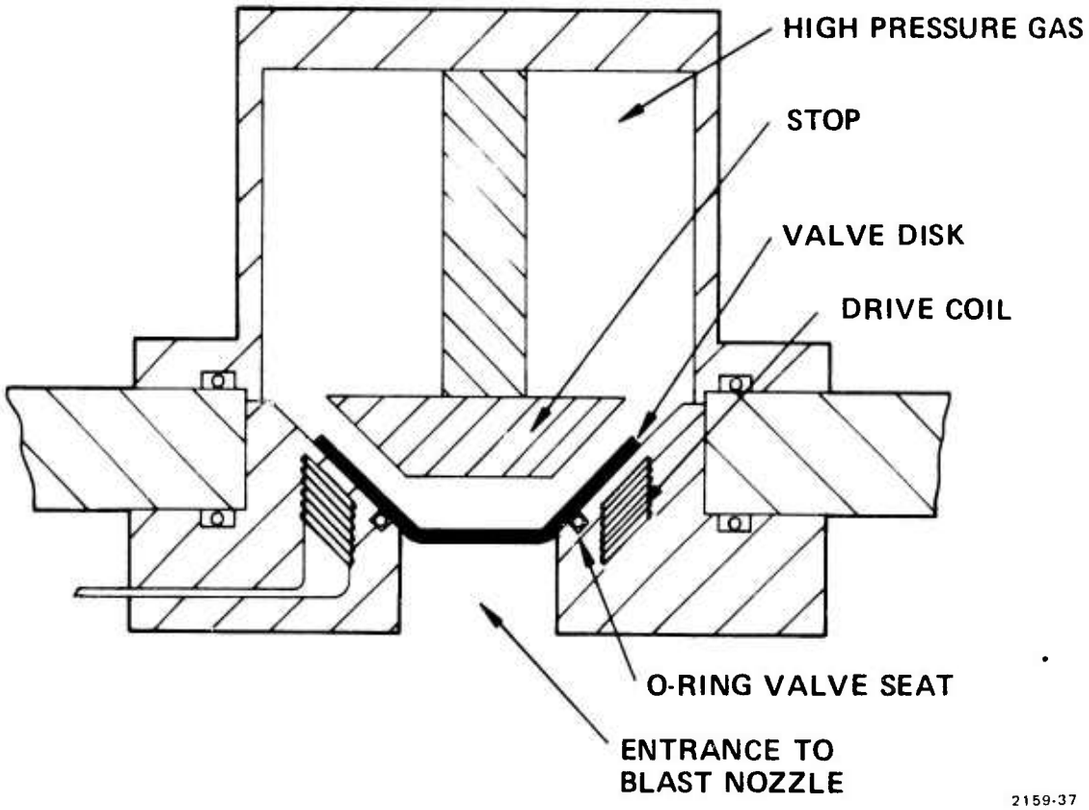

Fig. 11. Fast Acting Gas Valve.

The total number of operations in one sequence can be expected to be in the range of one hundred to several hundred shots, after which a cooling period is required. The energy consumption of such a switch is determined by the electrodynamic drive motor and should be on the order of 500 to 1000 J/shot (acceleration and deceleration pulse).

D. Experimental Verification of Design

Two areas of the conceptual design described in Section II-C above are not amenable to complete quantitative analysis. These are the torsion bar drive motor and the gas blasting system. These two items were therefore singled out for experimentation. This section describes these experiments and their results.

1. Drive Motor

a. Electrical – Measurements of inductance and torque were made on a full-scale but nonstructural model of the motor. An optical lever arm was used to measure angular position of the rotor. The test setup is shown in Fig. II-10. Inductance was measured by adding a known capacitance and measuring the ringing frequency. The rotor was spring restrained for the torque measurements and torque versus angular position calibrations were established with dead weights acting on a lever arm attached to the rotor. The current was maintained for several seconds at each data point to enable a reading of the steady state condition. Confirmation of analytical estimates within an order of magnitude were all that was desired. Circuit parameters and pulse amplitudes will be adjustable within a reasonable range during the final design stage, to achieve the necessary acceleration and deceleration of the torsion bar.

Correlation between tests and agreement with original estimates was good. The results are plotted in Fig. II-11. Torque is calculated from the change in inductance by

$$T = \frac{1}{2} I^2 \frac{\Delta L}{\Delta \theta}$$

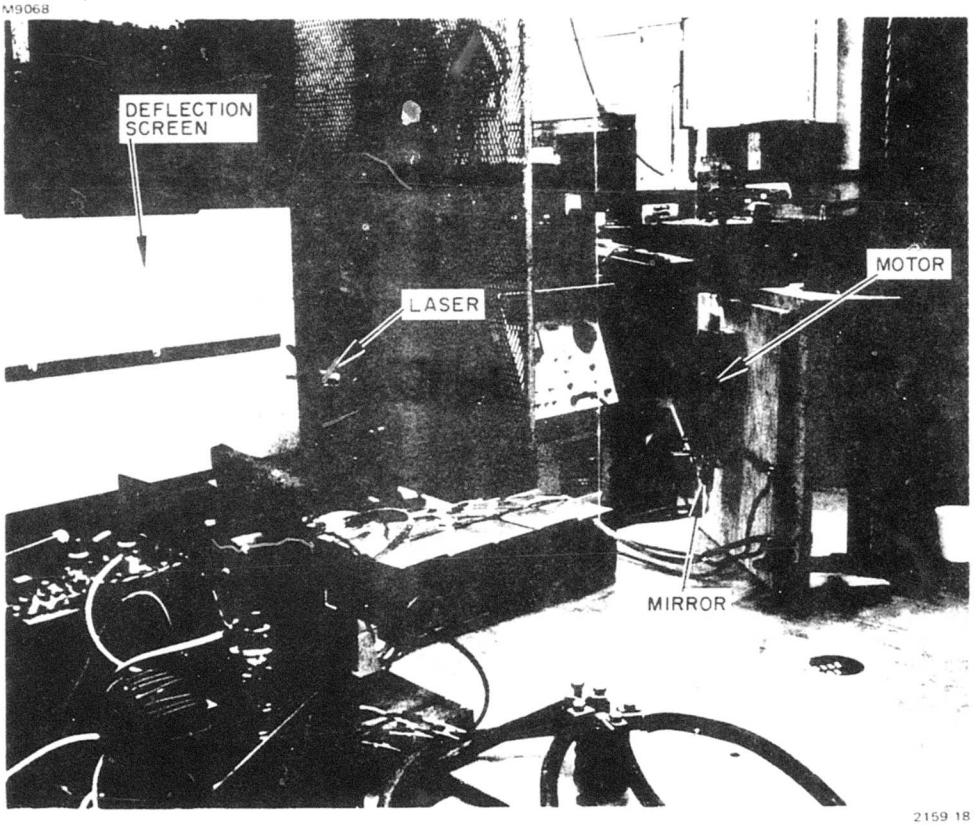

Fig. 12. Motor Test, Inductance and Torque.

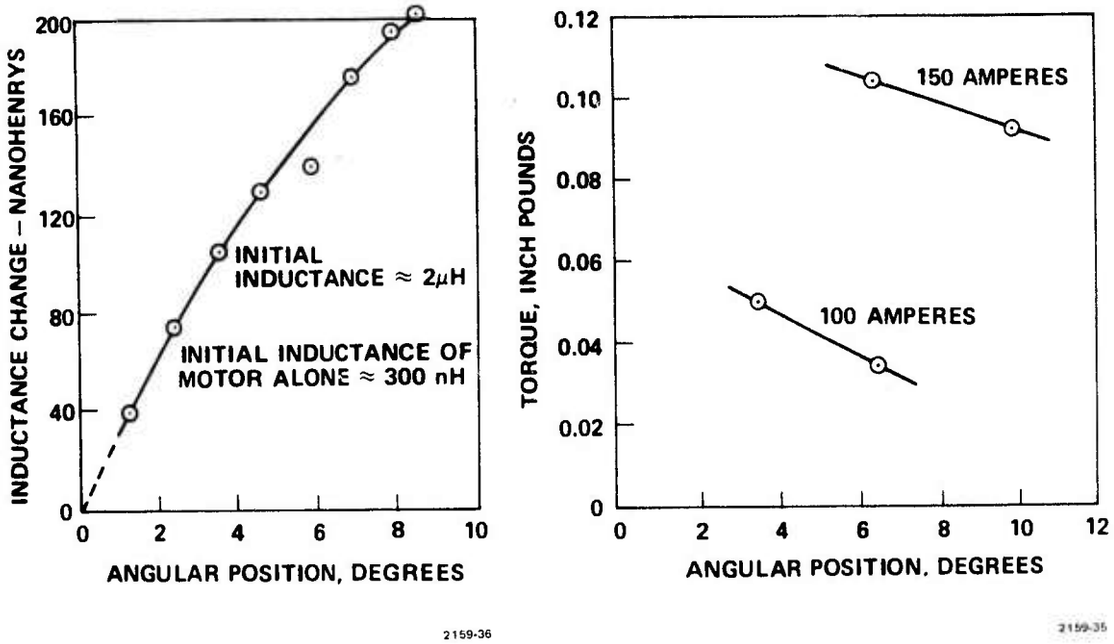

Fig. 13. Measured Motor Characteristics.

where T is the torque in newton-meters, I is the current in amperes, ΔL is the change in inductance in henrys, and $\Delta\theta$ is the change in angular separation between rotor and stator in radians.

The slope of the inductance curve at 5^{o} is 18 nH per degree. The torque calculated at 50 kA, after converting units is 11,400 in. -lb. The direct torque measurements at low currents at the 5^{o} position of the rotor are read from the plots as 0.042 in. -lb at 100 A and 0.11 in.-lb at 150 A. By scaling up in proportion to the square of the current, torque values of 10,500 and 12,200 in. -lb, respectively, are obtained for a 50 kA value of current.

b. Structural – Structural adequacy of fiberglass for the rotor and stator was indicated by a "locked rotor" test of one pair of motor vanes. The test sample is shown in Fig. II-12 and the test setup is shown in Fig. II-13. Fifty 50 kA, 300 μsec pulses were sustained with no evidence of deterioration.

Structural testing to failure by a drop test method was performed to determine the relative strengths of the assembly with the fiberglass laminations oriented radial, tangential and transverse to the motor axis. The test samples are sketched in Fig. II-14. The transverse orientation was the strongest of the three tested.

2. Gas Blasting System

An experimental gas blasting system was designed and fabricated to enable study of the gas value as a component and then studies of a gas blasted arc chute. In addition, the system could be used as a substitute for the entire mechanical switch for low current (to 2000 A) one-shot operation in early interrupter tube integration.

a. Apparatus – The components of the experimental system are identified in Fig. II-15. A photograph of the system is shown in Fig. II-16. A spare set of electrodes and an arc initiation rod are shown along side the system. Figure II-17 is a photograph of the aluminum valve disc, the nylon stop, and the O-ring valve seat.

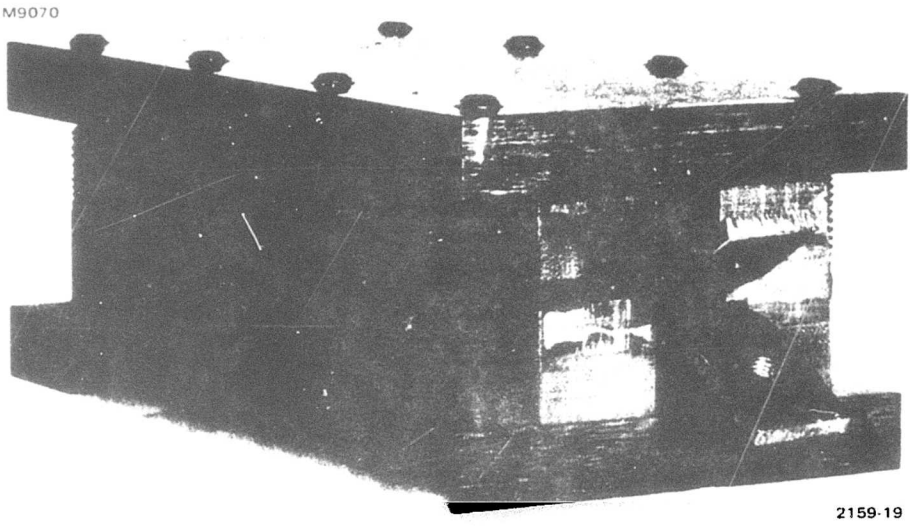

Fig. 14. Motor Structural Test Sample.

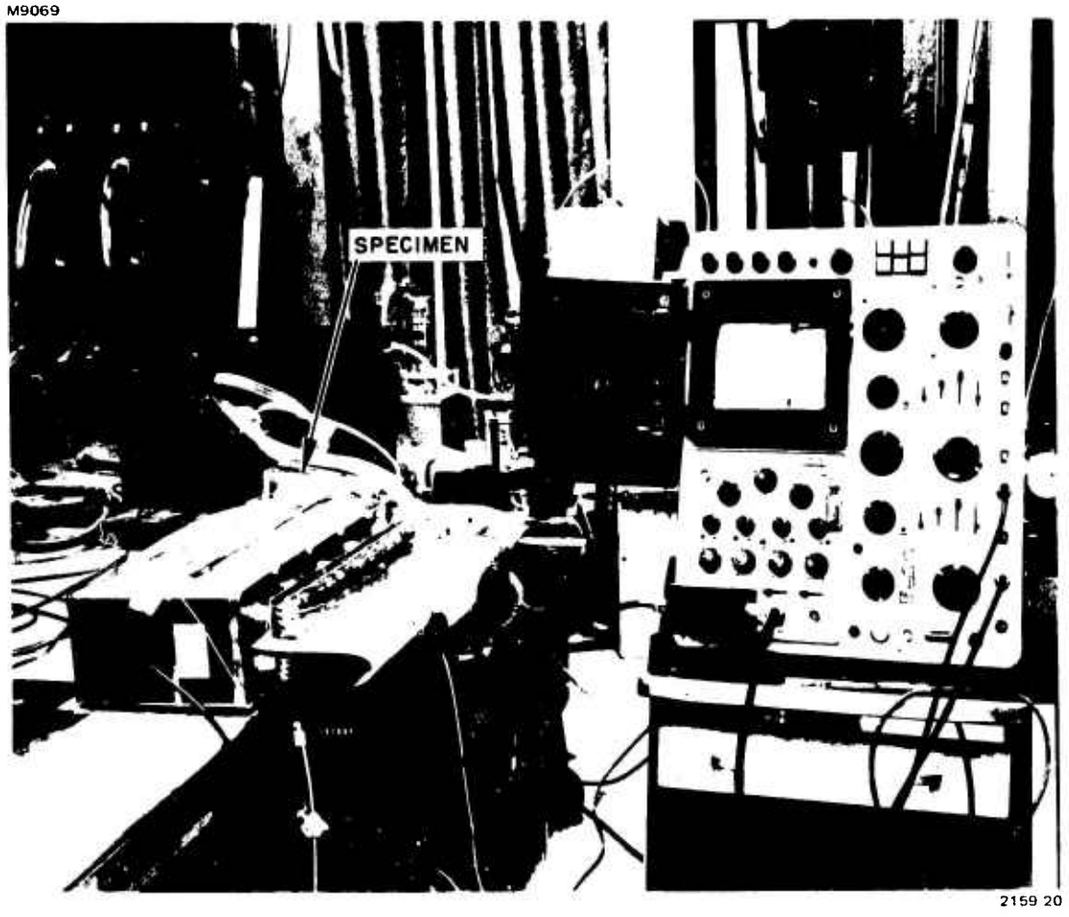

Fig. 15. Motor Structural Test.

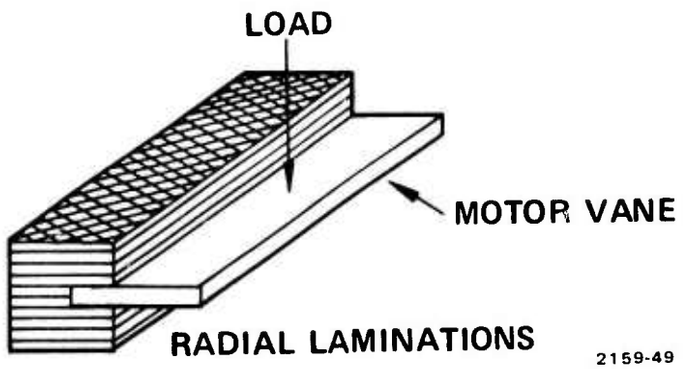

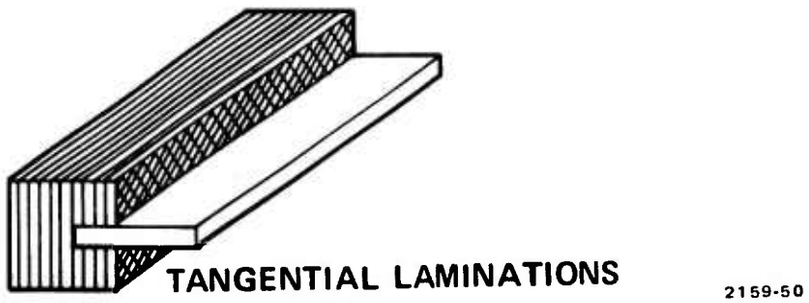

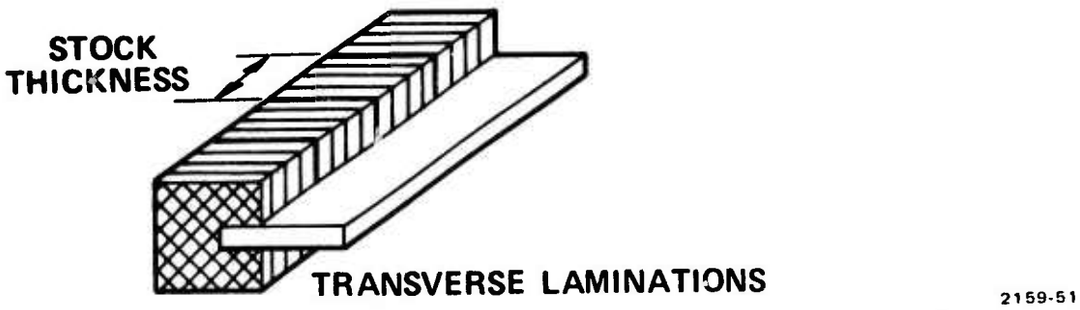

Fig. 16. Test Samples Used in Relative Strength Test Showing Orientation of Fiberglass Laminations.

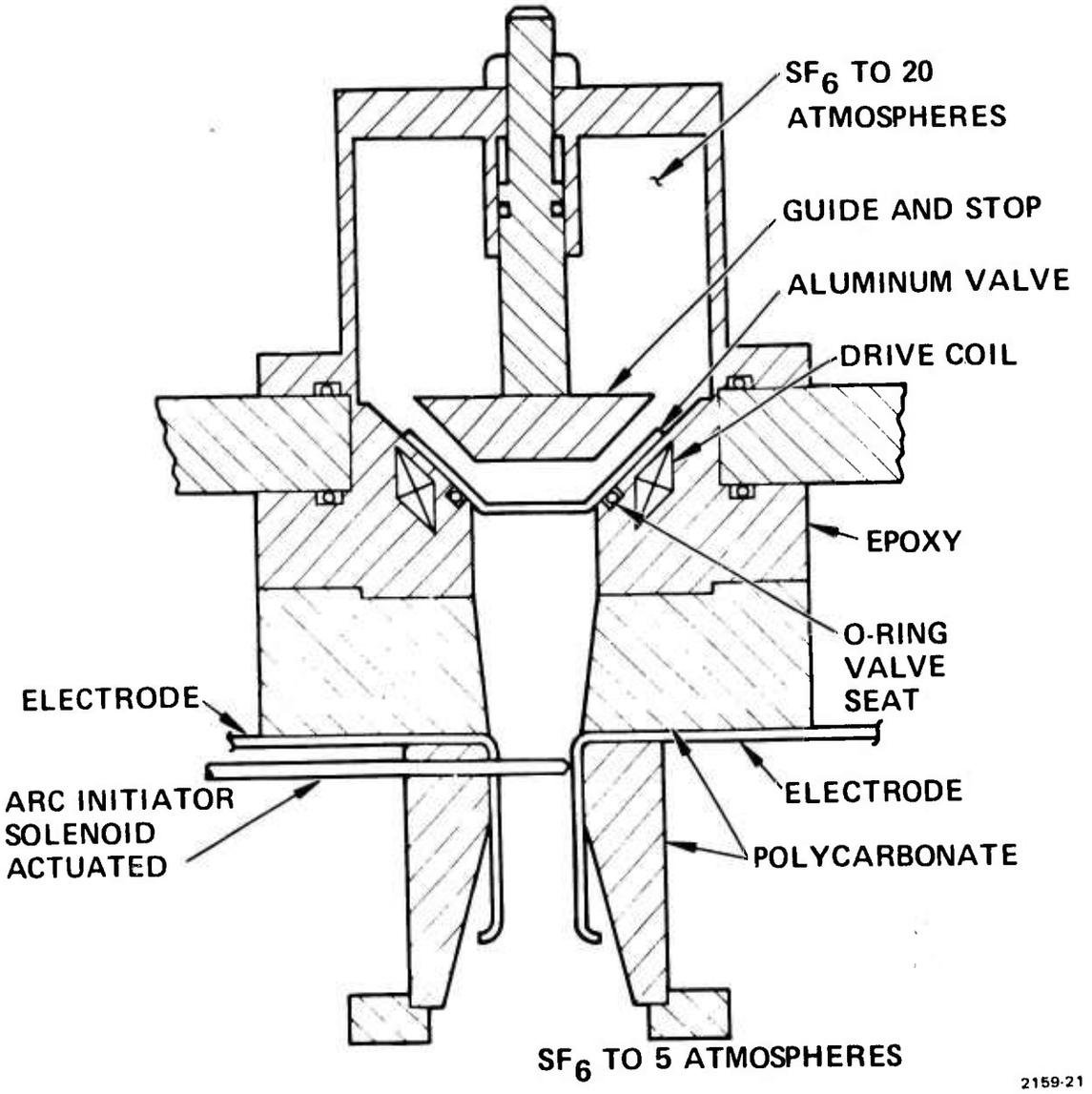

Fig. 17. Experimental Gas Blasting System.

M9426

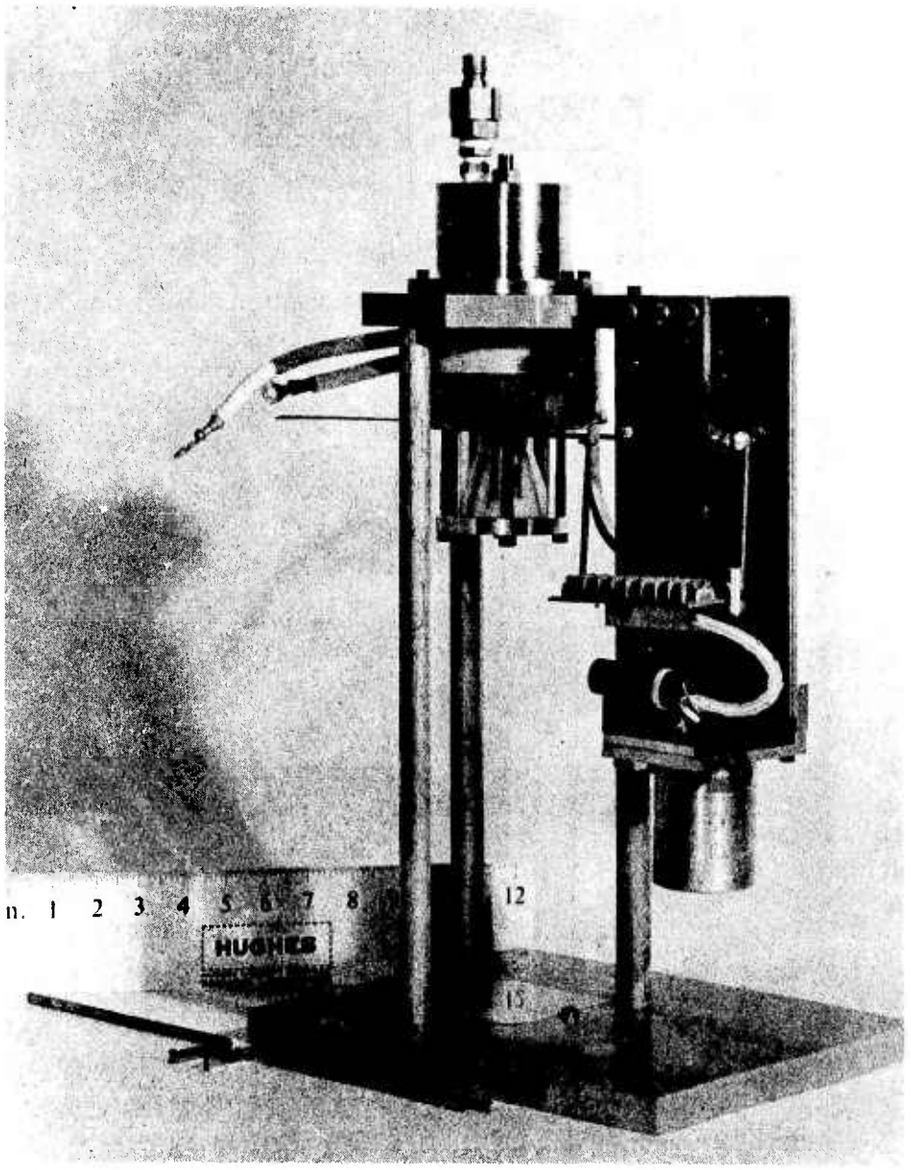

Fig. 18. Experimental Gas Blasting System.

M9428

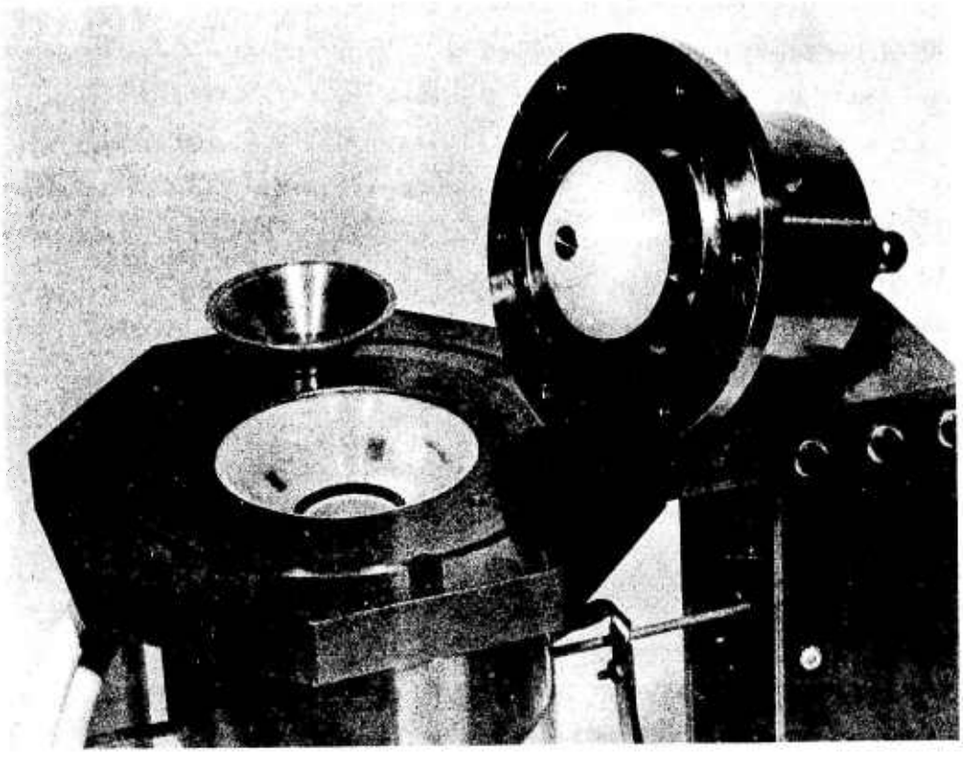

Fig. 19. Valve Disc, Stop, and Seat.

The drive coil contains 5 turns of 0.010 x 0.400 in. copper ribbon and was wound with laminated fiberglass tape between turns and continued for one turn on both the i.d. and o.d. of the coil. The fiberglass was thoroughly impregnated with wet epoxy before winding. A specially designed three-part mandrel enabled molding pressure to be applied as a final forming operation. The resultant coil was then cast into epoxy in a mold that has most of the finished dimensions of the part desired. The O-ring grooves and the back mounting face are machined. Figure II-18 is a photograph of a spare coil and a spare casting. The solenoid driven leverage mechanism which retracts the arc initiator rod of the arc chute is shown, with one support rail removed, in the photograph of Fig. II-19.

The gas valve is opened by discharging a capacitor bank through the driven coil. The arc initiator rod in the arc chute is retracted by discharging another capacitor bank through the solenoid, which then holds in the retracted position until manually switched off. The arc initiator rod retraction mechanism will not simulate the mechanical switch with regard to opening time. Therefore, to operate the arc chute with significant current, a circuit was devised that passes a low current during the time the arc is being drawn out and then raises the current for the gas blast experiments.

b. Experiments – Valve disc motion has been studied by microwave heterodyning techniques. The travel distance and velocity have been calibrated, by this method, as a function of both driver energy and gas (N_2) pressure. No difficulties are anticipated in operating with SF_6.

Preliminary tests have been performed on arc initiation by passing a low current (5 A) through the rod to the opposite electrode and then withdrawing the rod. When the rod was fully retracted, the current was increased to 70 A and the gas valve was activated. Figure II-20 shows the device in actual operation.

M9429

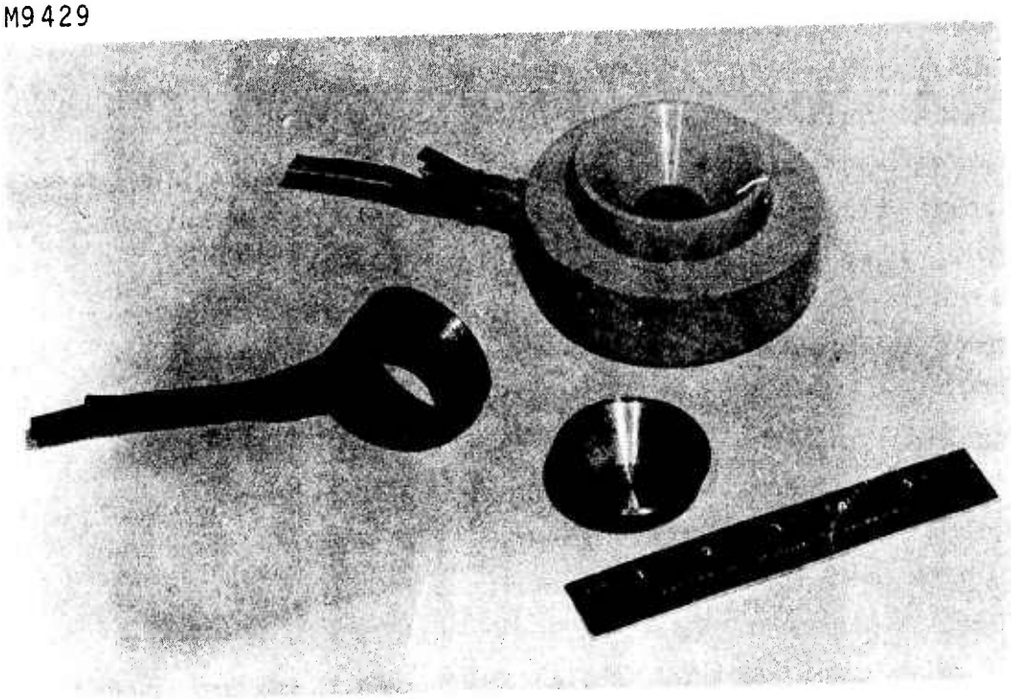

Fig. 20. Coil, Coil Casting, and Valve Disc.

M9427

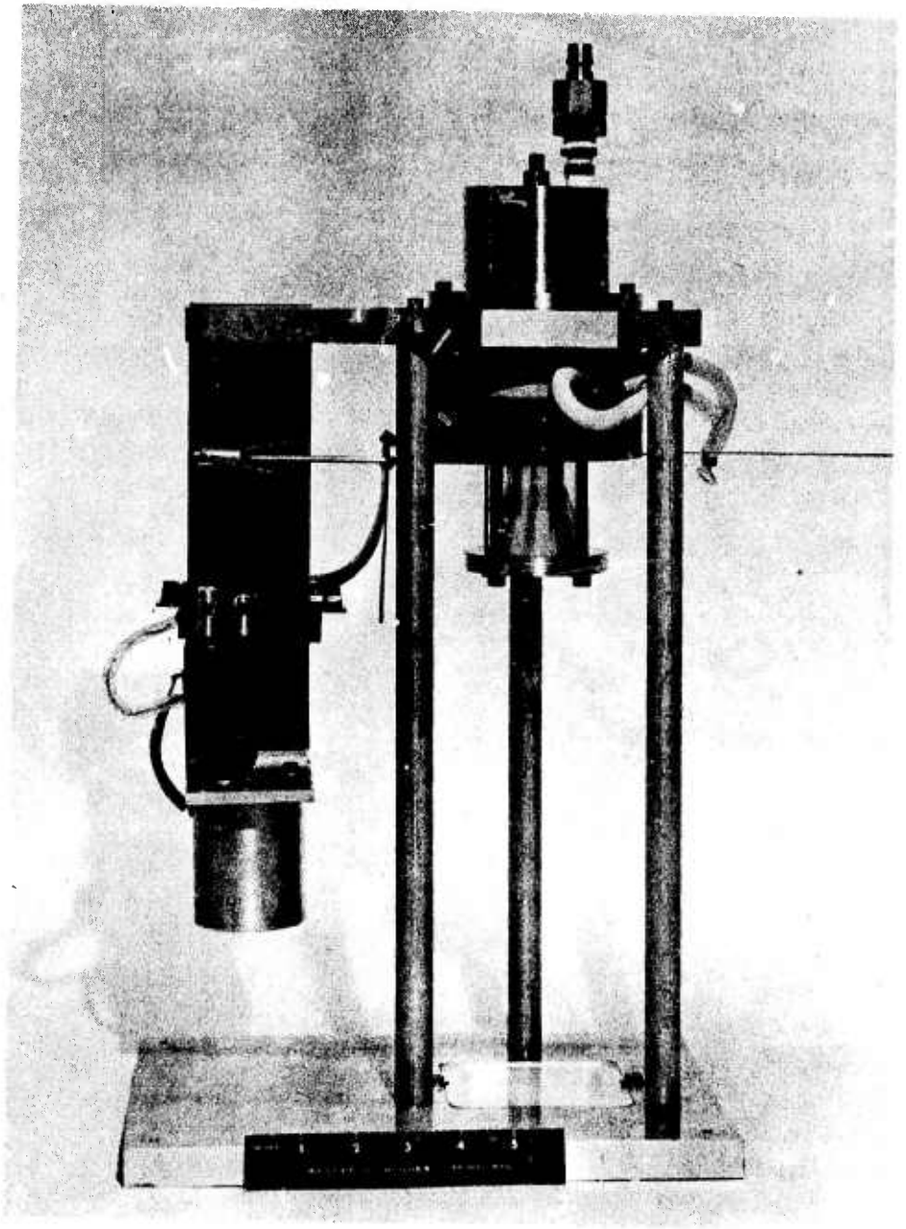

Fig. 21. Solenoid Driven Linkage Mechanism.

M9443

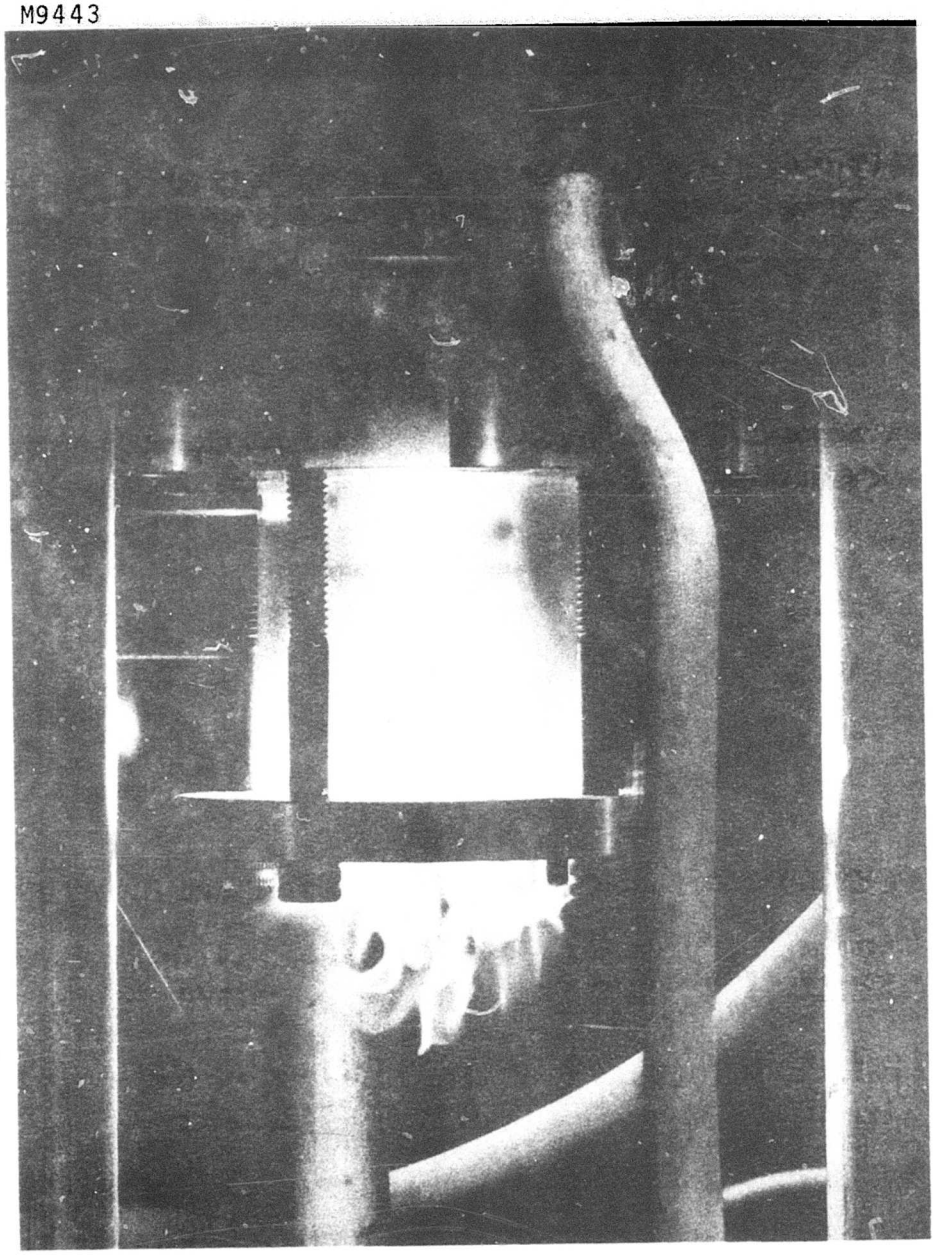

Fig. 22. Operating Gas Blasting System.

The prime objective of these tests is to demonstrate (1) that sufficient arc voltage can be generated by the gas blasting system to transfer the current to a shunt interrupter tube and (2) to show that the deionization time of the arc chute is less than the conduction time of the interrupter (typically 100 μsec).

This has been achieved at low current levels in initial tests. The top oscillogram in Fig. II-21 shows the arc voltage versus time (top trace) while the bottom trace shows the arc current versus time. When the arc voltage reached 500V (the conduction voltage of the shunt, 500 cm^2 interrupter tube), current transferred out of the arc chute (note the abrupt current fall) and into the interrupter (bottom trace of lower oscillogram). The tube was switched off after 90 μsec, interrupting the current flow against the driving capacitor voltage of 900V. These experiments are presently being extended to the 2.5 kA, 50 kV level.

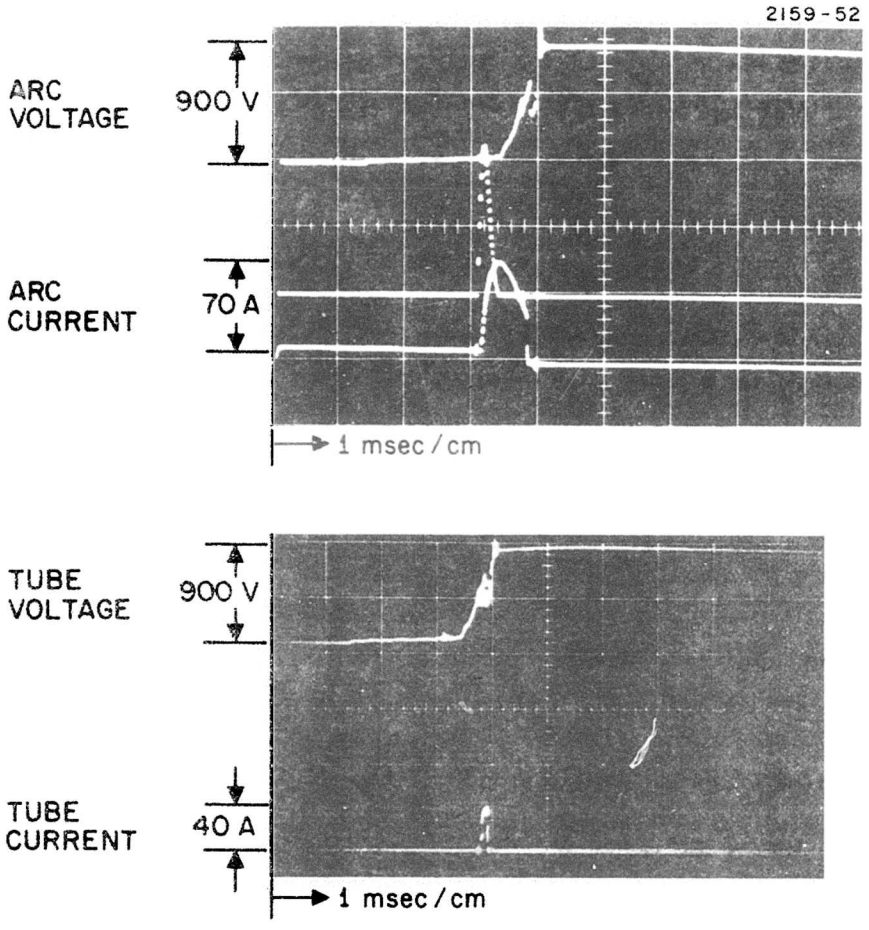

Fig. 23. Arc Voltage Generation and Current Transfer Waveforms.

E. Detailed Design

A layout of the mechanical switch is shown in a cutaway elevation view in Fig. II-22. Sectional views are shown in Figs. II-23, II-24 and II-25. The overall height as shown is 42-3/4 in. and the diameter of the largest flanges is just under 20 in. The bushings for the IES circuit each extend approximately 10 in. beyond the flanges and are located diametrically opposite one another.

In the following, we discuss detailed design points of each of the following items:

- Torsion bar
- Contacts
- Motor
- Motor pulser
- Gas blasting system
- Enclosure

The section concludes with a table listing the pertinent specifications of the complete mechanical switch.

1. Torsion Bar

The diameter and length of the torsion bar were calculated in Section II-C to be 1.65 cm (0.625 in.) and 23.5 cm (9.25 in.), respectively. The torsion bar will be fabricated from silico-manganese steel, Type 9260, which has been used extensively for torsion bars and is capable of the peak torsional stress of 7×10^9 cgs (110,000 PSI) even without the benefits of presetting. Presetting is the process of overloading the torsion bar as a final manufacturing operation to enhance the allowable working stress. Presetting is advantageous if the torsion bar will be stressed in only one direction in use, which will be the case in normal operation of the mechanical switch. However, at least in early working models, provision will be made for fail-safe survival in the event the deceleration pulse from the motor fails to occur properly.

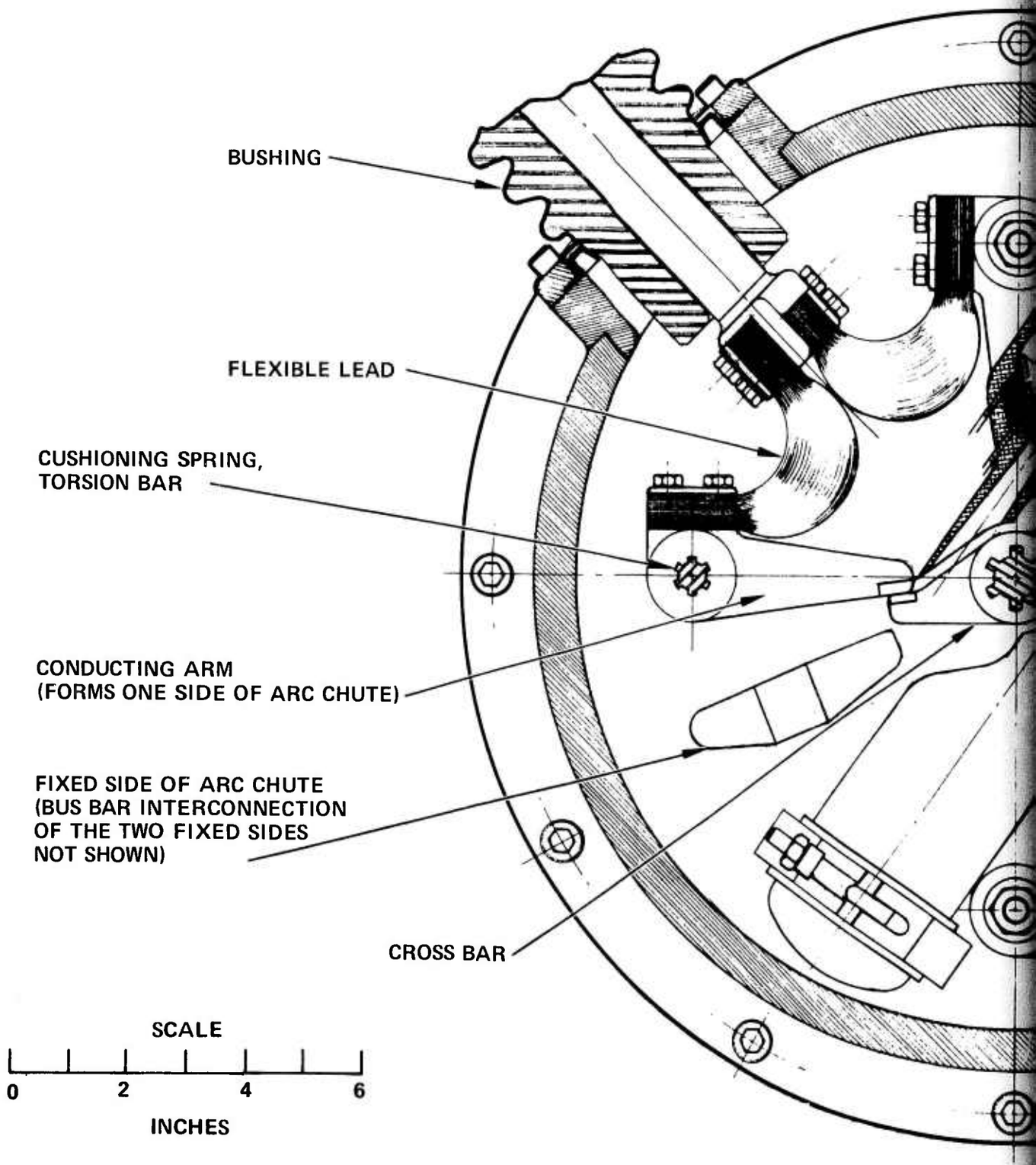

Fig. 24. Arcing Contacts.

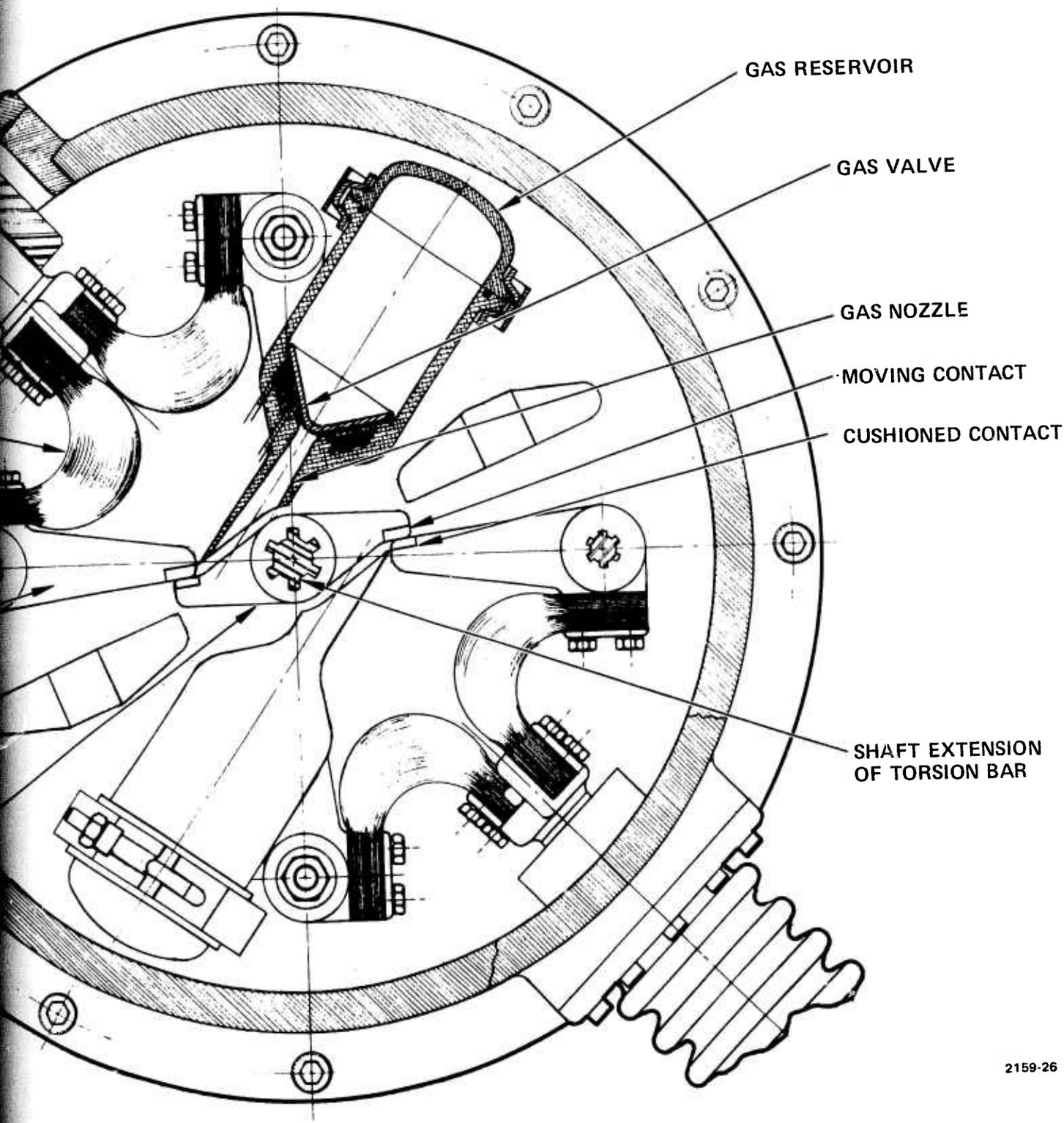

24. Arcing Contacts.

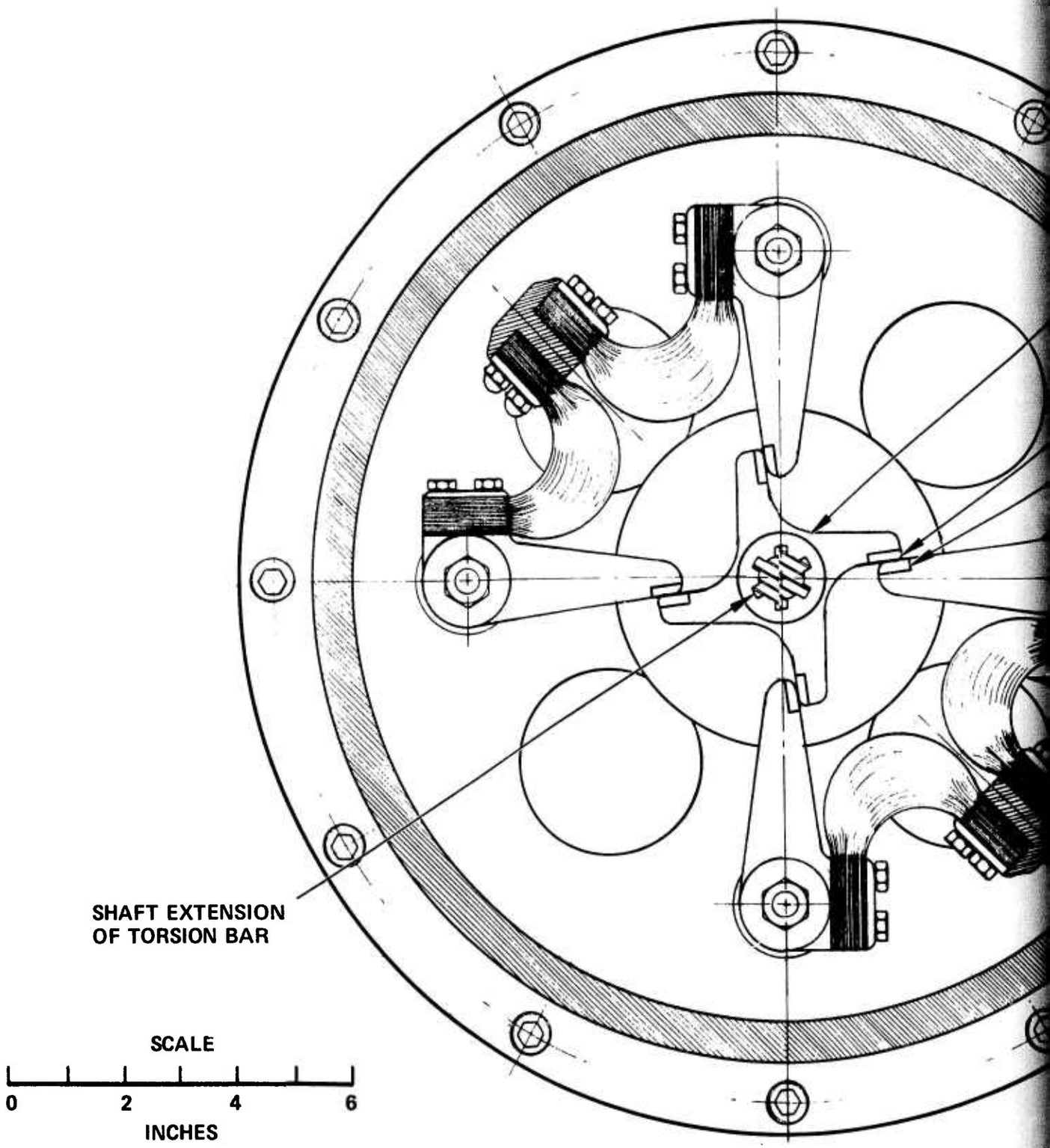

Fig. 25. Nonarcing Contacts.

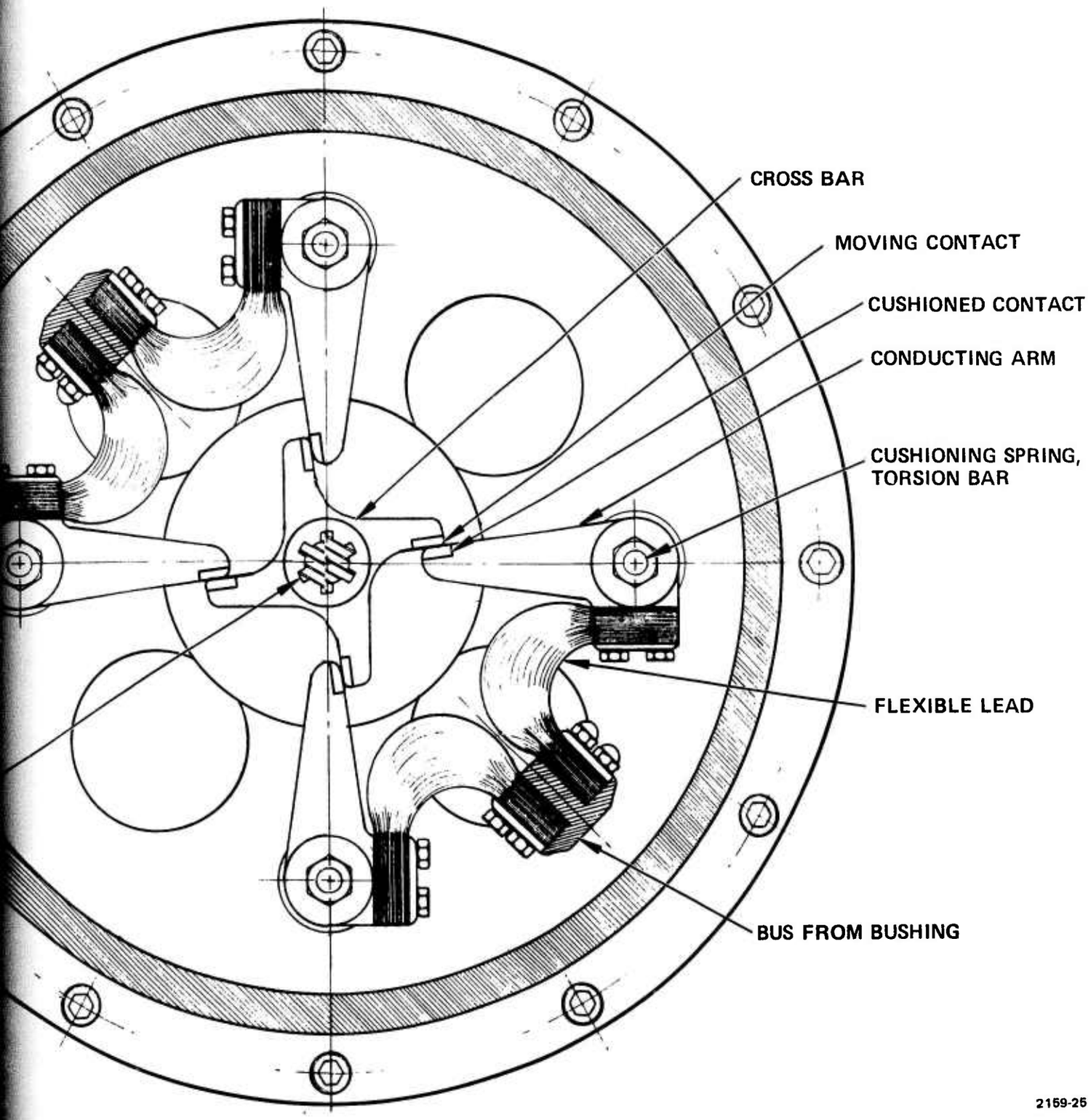

25. Nonarcing Contacts.

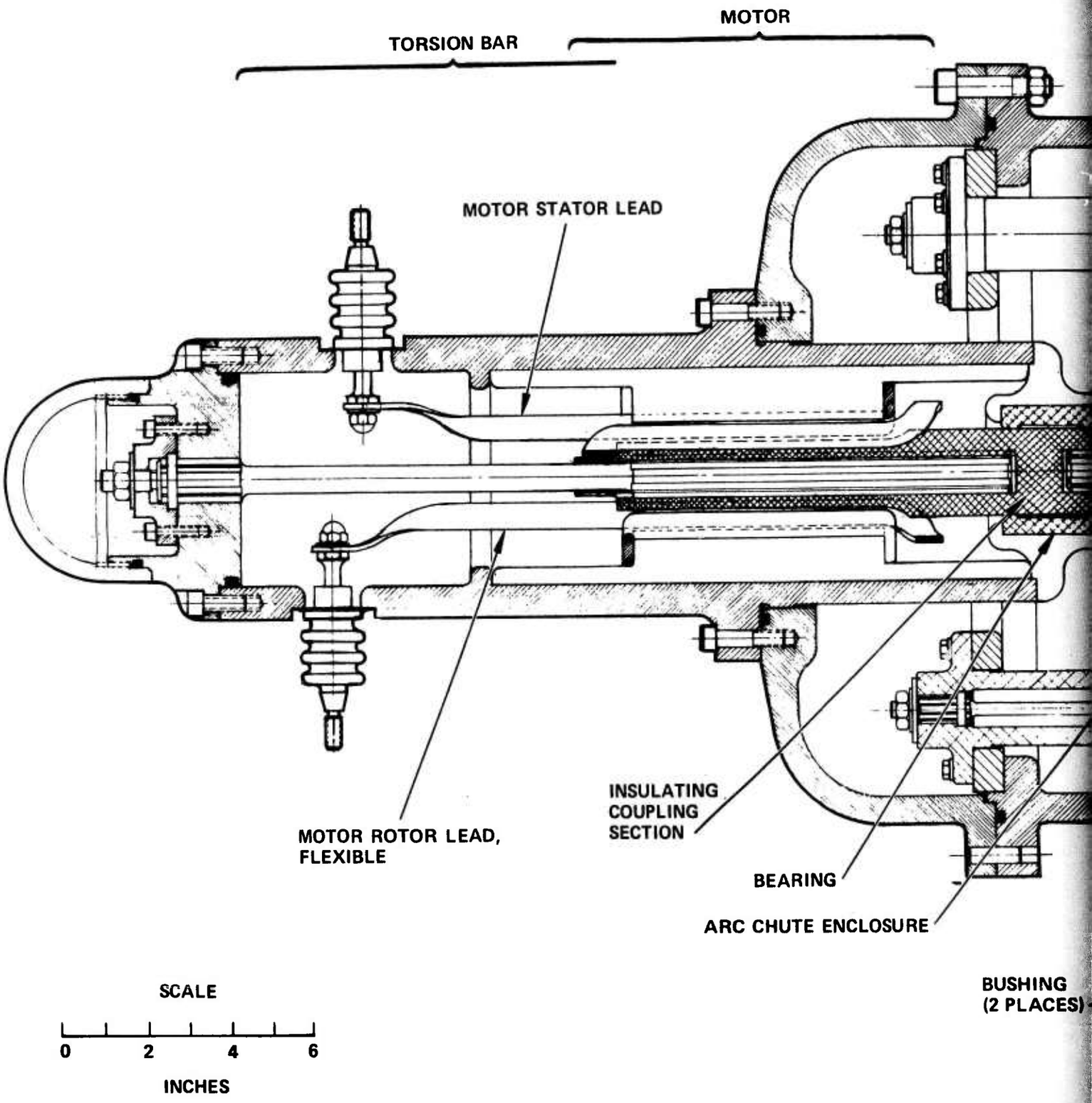

Fig. 26. Mechanical Switch.

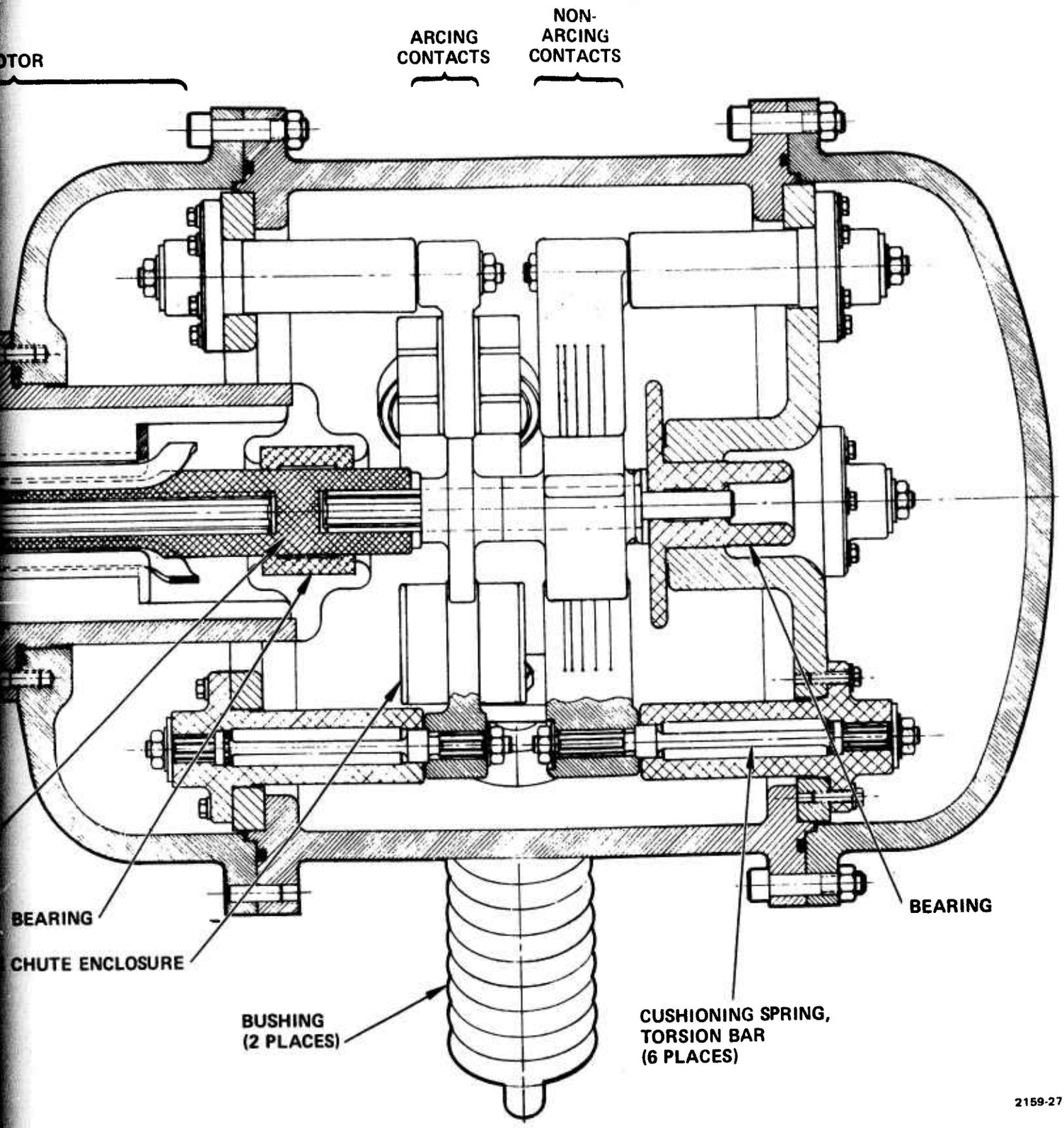

Mechanical Switch.

2

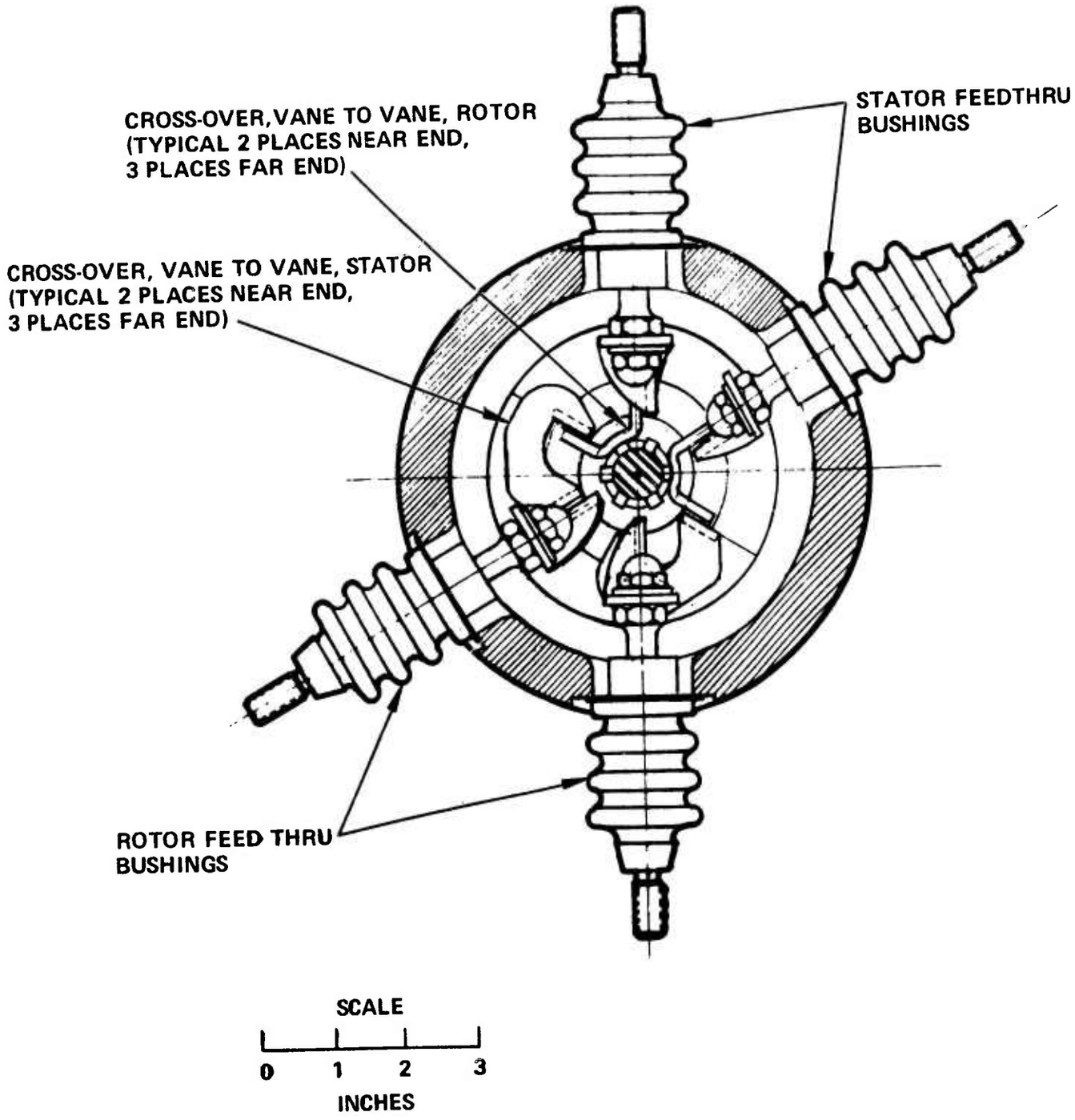
CROSS-OVER, VANE TO VANE, ROTOR
(TYPICAL 2 PLACES NEAR END,
3 PLACES FAR END)
STATOR FEEDTHRU
BUSHINGS
CROSS-OVER, VANE TO VANE, STATOR
(TYPICAL 2 PLACES NEAR END,
3 PLACES FAR END)
ROTOR FEED THRU
BUSHINGS
SCALE
0 1 2 3
INCHES

Fig. 27. Motor.

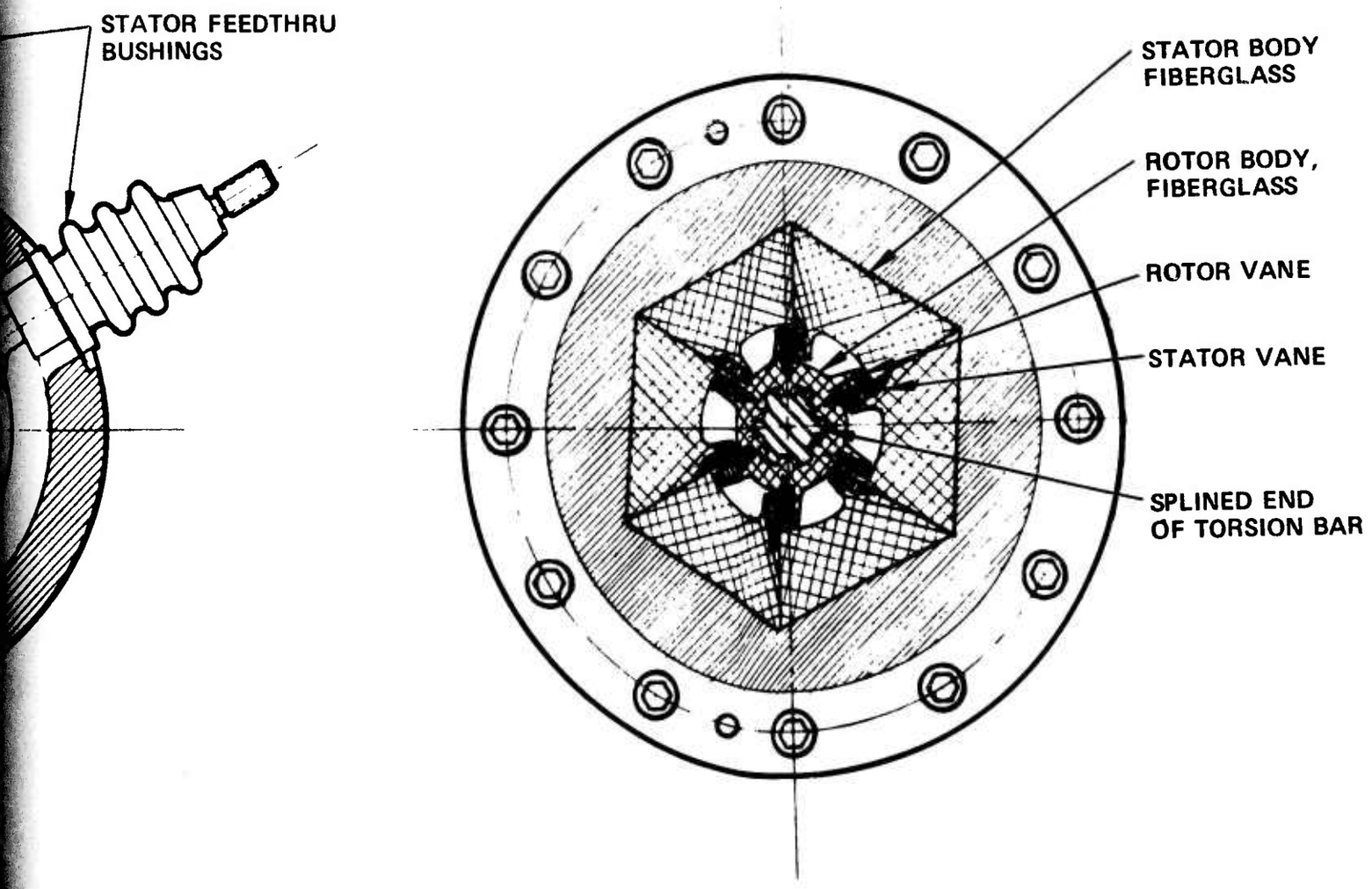

Fig. 27. Motor.

Without the deceleration pulse, the torsion bar would see a reversal of stress direction. A specific heat treatment schedule for the torsion bar will be given to avoid decarburization of the surface and to minimize distortion. Shotpeening will be used for surface conditioning.

Splines will be used at the anchor end and for attachment of the motor rotor at the free end. The transition from torsion bar diameter to the root diameter of the splines must be gradual to minimize stress concentration. The total active length of the torsion bar will increase by 1/4 in. to account for the tapers and fillets. Nonstandard, six-tooth, splines with parallel side teeth will be used. Involute splines are the usual choice for ease of accurate fabrication and for minimum stress concentration at the root of the teeth. An overriding consideration for the mechanical switch is the direction the spline teeth will load the fiberglass body of the motor rotor. Involute splines would exert a radial outward pressure which the fiberglass could not contain. Parallel side spline teeth will transmit the torque with nearly circumferential pressure; a load direction like that of the motor vanes.

Bearing support for the free end of the torsion bar (and the shaft extension which carries the contact crossbars) is provided by two polymeric slider journals. Rolling element bearings are not well suited to high acceleration starting. The layout drawing shows the midspan bearing running on a fiberglass o.d. Other bearing surfaces could be provided, if found necessary, and still maintain high voltage isolation of the shaft extension.

2. Contacts

The moving contacts are mounted in the tips of crossbars attached to the shaft extension of the torsion bar. The opposite contacts are named cushioned contacts rather than fixed contacts to be descriptive of the fact they are backed up by springs and experience some, although limited, motion. The cushioned contacts are mounted in the tips of conducting arms which are pivoted by torsion bar springs. The area in contact when the contacts are closed has a narrow dimension in the radial direction and actually approaches line contact because of the

rounding off of the edges of the contacts. Contact theory and practice assure that this is a satisfactory contact configuration. Eleven centimeter (4.3 in.) of contact length is shown in the layout presented. It is expected that this length can be reduced by a factor of 2. The contact length is divided into three segments; two 5 cm contact lengths are provided in the nonarcing contact section and one centimeter of contact length is provided for the arcing contact.

The arcing contact is distinguished by (1) different contact material (2) opens last and closes first (3) has a gas blast and arc chute associated with it. The last to open, first to close feature will be accomplished by the advanced position of the cushioned contacts relative to that of the cushioned contacts of the non-arcing contacts. The advancement of the cushioned contacts forward of those for the nonarcing contacts will be in the order of one millimeter (0.02 rad of moving contact rotation).

The nonarcing cushioned contacts and conducting arms on which they are mounted will be slit radially to form multiple contact fingers. This configuration is not only standard practice to decrease contact resistance but will serve to mask the effects of any contact bounce by decreasing the probability that all contact surfaces are parted at any one instant and hence draw an arc. To further ensure the later functioning of the contact fingers, the slits will be unequally spaced to form fingers of various widths. The fingers thereby will be tuned to slightly different frequencies. The prime controls of contact bounce will remain the properly timed and shaped deceleration pulse from the motor and the proper contact preload value.

The proper contact preload is predicted to be 40 lb per contact finger. Contact preload is necessary to decrease contact resistance and overcome electrodynamic blowoff which would result in contact bounce. Contact preload will be set in by rotation of the torsion bar cushioning springs and by a similar adjustment of the main drive torsion bar. Adjustment at both points is necessary to maintain the proper spacing of the vanes of the motor.

The arcing contacts will be sintered tungsten-copper with over 70% tungsten. The nonarcing contacts will be a high copper content material, hard enough to take the impact of rapid closing but still have a high conductivity and low contact resistance.

The preferred method of joining the contacts to their aluminum backing is by welding. Several recent attempts to accomplish this in-house on high tungsten content contacts were unsuccessful, but Mallory Metallurgical Company claims they can perform this operation. Screw fasteners offer an alternative method that is known to be satisfactory. The material chosen for the crossbar is a high conductivity aluminum with reasonable strength, i.e., Type 6101 heat treated. It is with this material that attempts would be made to develop welding techniques for the attachment of the contacts.

Erosion of the arcing contacts will be a limiting factor, along with temperature rise, in the determination of duration of the operating periods that can be obtained from a high current, repetitive mechanical switch. The gas blast will ensure rapid movement of the arc off the contacts and onto the arc chute which will greatly reduce the erosion of the contacts. The expectation is that this transfer of the arc from the contacts to the arc chute will occur in 90 μsec (i.e. 1/10 of the 900 μsec duration of the arcs). Published erosion rate data indicates 0.2 cm^2 of material loss per kA-sec per mating pair of contacts. At 20 kA, this erosion rate would be 4 cc/sec of arcing. At PRF = 5 Hz for 1 min (300 shots) the loss from the switch contacts would be $90 \times 10^{-6} \times 4 \approx 0.1$ cc per each of the two mating pairs of contacts. This loss would undoubtedly be intolerable. The published erosion rate data were obtained from experiments with arcs of much longer duration and it is recognized that a different regime may exist during very short duration arcs. That other regimes of arcing exist is evidenced by the fact that one investigating team published the finding that erosion rates decrease by a factor of 10 when the current is dropped below ≈1000 A. Another indication that the erosion calculated above is higher than will be found, is the survival of the contacts in 230 kV circuit breakers which are

tested at 43 kA rms at 60 Hz. One of the tests in a sequence of testing is open, rapid close, rapid open, close after 15 sec, rapid open and at each opening the arc lasts for 8 msec (1/2 cycle). Therefore the contacts see 24 msec of arcing at 43 kA in less than one minute, whereas in the switch herein, 27 msec of arcing at 20 kA in one minute (5 Hz, 1 min, 300 shots, 90 x 10^{-6} sec per shot of arcing) occurs.

The conclusion regarding contact erosion is that survival for one minute of operation at PRF = 5 Hz is expected, but that because of the material lost, the contact preload will require checking and probably need readjusting. Possibly, an automatic adjustment mechanism could be incorporated. Also, it seems probable that the contacts would require replacement after 600 shots or two 1-min operating periods at 5 Hz. Contact erosion is expected to increase in proportion to any PRF increase (at constant current), and therefore, it is expected that this fact (if not heat rise) would limit the duration of operation to less than one minute at PRF's > 5 Hz.

3. Motor

The motor design was covered extensively in Section II-C and was the subject of some experimental verification as reported in Section II-D. The rotor and stator vanes will each be formed into their sinuous configuration from a continuous strip of aluminum. The fiberglass rotor body, an extension of which will serve to isolate the motor from the extension shaft that carries the contact crossbars, will be made from either laminated NEMA Grade G-10 epoxy fiberglass as experimented with, or be a custom formed, epoxy fiberglass, filament wound component. The stator body can simply be built up from wedges of the G-10 material as shown in the sectional view of the motor. The stator body is shown fixed in the housing by the use of a broached hexagonal hole in the housing. The routing of the motor leads may have to be altered from that shown in the layout in order to produce a circuit with less inductance.

4. Motor Pulser

The electrodynamic drive motor requires a very high current (30 to 50 kA) to provide the necessary impulse. This is achieved by connecting a precharged capacitor bank to the motor by a triggered vacuum gap (GE No. ZR 7512). The pulser circuit is shown in Fig. II-26. The battery represents the (3 kV) HVDC supply. The total stored energy is 3 kJ of which 1 kJ is lost per switch operation. (The remaining 2 kJ is saved and only the 1 kJ need be replenished each shot.) At 5 Hz, this requires a 5 kW power supply. Size and weight estimates of the pulser are 5 ft^3 and 250 lb. The auxiliary power required is 5.5 kW, allowing 0.5 kW for losses.

5. Gas Blasting System

The gas blast must (1) move the arc off the contacts and onto the arc chute as quickly as possible, (2) extend and cool the arc to develop the arc voltage required to turn on the interrupter tube (preferably at a slow rate to begin with, followed by a rapid rise so that the dissipation of the arc is minimized), and (3) clear the gap of ionized products within the 100 μsec the tube is conducting, to develop the capability to withhold the required 100 kV.

The stored pressurized gas, fast acting valve system was chosen over the puffer approach to develop the gas blast. This choice (1) separates, to a large extent, the development of the torsion bar and its drive from the development of the gas blaster, (2) offers more, and more readily adjustable, parameters to work with in developing the proper blast to optimize performance of all three of the required functions, and (3) decreases the heat dissipated in the switch system.

The layout drawing incorporates a prototype version of the gas subsystem, in which the gas reservoir, drive coil and nozzle are formed in a one-piece epoxy fiberglass filament winding. Not shown is a larger holding reservoir outside the mechanical switch that replenishes the reservoir inside the mechanical switch in the period between shots.

The fixed side of the arc chute will be of an arc resistant material such as tungsten-copper. The other side of the arc chute is formed

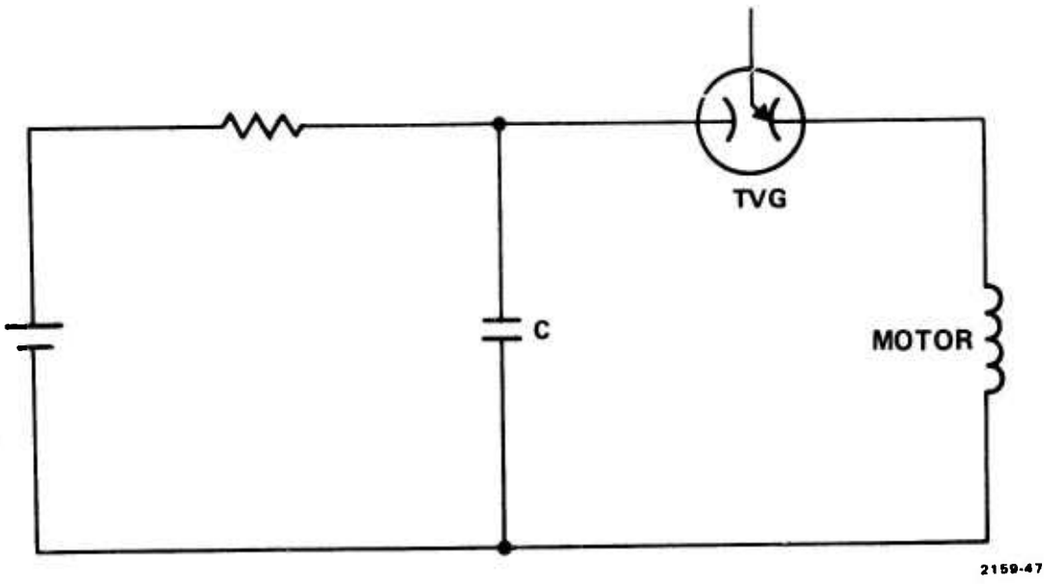

Fig. 28: Mechanical Switch Pulser Circuit.

by the conducting arm on which the cushioned contact is mounted. The conducting arm will be of copper or high conductivity aluminum but in either case will be faced on the arc chute side with tungsten-copper. Completing the enclosure of the gap formed by the arc chute electrodes will be a wall of polycarbonate. The function of this enclosure is to contain and guide the gas stream. However, because the surface of the polycarbonate will form a shunt conduction path between the electrodes, the enclosure cannot be as close fitting nor as complete as would be desired for optimum gas dynamics. Sonic flow at the contacts is a design objective of the gas path design.

6. Enclosure

The wall thickness of the enclosure shown in the layout drawing represents a conservatively designed aluminum pressure vessel and mounting structure. A significant weight reduction may be possible in a fully developed version but such a weight reduction program should follow gaining baselining experience with a rigid mounting structure. Not shown in the layout drawing are the coolant lines, the coolant plate-coils and other heat pickup routing of the coolant.

7. Specifications

The electrical and mechanical specifications of the mechanical switch are tabulated in Table II-1. A few comments regarding the entries will now be given. The nominal arc dissipation is based on an average arc voltage of 200 V for 900 μsec at the full 20 kA. The maximum operating time is based on heat build-up in the motor, gas valve and contact area. The size and weight shown is without motor coil and gas valve pulser.

F. Recloser

As described in the introduction to Section II, the recloser crowbars the load at the end of the load pulse (250 μsec) thereby saving the energy remaining in the storage inductor. A separate component is

TABLE II-1

Mechanical Switch Specifications

Item	Minimum	Maximum	Nominal	Comment
Voltage	0	100 kV	100 kV	
Current	100 A	20 kA	20 kA	
Current path resistance	30 μΩ	100 μΩ	40 μΩ	
Contact opening time	0.5 msec	1.3 msec	0.9 msec	
Arc dissipation per shot	2 kJ	7.5 kJ	3.6 kJ	20 kA
Repetition rate	none	50 Hz	5 Hz	Maximum based on IES versus CES tradeoff
Continuous operating time	none	1 min	1 min	5 Hz, 20 kA
Life	unk.	unk.	50,000 shots	
Contact maintenance time	unk.	5 min	2 min	5 Hz, 20 kA
Coolant flowrate	0.25 gpm	1.0 gpm	0.5 gpm	1 min on, 10 min cooldown
Weight	150 lb	325 lb	260 lb	Without auxiliaries
Volume	20 ft^3	35 ft^3	28 ft^3	Without auxiliaries
Auxiliaries — weight			250 lb	Motor coil and gas valve pulser at 5 Hz.
— volume			5 ft^3	
— power			5.5 kW	

required for this function because the mechanical switch contacts cannot reclose instantly, after being far enough apart to withstand the load voltage.

The recloser must be capable of meeting the following specifications:

Holdoff voltage	100 kV
Peak current (nominal)	14 kA
Conduction time	750 μsec
PRF	5 Hz

This corresponds to a conducted charge per pulse of 10.5 C. Under faulted load conditions where the recloser is used for load protection, the peak (nonrecurring) current will be 20 kA.

The most logical component choice for this kind of duty in an airborne environment is a triggered vacuum gap (TVG). Commercially available TVG's can meet these specifications. Two possible choices are GE 7534 and EG&G GP15BV (Hughes part No. 710122-3). These are designed to be operated in oil for maximum voltage operation and cooling. Operation of the EG&G gap has been demonstrated under the following conditions[4]:

Holdoff voltage	90 kV
Peak current	5 kA
Conduction time	1 msec
PRF	$\sim 10^3$ Hz (for 50 msec)

This clearly demonstrates the capability of TVG's to operate at nonzero PRF's provided all parameters are kept within reasonable operating limits.

Dissipation in the TVG can be computed in the following way. First, the dissipation during turn-on is approximately $V_o I_o T_o/6$ where V_o is the peak voltage, I_o is the peak current, T_o is the anode fall time, and a linear fall in voltage (and a linear rise in current) has been

assumed. Using V_o = 100 kV, I_o = 14 kA, and T_o = 0.3 μsec, we get a dissipation of 60 J. (The 0.3 μsec used for the anode fall time is based on an unpublished GE report by J. M. Lafferty.) Second, dissipation occurs during the conduction phase at a voltage drop ~50 V (Ref. 5) giving a dissipation during the 750 μsec pulse of 525 J. Taking the total dissipated energy to be 585 J per pulse, this gives a dissipated power of 2.9 kW at 5 Hz.

Thermal inertia of the copper electrodes will be used to store the dissipated energy during the operating time (one minute). Assuming 1 kg electrodes, the temperature rise will be about 200°C. This is far less than the processing temperature of 600°C and will not have any adverse effects. Cooldown during the off period will be accomplished by conduction and radiation to a cooled oil bath.

Trigger requirements for the GE gap are 5 kV and 150 A. This will be provided by a small pulser of conventional design with an auxiliary power requirement under 100 W. The volume and weight of the pulser will not exceed 0.25 ft^3 and 10 lb, respectively.

The range of operating parameters of a TVG is quite large. It will fire at voltages as low as 2 kV or as high as 120 kV. Currents as high as 100 kA and less than 100 A can be conducted. High PRF operation (>5 Hz) will cause greater electrode heating and consequently require the operating time to decrease if the electrode temperature rise is to be kept tolerable.

The GE TVG is cylindrical in shape with an overall length of 12 in. and a diameter of 6 in. This will be placed in an orientation independent oil filled enclosure containing a cooling oil and possibly an oil circulating pump. Overall dimensions will be 15 in. long, 9 in. in diameter, with an external bushing whose height is 6 in. This gives an overall volume of about 0.5 ft^3. The weight including TVG and oil will be about 25 lb.

The specifications for the recloser described in this subsection are listed in Table II-2.

TABLE II-2

Recloser Specifications

Item	Minimum	Maximum	Nominal	Comment
Voltage	2 kV	120 kV	100 kV	
Current	100 A	100 kA	14 kA	
Arc dissipation per shot	250 J	750 J	585 J	Depends on anode fall time and arc drop
Repetition rate	none	1 kHz	5 Hz	
Continuous operating time	none	unk.	1 min	5 Hz, 20 kA
Life	unk.	unk.	50,000 shots	
Weight			25 lb	Without auxiliaries
Volume			0.5 ft^3	Without auxiliaries
Auxiliaries — weight			10 lb	Trigger pulser at 5 Hz
— volume			0.25 ft^3	
— power			100 W	

G. BYPASS SWITCH SPECIFICATIONS

The mechanical switch specifications are listed in Table II-1 (Section II-E-7) while the recloser specifications have just been treated in the preceding section (Table II-2). We now bring these two components together to make the bypass switch, the composite specifications for which are given in Table II-3. This Table uses the most restrictive values from each of the two preceding Tables.

TABLE II-3

Bypass Switch Specifications

Item	Minimum	Maximum	Nominal	Comment
Voltage	2 kV	100 kV	100 kV	
Current	100 A	20 kA	20 kA	
Current path resistance	30 μΩ	100 μΩ	40 μΩ	
Dissipation per shot	4.0 kJ	14.1 kJ	6.5 kJ	Main circuit dissipation at 20 kA peak, 30% droop, 5 Hz
Repetition rate	none	50 Hz	5 Hz	Maximum based on CES versus IES tradeoff
Continuous operating time	none	1 min	1 min	5 Hz, 20 kA
Life	unk.	unk.	50,000 shots	
Contact maintenance time	unk.	5 min	2 min	5 Hz, 20 kA
Coolant flowrate	0.25 gpm	1.0 gpm	0.5 gpm	1 min on at 5 Hz, 20 kA 10 min cooldown
Weight	175 lb	350 lb	285 lb	without auxiliaries
Volume	20.5 ft^3	35.5 ft^3	28.5 ft^3	Without auxiliaries
Auxiliaries – weight			260 lb	Pulsers for mechanical switch
– volume			5.3 ft^3	and recloser at 5 Hz.
– power			5.6 kW	

III. INTERRUPTER TUBE

This section is devoted to a discussion of the interrupter (cross field) tube which is used to deionize the mechanical bypass switch. Section III-A is devoted to the present status of interrupter tube research and includes results for both 100 cm^2 and 500 cm^2 interrupters. Some of the work which is reported was performed under a separate Hughes-funded research program. Most significant is the operation of these interrupters at high current densities (5 A/cm^2) and high recovery rates (10 to 20 $kV/\mu sec$). The achievement of such high recovery rates eliminates the requirement for shunt, $\dot{V}$ limiting capacitors, the presence of which offsets the advantages of IES to a large extent.

Section III-B is devoted to the design of an interrupter capable of operation at the following ratings:

100 kV	peak voltage
20 kA	peak current
100 μsec	conduction time
5 Hz	PRF

This design is based on experience gained with the 100 cm^2 and 500 cm^2 interrupters. Section III-C presents the interrupter specifications and range of operating parameters in tabular form.

A. Present Status

1. 100 cm^2 Tube

The principal design features of the 100 cm^2 series of cross field interrupter tubes (XFT-100-x) are shown in Fig. III-1. Current is delivered to the anode via a high voltage feedthrough located at the top of the tube. The clearance of the feedthrough and the top end plate is minimized to prevent Paschen breakdown and to reduce plasma loss. The 20 mil thick cathode cylinder is made of tantalum and has

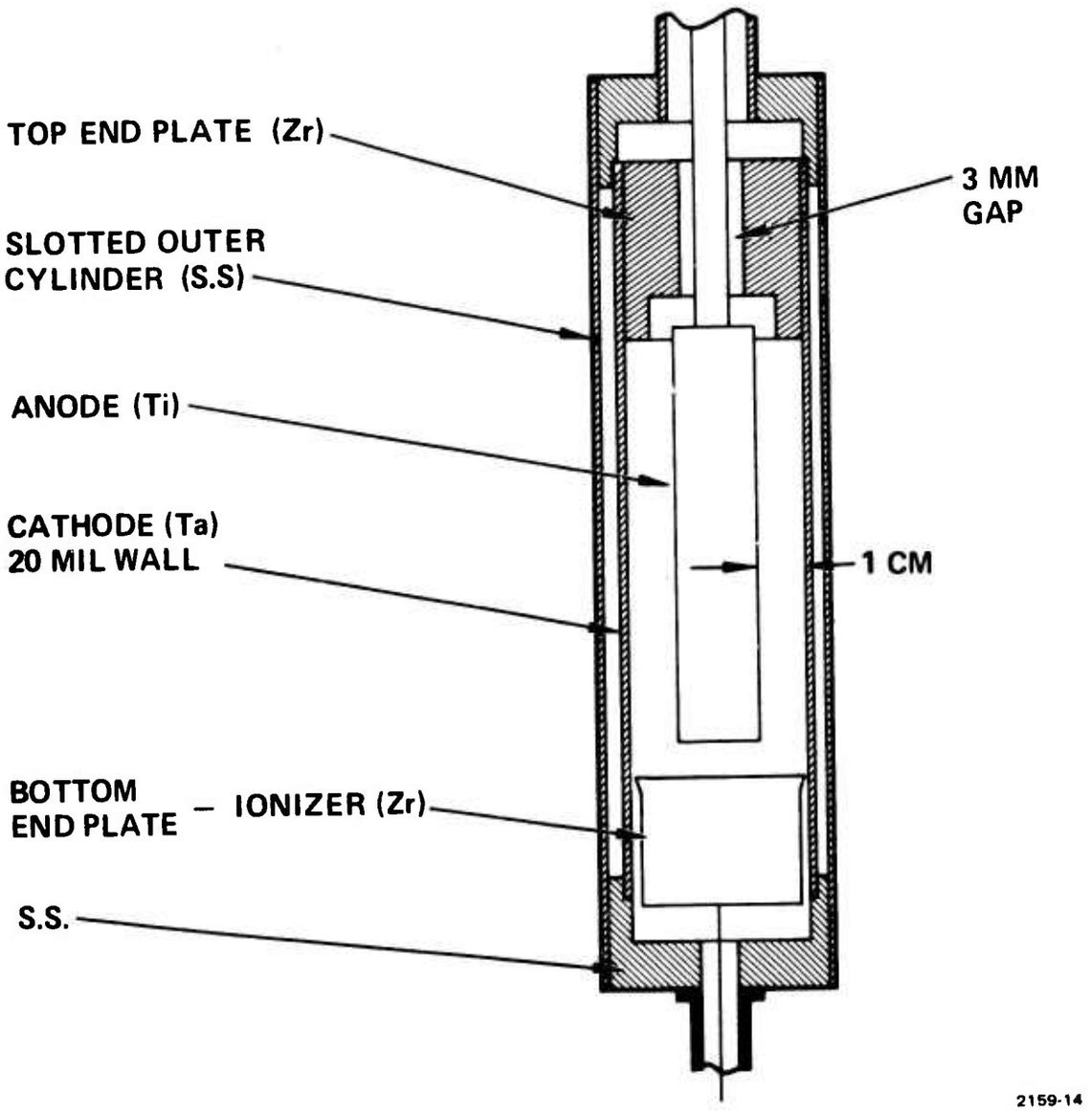

Fig. 29. 100 cm^2 Interrupter Tube.

approximately 100 cm^2 of its surface exposed to the plasma. The active cross field breakdown region is in the 1 cm anode-cathode gap located between the two end plates.

The lower end plate also serves as a preionizer. It is biased 5 to 10 kV negative relative to the cathode. Electrons are emitted from the sharp edge at its top by field emission. This provides a sufficient number of initial carriers to eliminate any significant jitter in the start-up time of the tube. A passive external spark gap is provided to limit the ionizer voltage when the tube enters the turn-off phase of its operation.

A photograph of a sealed off 100 cm^2 interrupter is shown in Fig. III-2. The tube is made entirely of metal-ceramic materials and is bakeable to 400°C. Visible through the glass vacuum envelope is the stainless steel support cylinder (see Fig. III-1).

The magnetic field is supplied, typically, by a hydrogen thyratron in series with a 2 kV, 1 μf capacitor and a 50-turn magnetic field coil. A typical test circuit for the tube is shown in Fig. III-3. The magnetic pulse lasts approximately 50 μsec. During this time the main capacitor (C) discharges through the inductor (L) and the cross field tube. The rate of rise of the current is determined by $\dot{I} = (v - \Phi_o)/L$ where v is the capacitor voltage and Φ_o is the tube voltage drop (300 to 500 V). The parameters of the circuit, particularly the charging voltages, are adjusted to yield the desired current (I_o) at the time when the tube begins to turn off.

The fall time of the current during turn off (Δt) is independent of the current amplitude. This time is about 5 μsec during normal interruption. Subsequently the voltage across the tube during interruption rises to a maximum value given by

$$\phi_{max} \approx v + \frac{I_o L}{\Delta t}$$

at a time when the current has fallen to about one-half of its initial value. Such a set of current and voltage waveforms is shown in

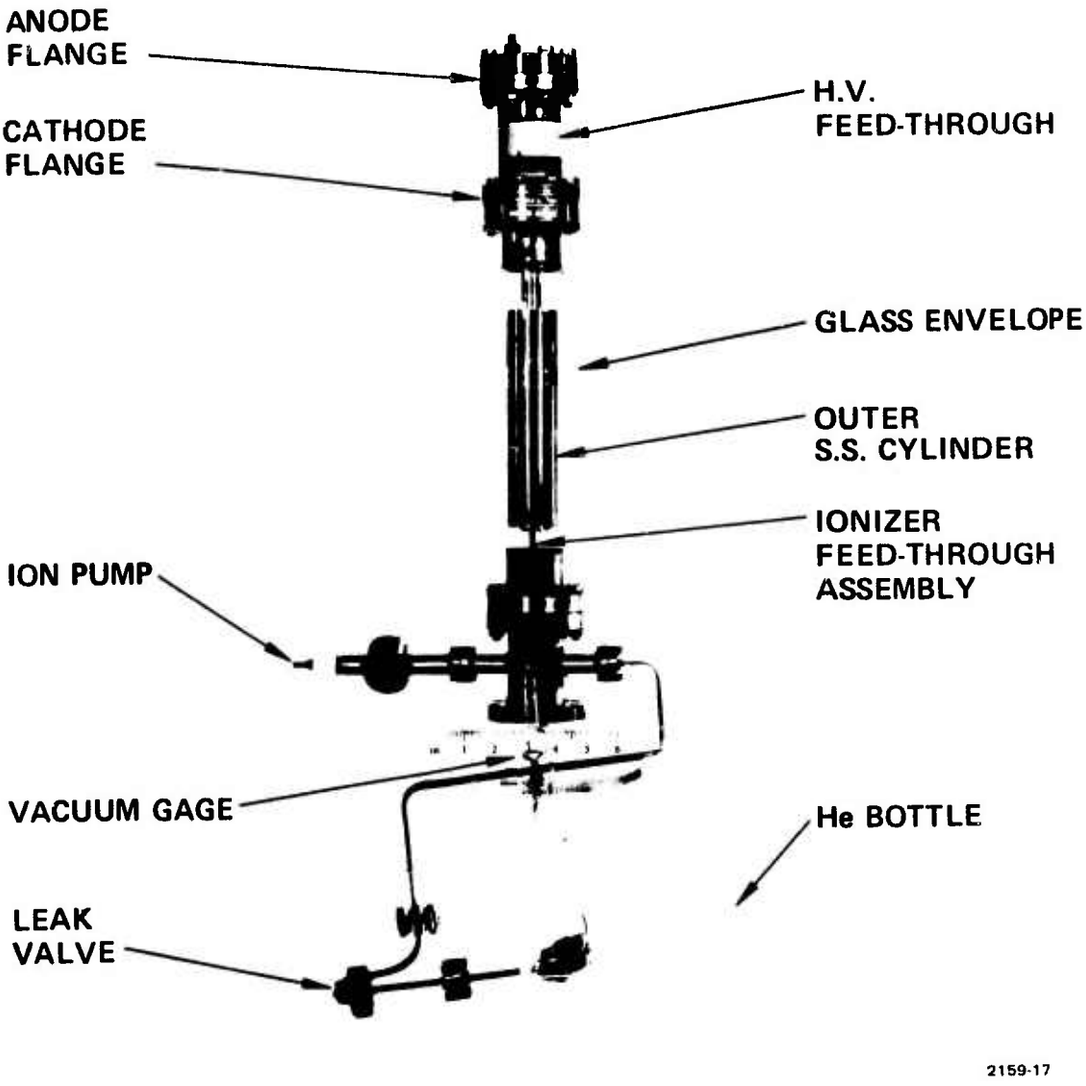

Fig. 30. Sealed Off 100 cm^2 Interrupter Tube.

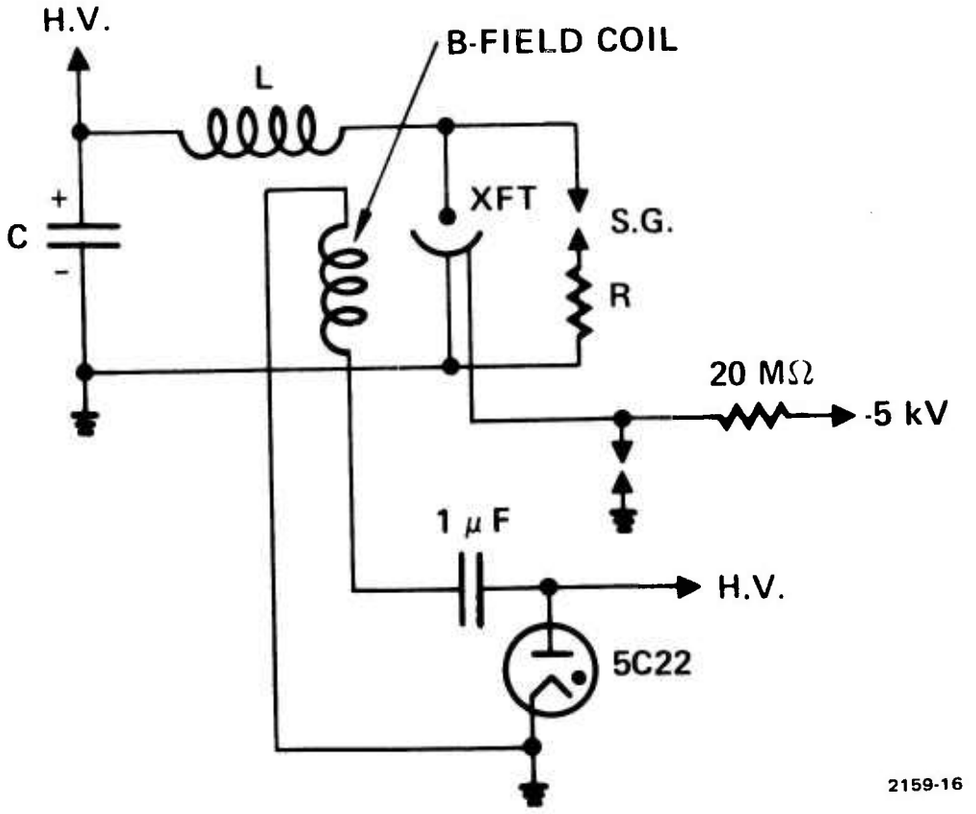

Fig. 31. Interrupter Tube Test Circuit.

Fig. III-4. This oscillogram shows three superimposed and chopped traces obtained with XFT-100-2.

After this photograph was taken, a circuit was designed to trigger the tube when the capacitor voltage v reached a preset value. This stabilized the peak current to the point that a series of 1000 consecutive shots was run at over 500 A and 40 kV without any failures. No capacitor or spark gap was used to limit the voltage rise across the tube. It is generally true that all of the tubes tested did not require any sort of $\dot{V}$ limiter. Since the peak voltage of 40 kV was reached in about 2.5 μsec, one may assign a $\dot{V}$ of 16 kV/μsec to this series of shots.

The principal cause of jitter was found to be variations in pressure. These tubes usually pump themselves down (gas clean-up) during operation. The normal operating range is 36 to 60 mTorr of helium. If the pressure is held to ±3%, one may expect the jitter in turn-off and turn-on times will be less than one microsecond.

At reduced pressures the voltage and magnetic field ranges within which the tubes will operate are derated in a complicated manner. The current growth rate is affected and subsequently the magnetic field pulse shape internal to the cathode (both in space and time) is critical. Figure III-5 depicts the ignition characteristics for two tubes with normal (~50 mTorr) and low (~30 mTorr) pressures. The minimum voltage at which the current will start is 350 to 500 V and the magnetic field on the order of 120 G.

When the magnetic field is held on by using a dc rather than a pulsed power supply, the breakdown curve is shown in Fig. III-6. Also shown is the effect of distorting the magnetic field by tilting the field coil by 9^{o}. Two branches are observed. Inside the upper branch, the tube has a high voltage drop during conduction. The dotted portion is where that voltage drop just equals the applied voltage. To the right of the upper branch the tube will not conduct until the magnetic field is made large enough to cause ignition in the lower branch.

Once all the external parameters, such as voltage, pressure, peak current, magnetic field pulse shape, etc., have been established,

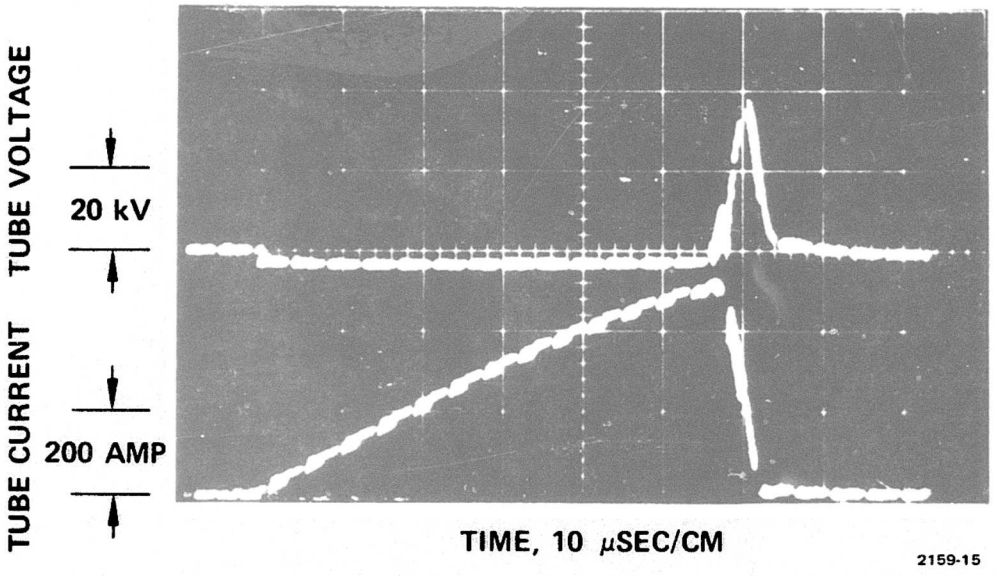

Fig. 32. Current-Voltage Waveforms for XFT-100-2.

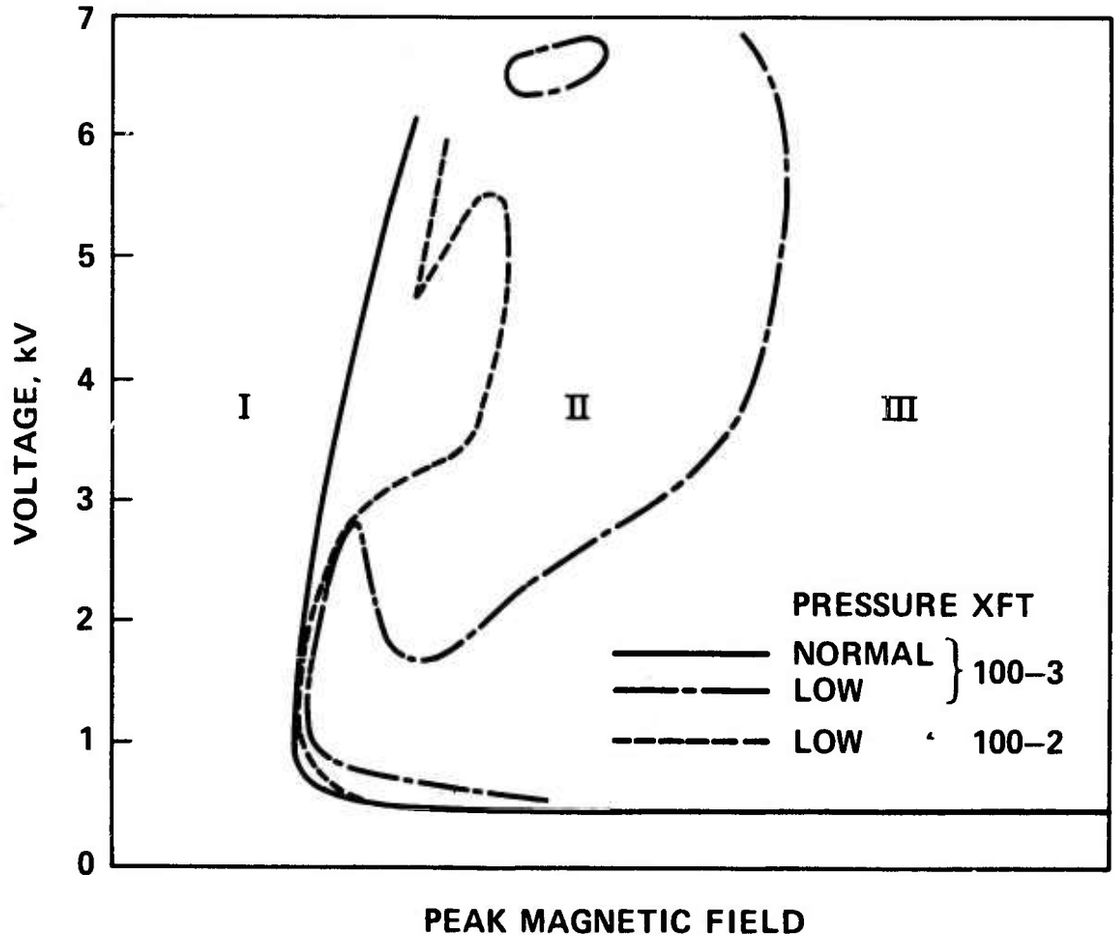

Fig. 34. Ignition Characteristics Showing Pressure Dependence.

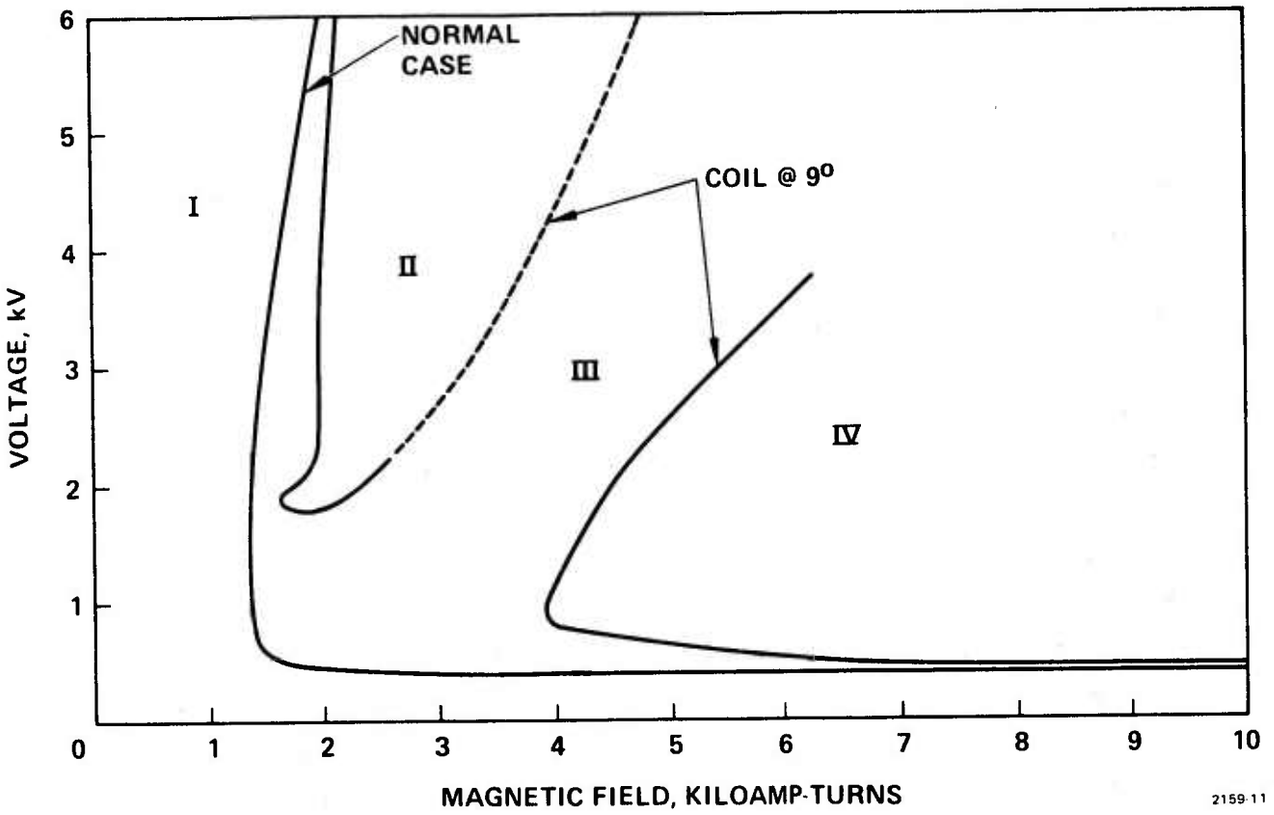

Fig. 35. Ignition Characteristics of XFT-100-4 Showing Effect of Coil Alignment.

there remains the problem of conditioning the tube. Since successful operation of the cross-field tube relies upon the correct surface properties of the cathode and anode, care must be taken in starting with a clean surface and preserving that surface. In practice, the tubes are chemically cleaned, assembled, evacuated, and baked out. Following this, the surfaces are aged under operating conditions until the arcing ceases to be random. It may be assumed that contaminants are both sputter buried on the anode and distributed in regions where the plasma is not active. By stepping up the current density slowly, one eventually establishes a point at which the arcs become predictable.

Empirically, arcs occur during the turn-off phase of the current pulse. The voltage rises to approximately one-half of its peak value and then abruptly drops to near zero, while the current stops falling and rises according to how much voltage remains in the driving capacitor. These arcs are characteristic of the upper performance levels of the tube although the same phenomenon may occur at lower levels, e.g., Fig. III-7(a). By reducing the peak current a few percent, arcs will not occur and the voltage will rise uninhibited to its peak value.

The time at which arcs occur corresponds to the maximum of the electric field which is believed to exist in the plasma sheath between the cathode and the plasma. Figure III-7(b) shows the relative arcing probability for values of the current after the peak current has been reached, i.e., the abscissa maps onto points on the falling current of Fig. III-7(b). The electric field should scale as the current density j squared times the tube voltage ϕ

$$E \sim \left(j^2 \phi\right)^{1/4}$$

A comparison of a contour of constant E and the maximum current density and peak voltage obtained with several tubes and circuit configurations is shown in Fig. III-8. The phenomenon which restricts the I, V operating range of the tube is thought to be field emission induced arcs. Therefore, surface roughness, which is a statistical property of the tube

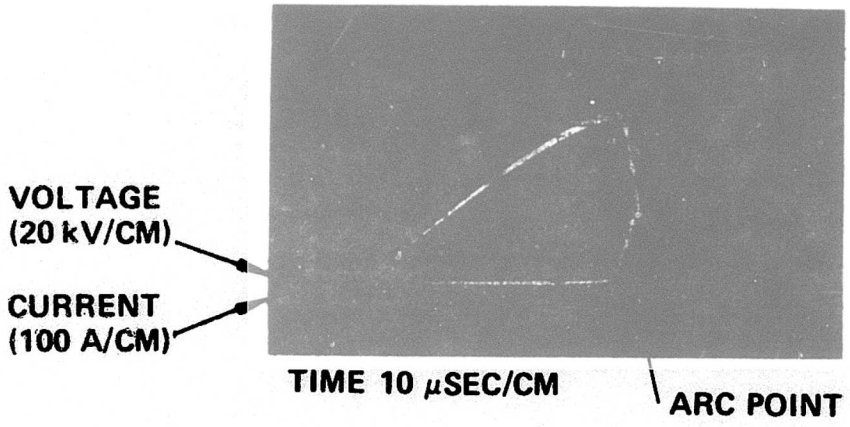

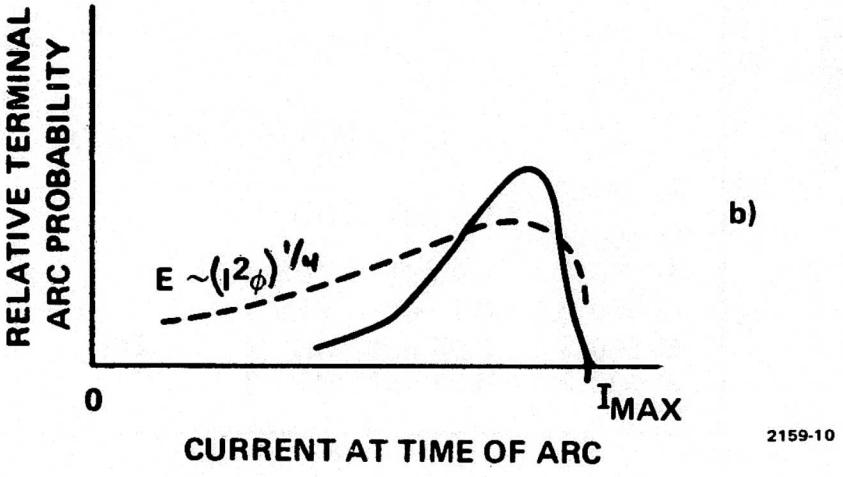

Fig. 35. Glow to Arc Transition During Interruption (After Terminal Arc Rate has been Reached). (a) Current-Voltage Waveforms. (b) Relative Arc Probability.

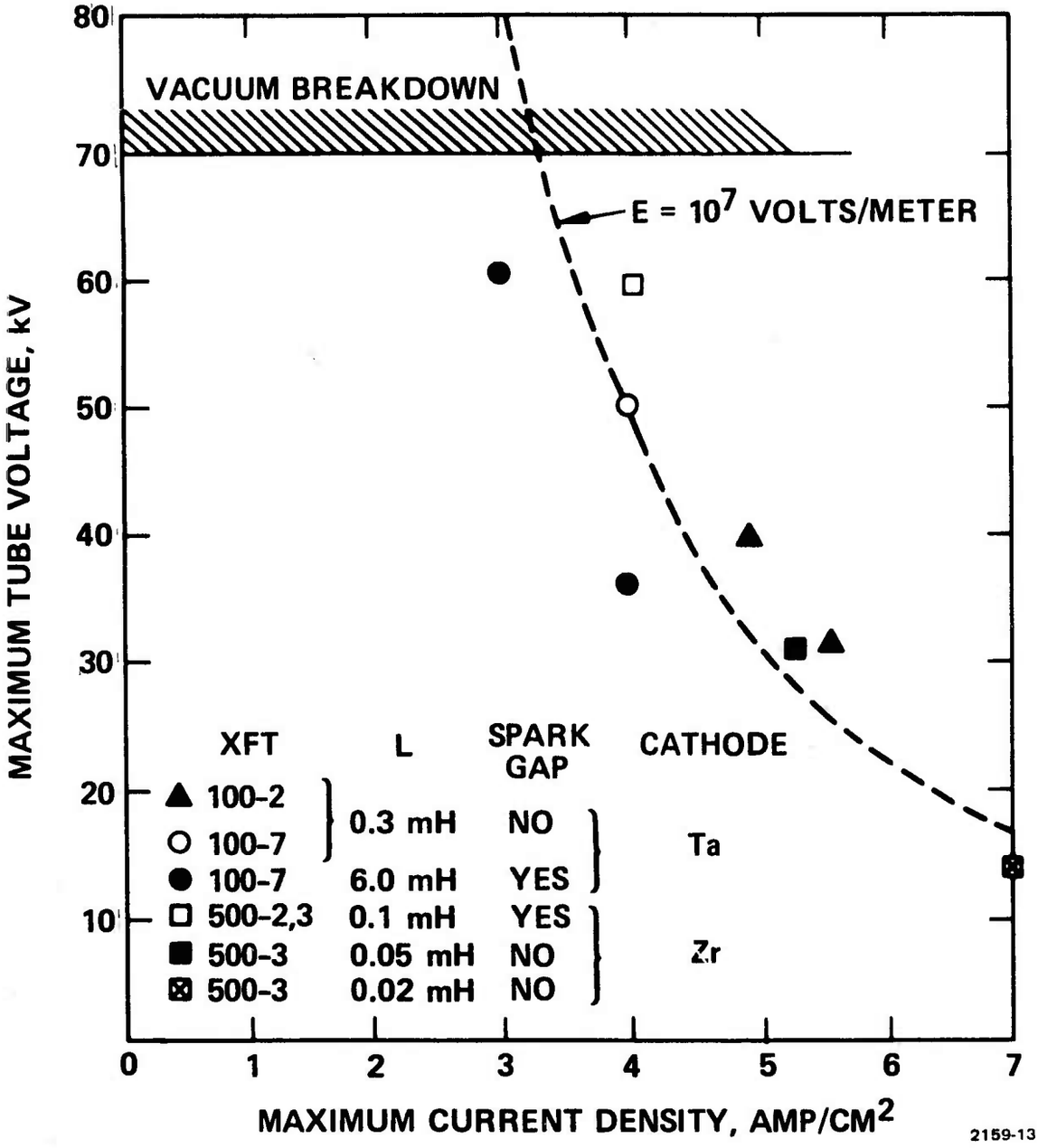

Fig. 36. Maximum Reliable Value of Current and Voltage for Several Interrupter Tubes.

after each good shot, will affect the outcome of the next shot. It is not known if the data shown in Fig. III-8 are entirely representative of all cathode materials, or if surface roughness can be reduced by preconditioning procedures not yet attempted. The spark gap referred to in Fig. III-8 is the parallel gap used to limit the peak voltage. When it is not used, all the inductor energy is dissipated in the tube.

A power conditioning circuit has been constructed (separate from this contract effort) for the purpose of running a 100 cm^2 tube at high rep rate (~5 Hz). The circuit diagram is shown in Fig. III-9, and a photograph of the portable unit in Fig. III-10. The triggered vacuum gap (TVG) is used to allow current to rise in the inductor and to simulate a bypass switch. After about 2 msec, the current has reached a maximum of 500 A and the tube (XFT) is turned on. The 50 μf capacitor discharges through the XFT and applies a reverse voltage on the TVG. This temporarily quenches the current flowing through the TVG and transfers it to the 50 μf capacitor and XFT. After about 50 to 60 μs, the TVG is deionized and the XFT is turned off. The voltage rises and the spark gap transfers the current to the load, in this case a 100 Ω resistor. Since the inductor was chosen to store about 750 J, the decay time of the current is long compared with the time required for the voltage to reach 50 kV. Simultaneous traces of the current and voltage are shown in Fig. III-11. Figure III-12 shows operation of a tube at approximately 5 Hz. The solid circles on Fig. III-8 represent operating points at this repetition rate.

2. <u>500 cm^2 Tube</u>

Figure III-13 is a line drawing of the 500 cm^2 tube now in operation at over 2000 A and 50 to 60 kV. A photograph of this tube (XFT-500-3) is shown in Fig. III-14. The cathode material is zirconium. The other principal differences between it and the 100 cm^2 tubes, besides the area, are the small ionizer electrode and the internal magnetic field coil. The design of the internal field coil appears to have been a failure. The most likely cause was field errors near the feed-ins to the single

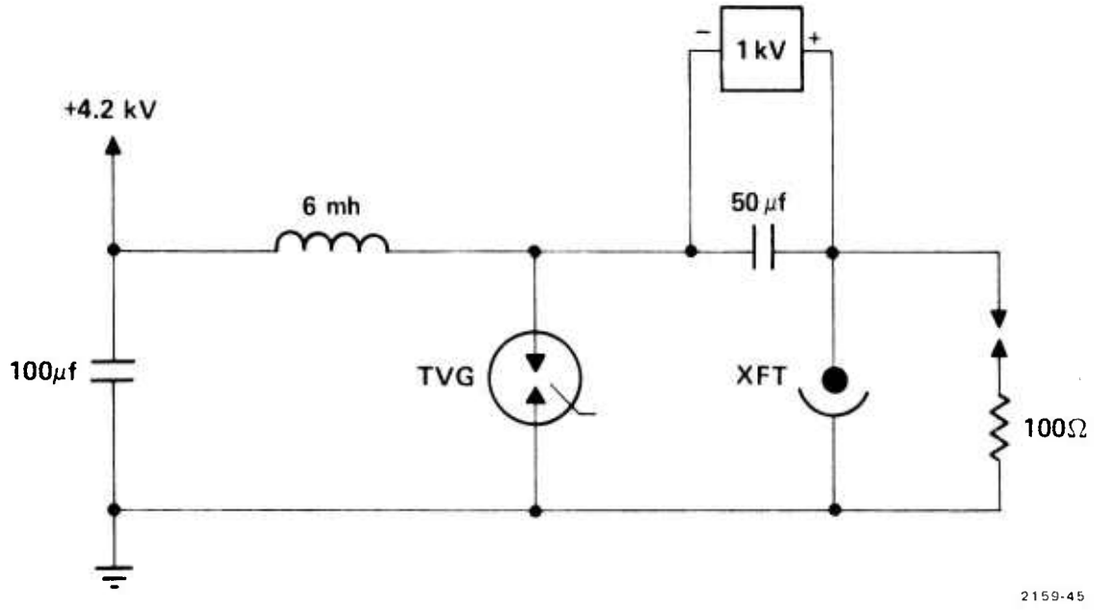

Fig. 37. Power Conditioning Circuit.

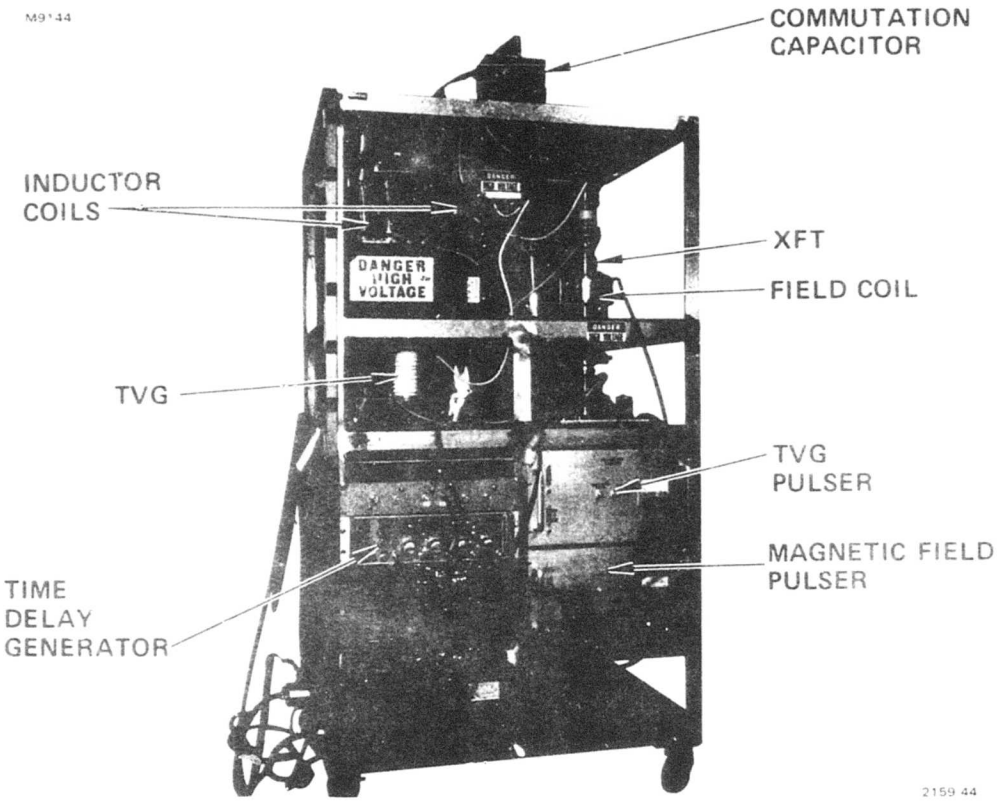

Fig. 38. Power Conditioning Unit.

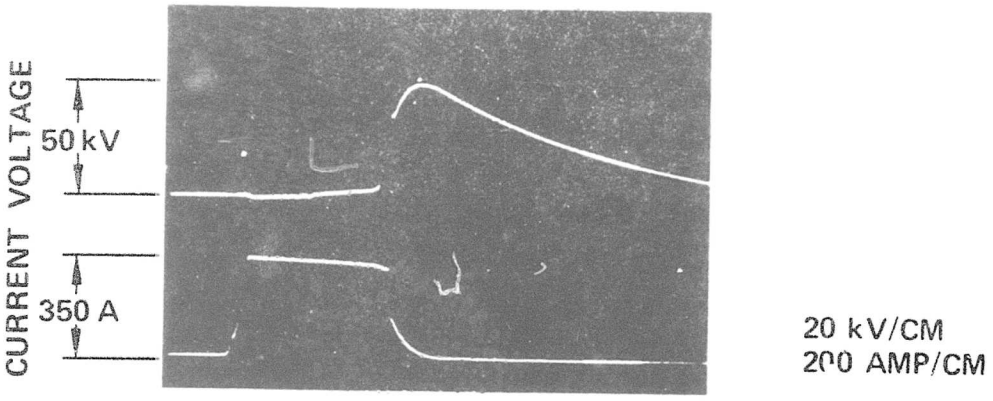

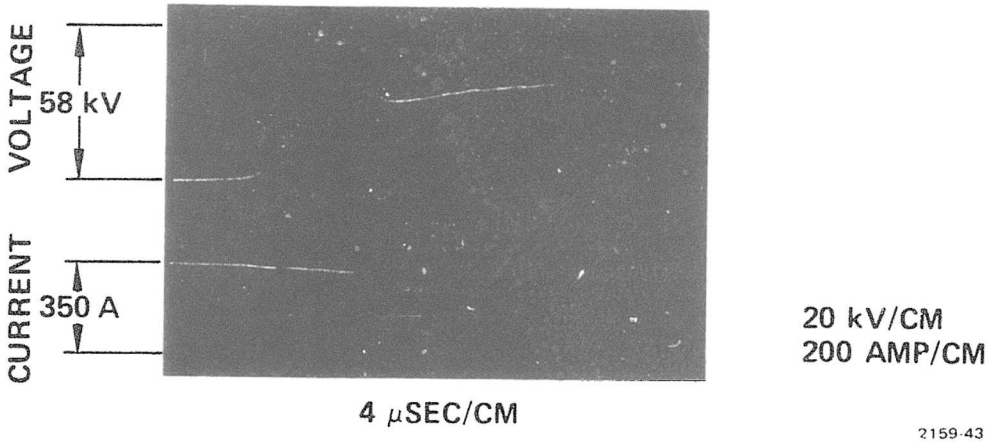

Fig. 39. Current-Voltage Waveforms for 100 cm^2 Interrupter Tube.

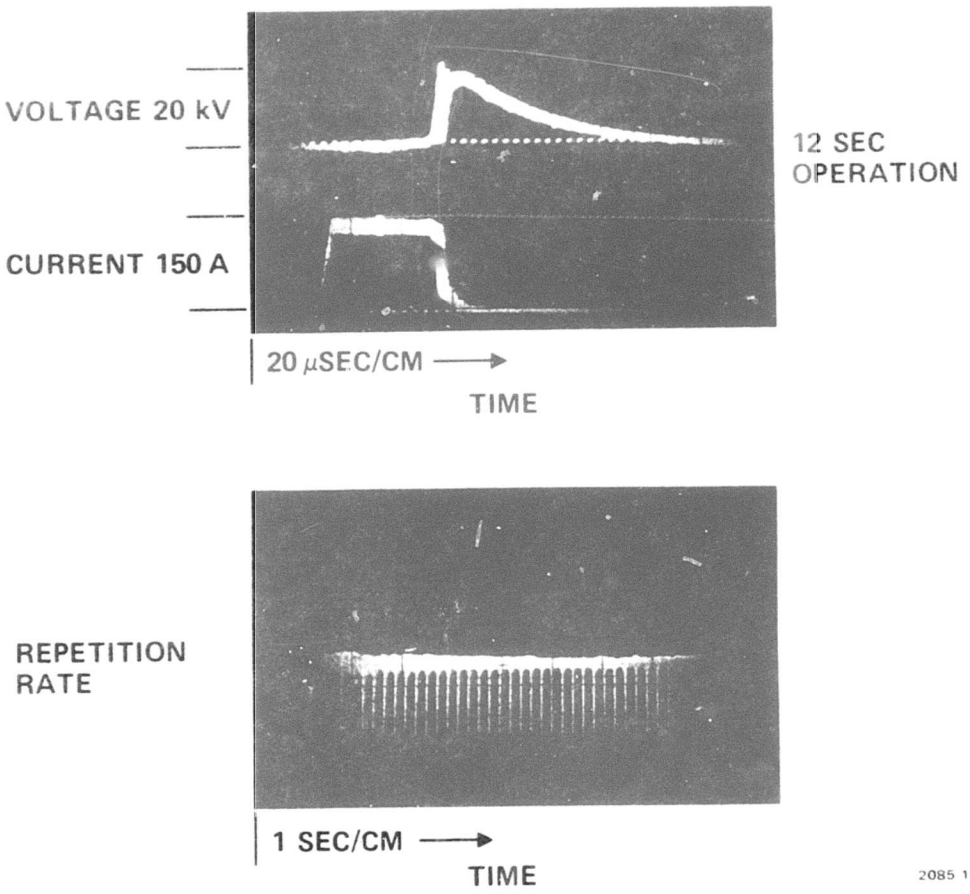

Fig. 40. 5 Hz Operation of 100 cm^2 Interrupter Tube.

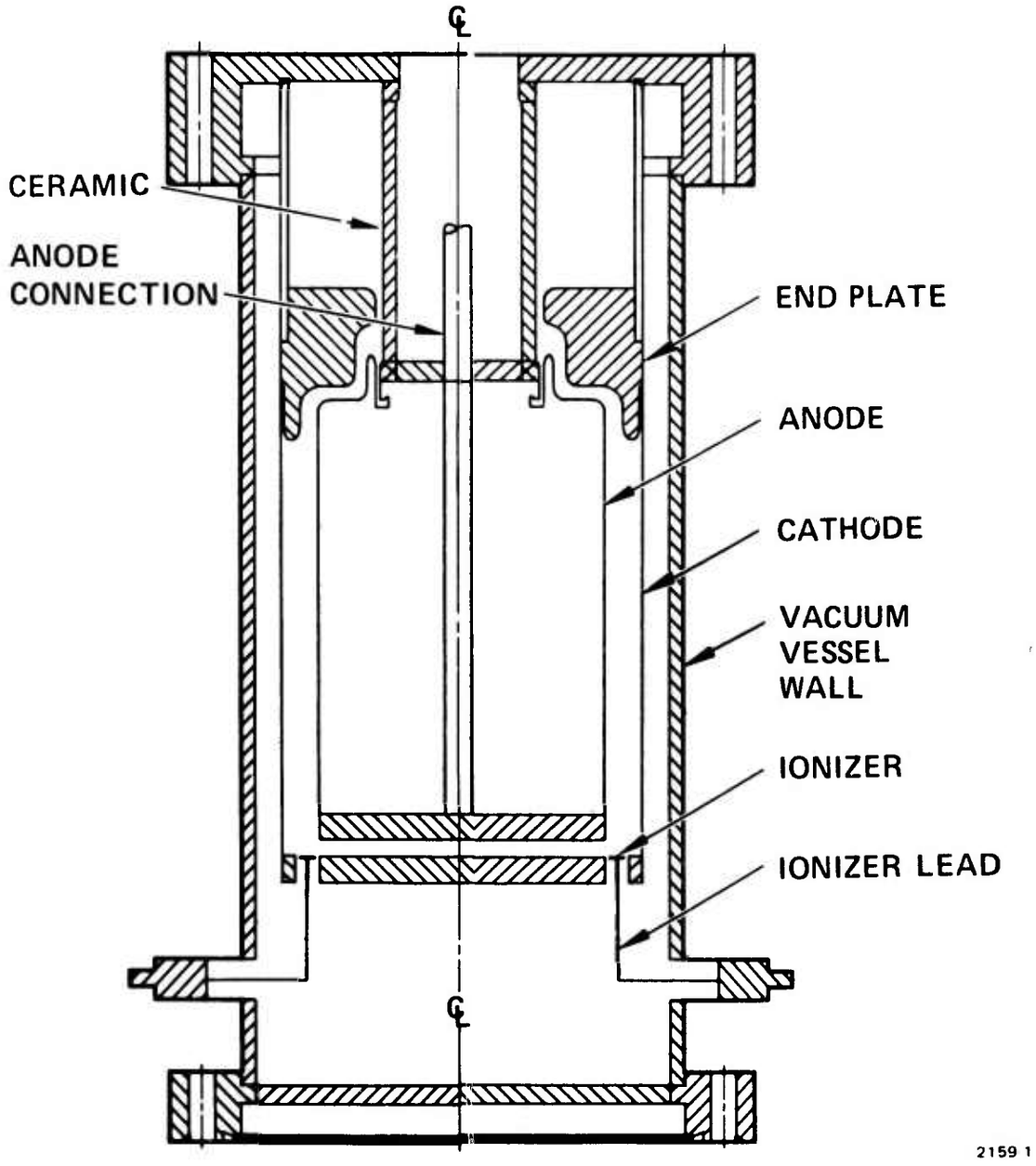

Fig. 41. 500 cm^2 Interrupter Tube.

Fig. 42
500 cm^2 Interrupter Tube
with Feedthrough Bushing.

turn coil, resulting in excessive plasma loss. Rather than driving the coil at the necessary 10,000 A we resorted to an external field coil. This limited control over the internal field strength because of eddy currents in the stainless steel vacuum envelope. However, the performance of both of the 500 cm^2 tubes actually tested was wholly satisfactory. The conditioning times were comparable to the 100 cm^2 tubes even though the 500 cm^2 tubes were not baked out. The slight improvement in maximum performance level over the 100 cm^2 tubes may be geometric in origin, but the use of zirconium as a cathode material instead of tantalum may also have a bearing. Typical turn-off traces with and without parallel spark gaps are shown in Figs. III-15 and III-16.

B. Detailed Design

Having covered the present status of high current density, high recovery rate interrupter tubes, we now turn to the detailed design of an interrupter suitable for operation at the following ratings:

100 kV	peak voltage
20 kA	peak current
100 μsec	conduction time
5 Hz	PRF

The design of this interrupter is based on the extensive experience in high power interrupter tube design gained during the course of the High Voltage Systems Program at Hughes. A simplified line drawing showing the principal tube parts is shown in Fig. III-17.

The tube basically consists of two coaxial, cylindrical electrodes with a 1 cm spacing. Both electrodes are liquid cooled and insulated from one another for 100 kV. The active cathode surface area (adjacent to the magnetic field coil) is 2000 cm^2 which, at 5 A/cm^2, gives 10 kA current carrying capacity. Extension of the current density to 10 A/cm^2 at the same high recovery rate or use of a larger field coil to utilize the entire cathode surface area should allow for 20 kA operation. The tube

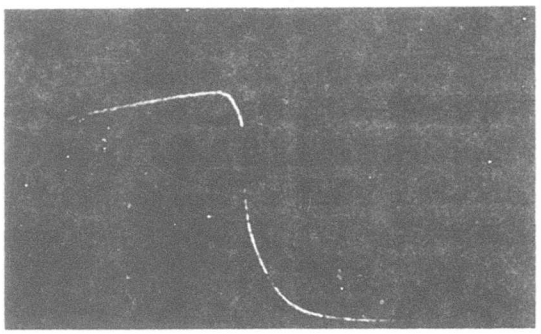

TUBE CURRENT

500 A/CM

5μSEC/CM

2159-40

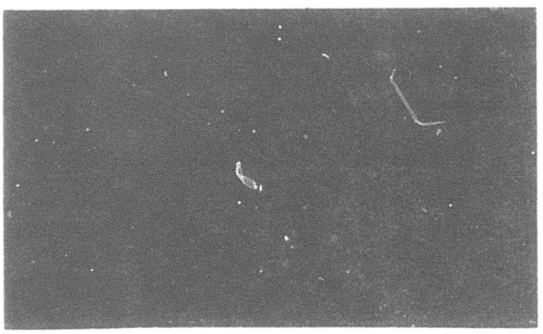

TUBE VOLTAGE

20 kV/CM

5μSEC/CM

2159-41

Fig. 43. Interruption Waveforms with Spark Gap for XFT-500-2.

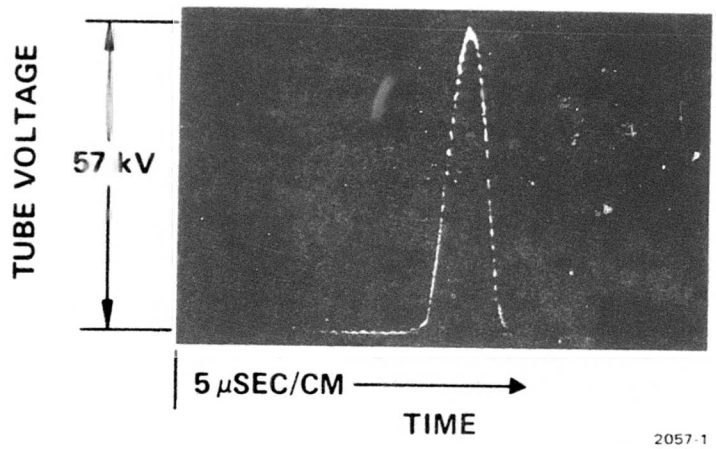

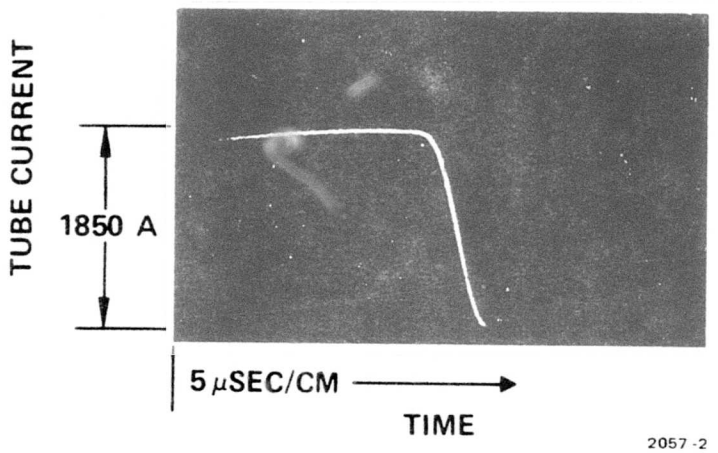

Fig. 44. Interruption Waveforms Without Spark Gap for XFT-500-2.

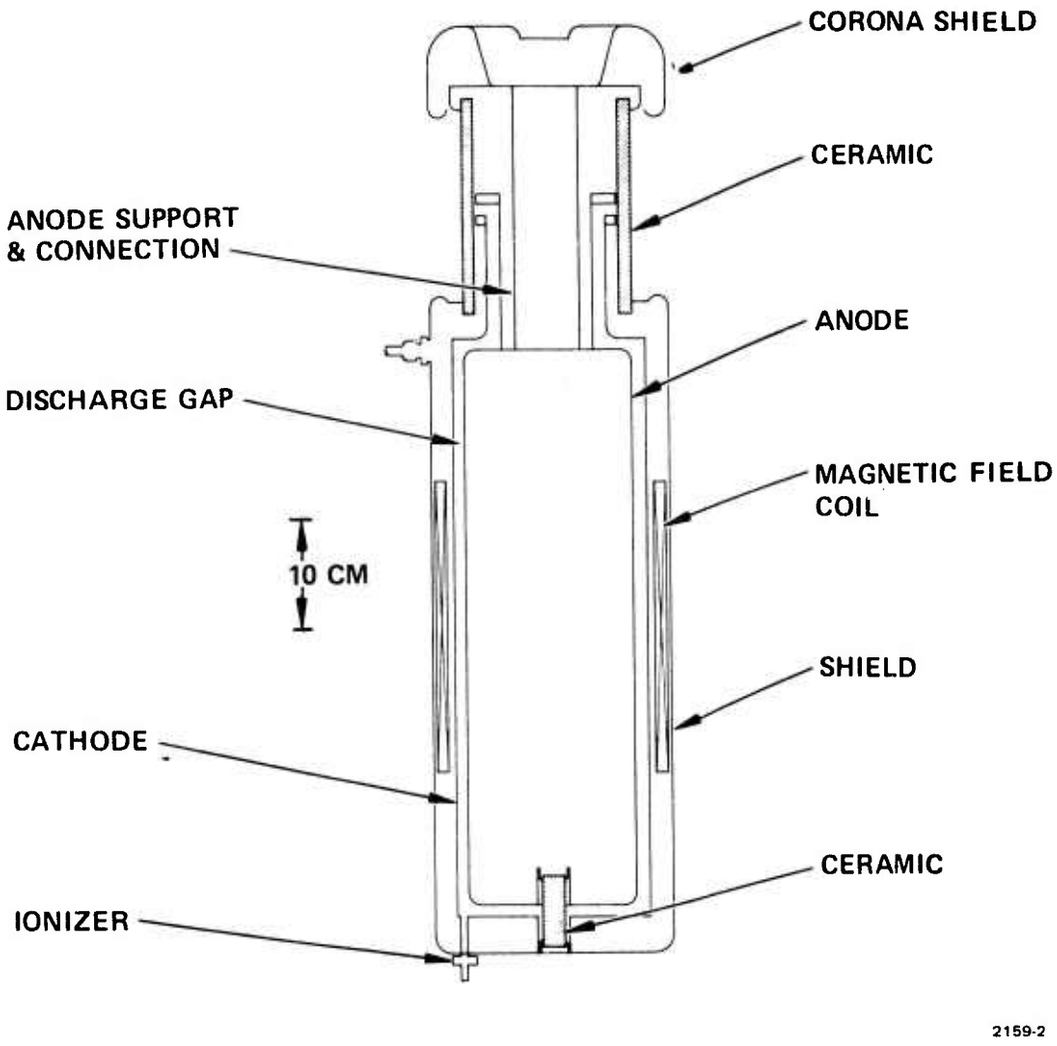

Fig. 45. 100 kV, 20 kA Interrupter Tube.

is fitted with a gas pressure controller and an ionizer to provide microsecond ignition. The choice of gas, materials and liquid flowrate, life, and the design of the magnetic field coil and pulser have all been determined and are treated in detail below.

1. Gas and Materials

The best choice of gas has been found to be helium because it produces minimal sputter deposits and thereby increases tube life. In addition, it does not chemically combine with sputtered material and therefore has a low clean-up rate. Finally, it has one of the best Paschen curves of any gas, allowing for the highest possible pressure (and hence lowest conduction voltage) consistent with high voltage holdoff.

The optimum material for the electrodes is an inclusion-free, refractory metal such as tantalum or tungsten. The absence of insulating inclusions is known to inhibit arc formation, as is the high melting point. These heavy metals are also sputter resistant because of the large disparity in the mass between tantalum or tungsten and helium.

Those parts of the tube not in contact with the plasma discharge can be made of stainless steel, high alumina ceramics and other materials compatible with high power, metal-ceramic tubes.

2. Liquid Flowrate

Dissipation occurs in an interrupter tube both during conduction and interruption. The conduction dissipation can be calculated from

$$P_c = I_o V \nu \tau_c$$

where

ν = PRF
I_o = current
V = discharge voltage
τ_c = conduction time

Using ν = 5 Hz, I_o = 20 kA, V = 500 V, and τ_c = 100 μsec, we get P_c = 5 kW.

The interruption dissipation can be computed from

$$P_I = V_o I_o \tau_I \nu$$

where

V_o = peak voltage

τ_I = voltage rise time or current fall time

The above equation assumes a linear voltage rise to V_o in time τ_I followed by a linear current fall to zero also in a time τ_I. Using V_o = 100 kV and τ_I = 5 μsec (typical), we get P_I = 50 kW (also at 5 Hz). Thus, we can neglect the conduction dissipation relative to the interruption dissipation and simply set the cooling requirement to approximately 50 kW.

To be well within the state of the art of cw liquid cooling techniques, the dissipated power density should not exceed 100 W/cm^2. Using both electrodes, we have 4000 cm^2 available to dissipate 50 kW, giving a cooling density of 12.5 W/cm^2, which is a very conservative requirement. To be consistent with the present system concept of 1 min on, 10 min off, however, we only need to remove heat at 10% of the rate it is deposited, namely 5 kW. Using glycol and allowing a 50°C rise between inlet and outlet, less than 0.5 gpm is required. This is easily achieved.

3. Life

End of life occurs when the build-up of sputter deposits on the anode begin to flake off. The charge density conducted by the tube when this point is reached can be calculated from

$$\sigma = \frac{tNe}{t_m S} \qquad C/cm^2$$

where

t = thickness of film when flaking begins

N = number of atoms/monolayer

e = electronic charge

t_m = thickness of monolayer

S = sputter yield (atoms sputtered per incident ion)

For a helium tantalum combination,

$t = 2.5 \times 10^{-4}$ cm (pessimistic value)

$N = 10^{15}/cm^2$

$t_m = 2 \times 10^{-8}$ cm

$S = 10^{-2}$

Thus, $\sigma = 2.5 \times 10^2 C/cm^2$. At 10 A/cm^2 for 100 μsec/shot, this gives a life of 250,000 shots.

4. Gas Pressure Control

During operation, helium is gradually lost by sputter burial. This gas must be replenished in order to keep the gas pressure within a predetermined range (typically 30 to 80 mTorr). This is accomplished by a gas refill system, the block diagram of which is shown in Fig. III-18. Operation is as follows: A thermocouple gauge tube reads the tube pressure continuously. When the pressure falls below a set value, the valve is opened and gas flows into the tube at a controlled rate. (Either a high flow impedance or a metering volume and second valve is used to avoid overfilling.) When the tube pressure has reached the upper set point, the valve is closed. Tube operation can continue during the refill process.

The gauge controller occupies 1 ft^3, weighs 25 lb and requires approximately 25 W of auxiliary power. The size and weight of the valve, gas reservoir, and gauge tube is negligible.

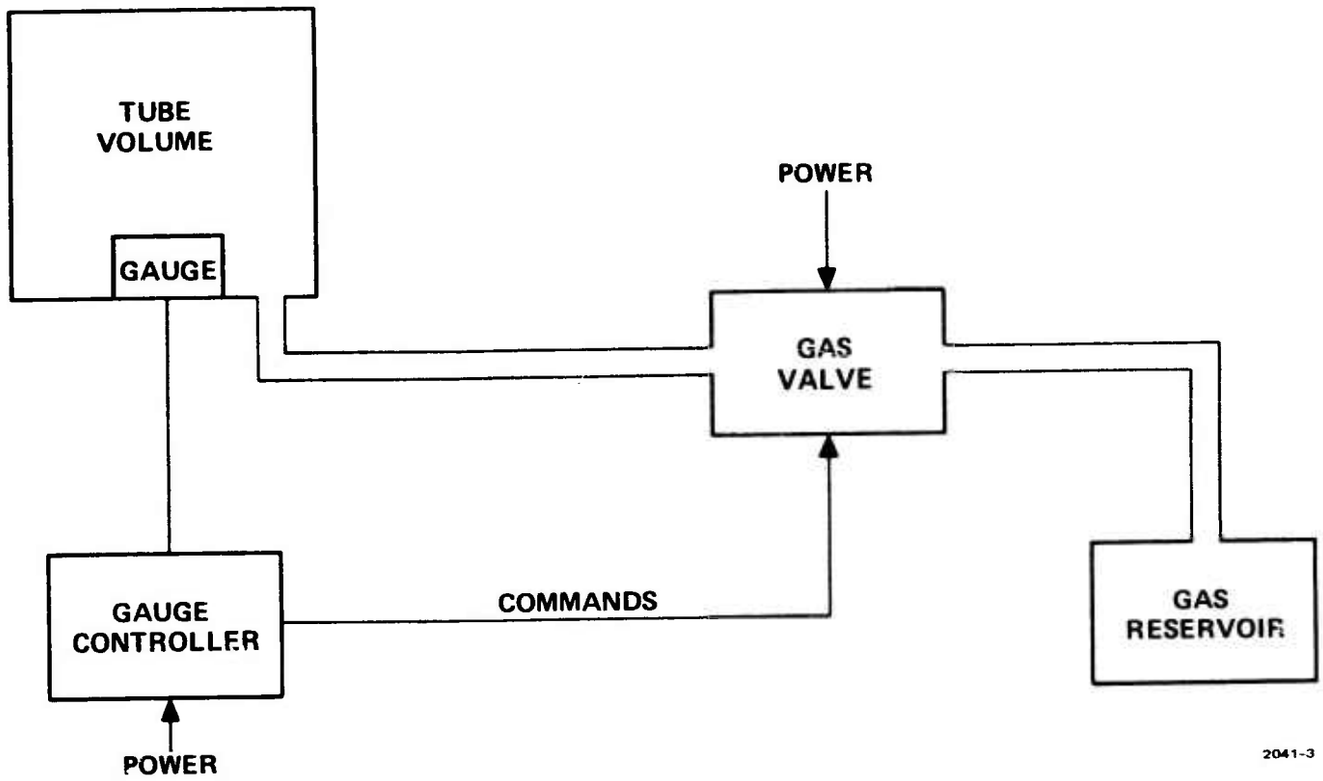

Fig. 46. Pressure Controller Block Diagram.

5. Ionizer

A source of electrons is necessary to assure ignition with minimum jitter (~1 μsec). This source is a field emitting point which directs a beam of electrons into the interelectrode space from the base of the tube. A detailed drawing of the ionizer and feedthrough bushing is shown in Fig. III-19.

Experiments with an ionizer of similar design have shown that satisfactory ignition occurs when the emitter is biased 5 to 10 kV negative with respect to the cathode (ground) and a current ~μA flows. This gives the ionizer and auxiliary power requirement of 1 W. The ionizer power supply will occupy a volume of 0.1 ft^3 and weight 10 lb.

6. Magnetic Field Coil and Pulser

The coil shown in Fig. III-17 has an inductance of 250 μH, 50 turns, and requires 100 A to generate a 100 G field inside the interelectrode space. Using a simple LC circuit to provide a 200 μsec half period with a 200 A current peak, we will have 134 μsec during which the current exceeds 100 A (and the field exceeds 100 G). Only 5 J are stored in the field, requiring a 17 μF capacitor charged to 770 V. The circuit and field waveform is shown in Fig. III-20. The tube T is a conventional hydrogen thyratron such as the 5C22.

The pulser of Fig. III-20 will require approximately 100 W of power, including filament and grid drive power. The pulser will require about 0.5 ft^3 of volume and weigh about 25 lb.

7. Design Drawing

A detailed design drawing of the proposed interrupter tube for this application is shown in Fig. III-21. Some of the essential design points are described below.

Anode cooling is introduced and discharged via pipes running the length of the feedthrough bushing. The anode and cathode both have liquid cooling jackets with flow diverters to ensure proper fluid motion and eliminate the possibility of hot spots. The anode cooling lines will

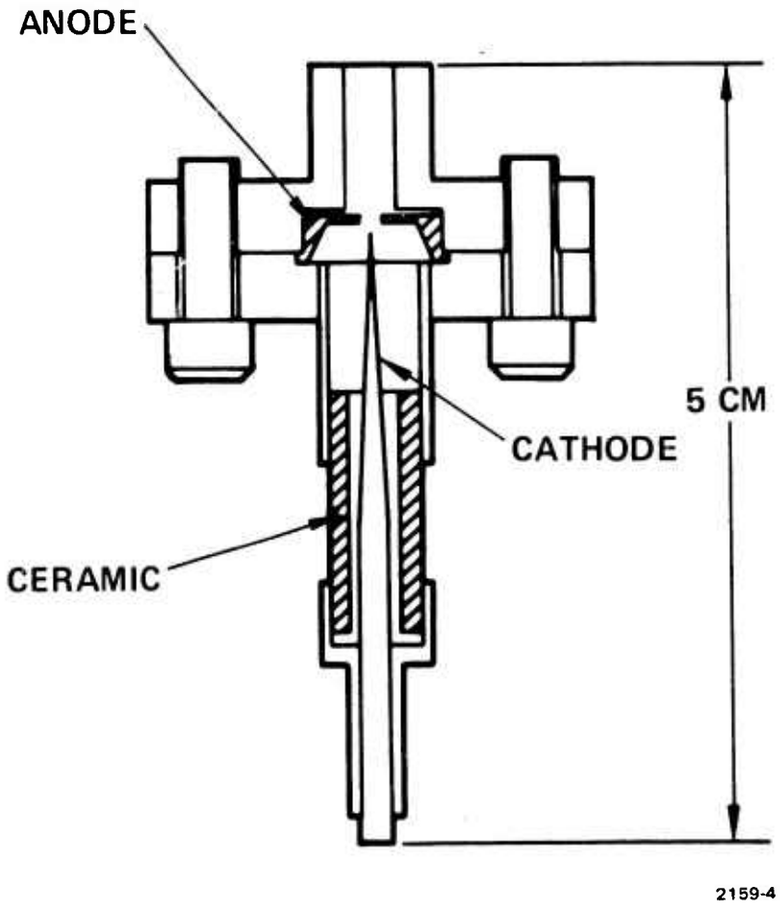

Fig. 47. Ionizer and Feedthrough Bushing.

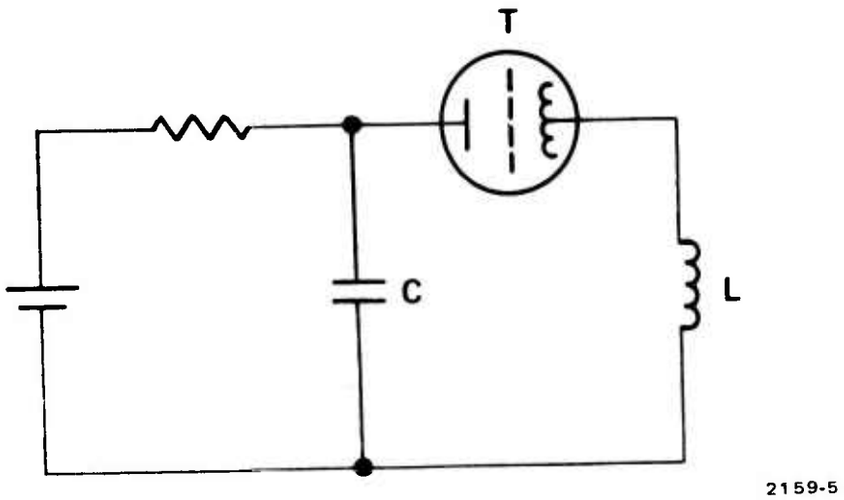

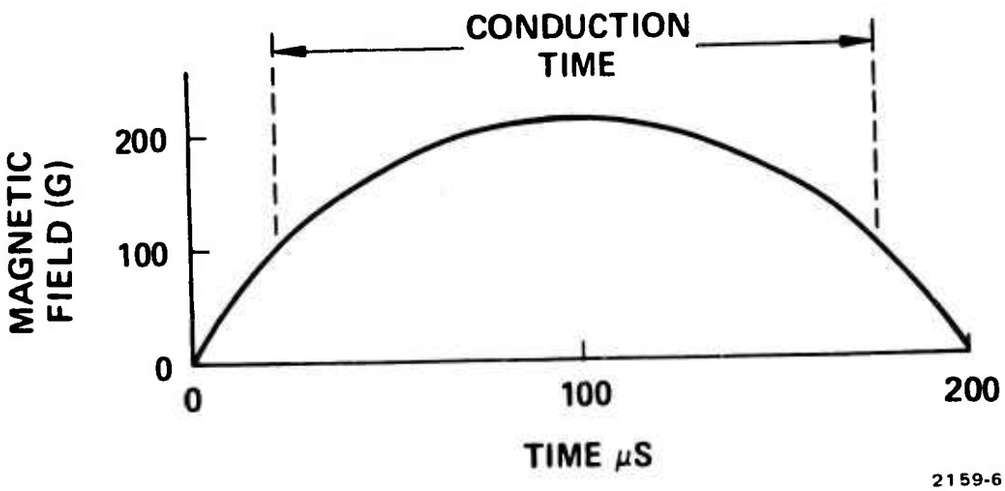

Fig. 48. Magnetic Field Pulser-Circuit and Field Waveform.

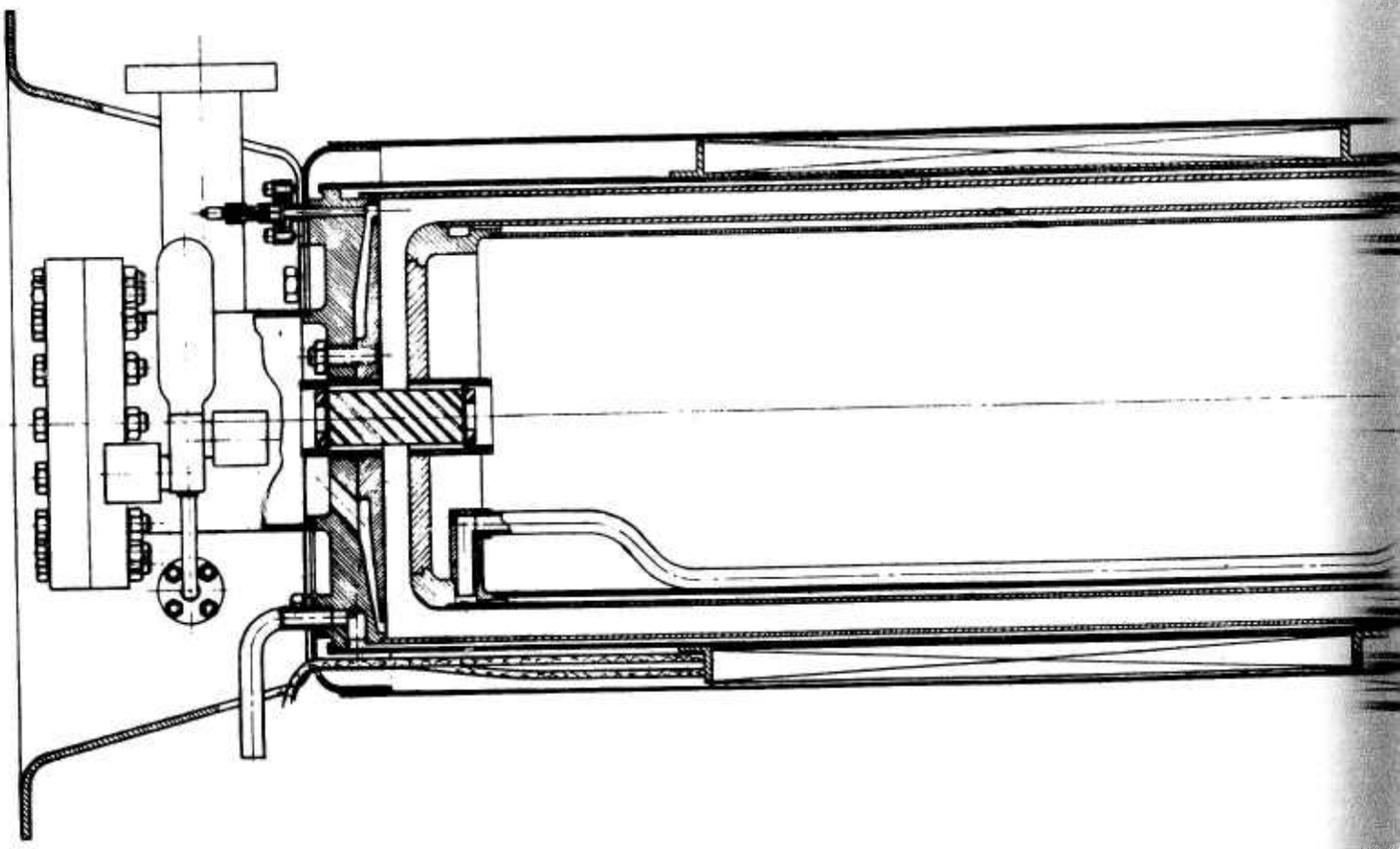

Fig. 49. 100 kV, 20 kA Interru

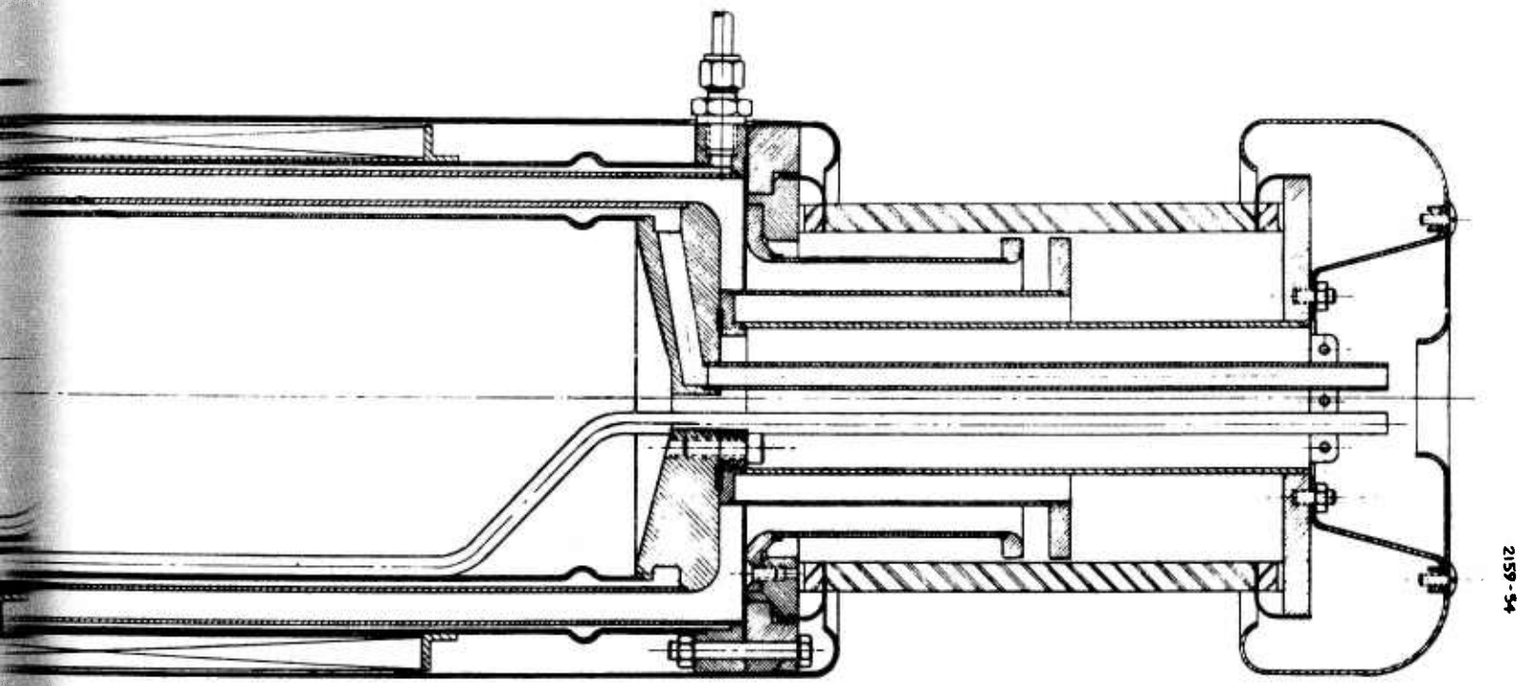

100 kV, 20 kA Interrupter Tube.

connect to the heat exchanger by Tygon tubing capable of withstanding 100 kV between tube and heat exchanger. The cathode cooling jacket may be slit vertically to minimize the flow of eddy currents when the field coil is switched off.

This tube is designed to operate completely sealed after processing. For that reason it has been supplied with a pressure gauge and a gas refill system. The 1/4 l gas reservoir with two adjacent metering valves is shown at the base of the tube in Fig. III-21. The pump out port is shown at the base. The tube will be permanently tipped off at this point or valved off with a bakeable valve. The ionizer can also be seen at the bottom of the tube, parallel with the interelectrode gap. The field coil is contained in a shield to limit the propagation of stray fields away from the tube. Current leads to the coil enter the shield at the bottom. A special support insulator for the anode has been added at the anode base to provide better stability of the relatively long anode cylinder.

Figure III-22 is a view up from under the tube. The thermocouple gauge tube and leads can be seen as well as the gas refill system. An overall weight estimate of the tube is 202 lb and the volume is 1.5 ft^3.

C. Specifications

In this section, the data presented in Section III-B above is brought together and placed in tabular form for easy reference (Table III-1). Also included is an estimate of the range of operating parameters.

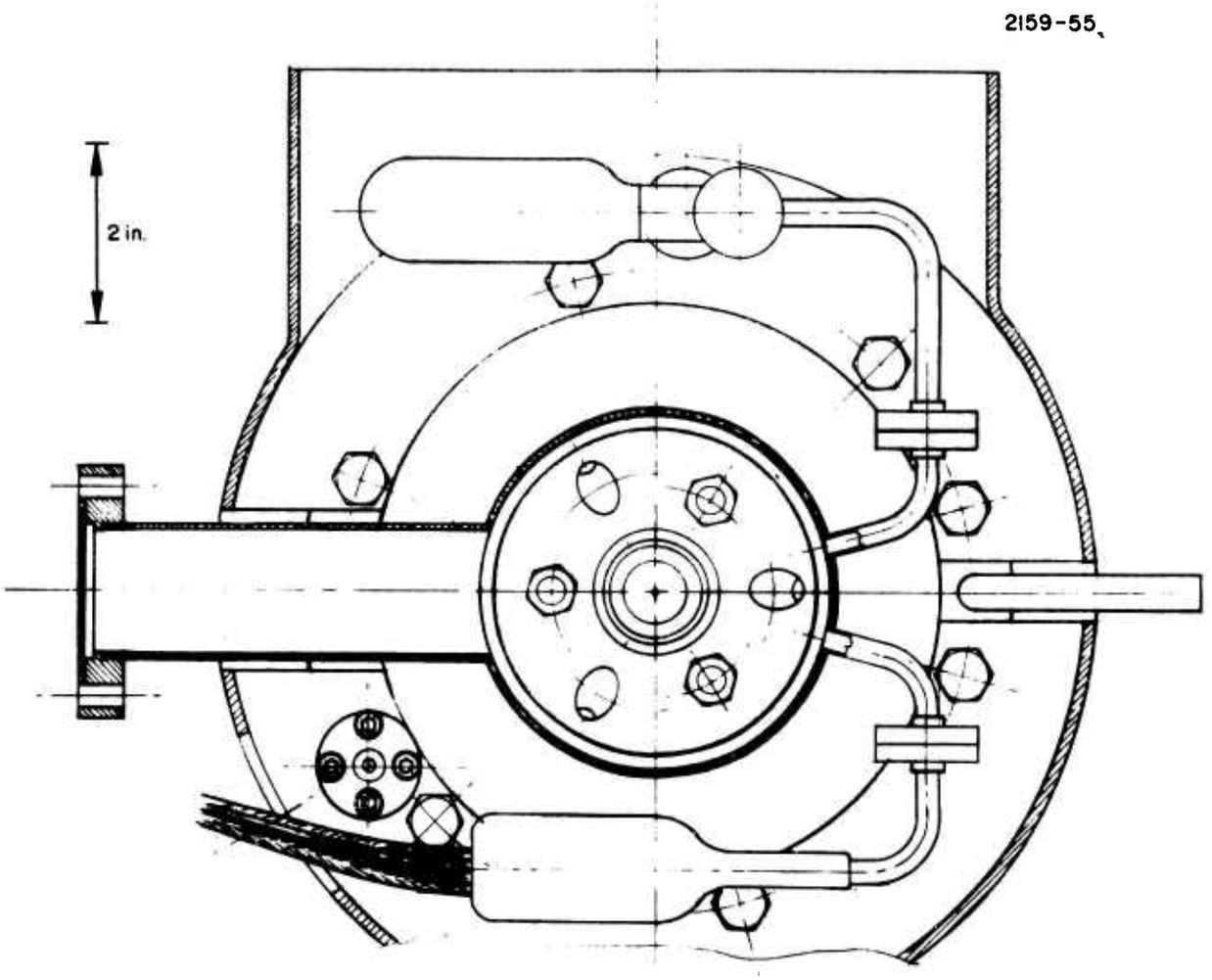

Fig. 50. View of 100 kV, 20 kA Interrupter Tube Looking up from Base.

TABLE III-1

Interrupter Specifications

Item	Minimum	Maximum	Nominal	Comment
Voltage	1 kV	100 kV	100 kV	
Current	1 A	20 kA	20 kA	
Conduction time	10 μsec	200 μsec	100 μsec	
Dissipation per shot	5 kJ	15 kJ	10 kJ	100 kV, 20 kA
Repetition rate	none	50 Hz	5 Hz	Maximum based on CES versus IES tradeoff
Continuous operating time	none	1 min	1 min	5 Hz, 100 kV, 20 kA
Life	10^5 shots	5×10^5 shots	2.5×10^5 shots	10 A/cm^2, 100 μsec
Coolant flowrate	0.25 gpm	1.0 gpm	0.5 gpm	1 min on at 5 Hz, 20 kA, 10 min cooldown
Weight	150 lb	250 lb	202 lb	Without auxiliaries
Volume	1.5 ft^3	2.0 ft^3	1.5 ft^3	Without auxiliaries
Auxiliaries – weight			60 lb	Pressure controller, ionizer, and magnetic field pulser at 5 Hz.
– volume			1.6 ft^3	
– power			126 W	

IV. SWITCH SYSTEM

The complete switch system consists of four major components:

- Bypass switch
- Interrupter tube
- Heat exchanger
- Control and auxiliary power unit

In this section, we treat the heat exchanger and the control and auxiliary power unit, in order to determine their size, weight, and auxiliary power requirements. The section concludes with an overall view of the complete switch system, including the physical configuration and operating specifications.

In Section II-G, the auxiliaries of the bypass switch were listed, along with sizes and weights. The two auxiliaries were (1) mechanical switch and gas valve pulser and (2) recloser trigger pulser. In Section III-C, the auxiliaries of the interrupter tube were also listed. These were (1) magnetic field pulser, (2) ionizer and (3) gas pressure controller. These auxiliaries were summed up so that the complete size, weight, and auxiliary power requirements for each of the two main switch components, bypass and interrupter could be determined. In this section, we consider that these auxiliaries are located in an auxiliary unit physically away from the two switch components. Thus, the control and auxiliary power unit will house the following items:

- Mechanical switch coil and gas valve pulser
- Recloser trigger pulser
- Tube pressure controller
- Tube ionizer supply
- Tube magnetic field pulser

The overall system will then consist of four separate components: tube, bypass switch (both without auxiliaries), heat exchanger and the control and auxiliary power unit.

A. Heat Exchanger

The dissipation of the switch system when operating at 20 kA and a PRF of 5 Hz is:

Interrupter Tube	50 kW	
Mechanical Switch	35 kW	(includes 5 kW motor and gas valve dissipation)
Recloser	3 kW	
	88 kW	

With one minute of continuous operation and ten minutes off, cooling at the rate of 8.8 kW average is required. Circulating coolant during the off period will be the primary source of cooling. Thermal inertia of the components of the switch system will be utilized as the primary means of limiting temperature rise during operation. A conventional liquid-to-air heat exchanger of the required capacity occupies a volume of 2 cubic feet, weighs 200 lb and has a power consumption of 1 kW to operate the coolant pump and an air fan.

High voltage isolation where required along the coolant path, such as between the anode of the tube and the grounded heat exchanger, can be provided by passing the dielectric fluid through a section of insulating tubing approximately three feet in length.

B. Controls and Auxiliary Power Unit

A single interruption of an IES circuit requires the following things to happen:

- Mechanical switch coil and gas valve energizes
- Interrupter tube magnetic field energizes

- Recloser fires
- Mechanical switch coil refires to damp contact closure

These four things happen in sequence. Starting with the activation of the mechanical switch coil at time zero, a four channel time delay generator is necessary. Channel 1 delays the firing of the interrupter tube for 900 μsec from time zero, allowing the mechanical switch to open fully. Channel 2 delays firing of the recloser for an additional 350 μsec, shorting the load and saving the energy remaining in the storage inductor. Channel 3 pulses the mechanical switch coil after an additional 750 μsec, and channel 4 restarts the entire sequence after an additional 198 msec. This time delay sequencer is of conventional design, requires negligible auxiliary power and contributes little size and weight. The sequencer will be provided with low impedance outputs, suitable for directly driving SCR's which, in turn, will drive the gates of the closing switches for the three pulsers for the mechanical switch coil and gas valve, interrupter tube magnetic field, and recloser.

Table IV-1 lists the various components that make up the controls. Included is the interrupter tube pressure controller. It can be seen from the table that the controls occupy 7.3 ft^3, weigh 335 lb, and require an auxiliary power of 5.8 kW.

The auxiliary power unit (APU) is physically part of the control center. Reference to Fig. IV-1 shows the power distribution and control layout. The APU supplies continuous power to the controls, the heat exchanger and the interrupter tube icnizer. The controls, in turn, supply pulse power to the bypass switch and interrupter. The APU contains only a 1 W power supply for the ionizer which requires only 0.1 ft^3 and 10 lb. The APU also serves as a distribution center for the 6.8 kW of power required by the controls (5.8 kW), heat exchanger (1 kW) and ionizer (1 W). Assuming negligible APU power losses, a reasonable size and weight would be 1 ft^3 and 25 lb. Thus, the total size and weight of the combined controls and APU console is 8.3 ft^3 and 360 lb. A total of 6.8 kW of auxiliary aircraft power is required.

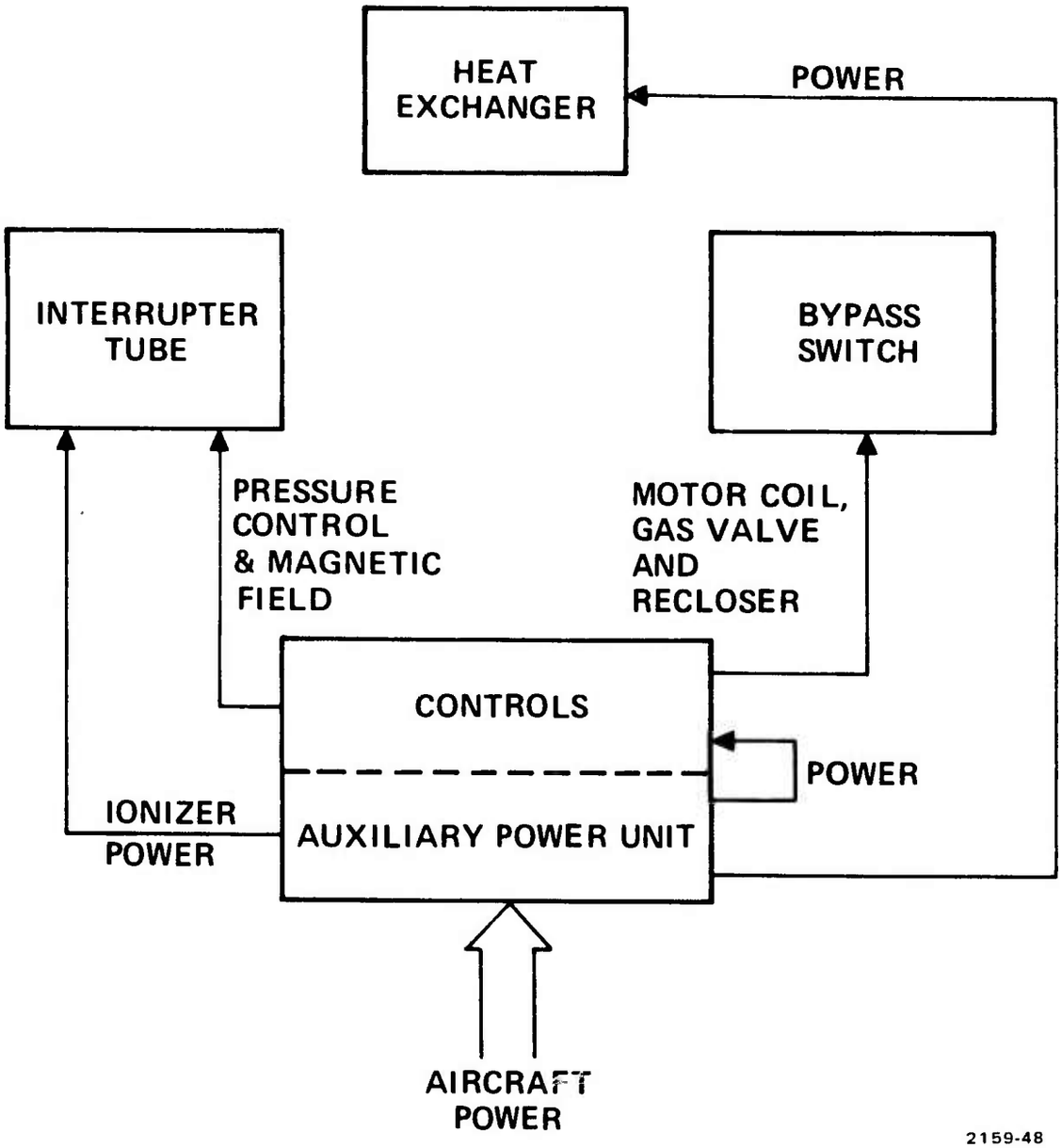

Fig. 51. Power Distribution and Control System.

TABLE IV-1

Controls

Item	Size, ft^3	Weight, lb	Required Power, kw
Sequencer	0.5	25	0.1
Mechanical switch coil and gas valve pulser	5.0	250	5.5
Interrupter tube magnetic field pulser	0.5	25	0.1
Recloser pulser	0.25	10	0.1
Interrupter tube gauge controller	1.0	25	0.025
	7.3	335	5.8

C. Switch Configuration and Specification

The four components making up the complete switch are the bypass switch, the interrupter tube, the heat exchanger and the control and auxiliary power unit. The size, weight, and auxiliary power requirements of each of these components are listed in Table IV-2. Figure IV-2 is an artists conception of one possible layout of these four components. (The packing density can be considerably greater than shown).

Table IV-3 contains a set of specifications for the complete switch system. This table is derived from the bypass switch and inter interrupter tube specifications listed in Sections II-G and III-C, respectively. When one component had a range of operating parameters

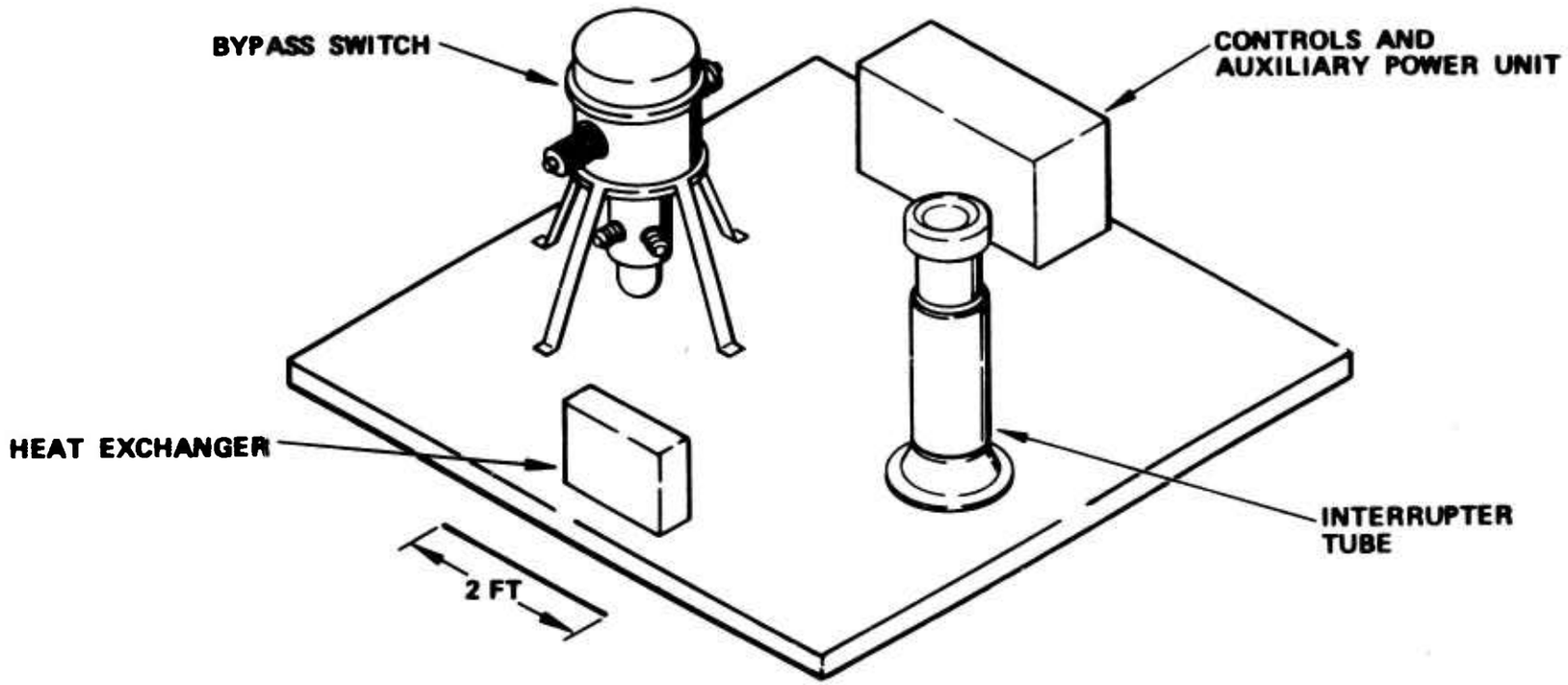

Fig. 52. Artists Sketch of Hughes Switch System.

different from another component, the narrowest range was chosen. The principal result is that the complete Hughes IES switch system will weigh about 1000 lb, occupy about 40 ft^3, and require about 7 kW of auxiliary power.

TABLE IV-2

Size, Weight, and Auxiliary Power Requirements of Four Primary Switch Components

	Size, ft^3	Weight, lb	Power, kw
Bypass Switch	28.5	285	-0-
Interrupter Tube	1.5	202	-0-
Heat Exchanger	2.0	200	1.0
Controls and Auxiliary Power Unit			
Controls	7.3	335	5.8
Auxiliary power unit	1.0	25	-0-
Ionizer (located in APU)	0.1	10	nil
	40.35	1057	6.8

TABLE IV-3

Switch Specifications

Item	Minimum	Maximum	Nominal	Comment
Voltage	2 kV	100 kV	100 kV	
Current	100 A	20 kA	20 kA	
Dissipation per shot	9.0 kJ	29.1 kJ	16.5 kJ	Main circuit dissipation at 20 kA, 30% droop, 5 Hz
Repetition rate	none	50 Hz	5 Hz	Maximum based on CES vs IES tradeoff
Continuous operate time	none	1 min	1 min	5 Hz, 20 kA
Life	unk.	unk.	50,000 shots	
Maintenance time	unk.	5 min	2 min	5 Hz, 20 kA
Coolant flowrate	0.5 gpm	2.0 gpm	1.0 gpm	10 min cooldown
Weight - bypass and interrupter complete system	325 lb 395 lb	600 lb 1170 lb	487 lb 1057 lb	
Volume - bypass and interrupter complete system	22 ft^3 32.4 ft^3	37.5 ft^3 47.4 ft^3	30 ft^3 40.4 ft^3	
Auxiliary power			6.8 kW	

V. INDUCTIVE ENERGY STORAGE MODULATOR

The purpose of this section is to carry out an analysis of an IES modulator capable of operating to the following specifications:

100 kV	load voltage
20 kA	peak current
5 Hz	pulse repetition rate
250 μsec	pulse duration

In addition, we have assumed a tolerable current droop of 30%. Once the analysis has been completed and the component values have been determined, we will then evaluate the size and weight of the resulting modulator using the latest available data for the size and weight of the individual components. The switch used in this evaluation will, of course, be the Hughes switch described previously in this report.

A. Analysis

The energy E_o delivered to a constant voltage load V_o by an average current $\bar{I}$ over a time τ is

$$E_o = V_o \bar{I} \tau \tag{1}$$

When an inductance is connected to a constant voltage load, current in the inductor decays at a constant rate from an initial value I_o to a final value fI_o, where $f \leq 1$ and is called the current droop factor. The average current

$$\bar{I} = \frac{(1 + f)}{2} I_o \tag{2}$$

Substituting eq. (2) into eq. (1)

$$E_o = V_o \tau I_o \frac{(1 + f)}{2} \tag{3}$$

The magnitude of the inductance L may now be computed from

$$L = \frac{V_o}{\dot{I}} \tag{4}$$

where

$$\dot{I} = \frac{I_o - fI_o}{\tau} \tag{5}$$

Substituting eq. (5) into eq. (4),

$$L = \frac{V_o \tau}{I_o (1 - f)} \tag{6}$$

The voltage of the prime mover V_{pm} must be

$$V_{pm} = \frac{L I_o}{\tau'} (1 - f) \tag{7}$$

where τ' is the interpulse period. Finally, the energy stored in the storage inductor is

$$E_s = E_o + \frac{1}{2} L (fI_o)^2 \tag{8}$$

where the first term is the energy delivered to the load and the second term is the energy remaining in the inductor at the end of the load pulse. Substituting eq. (3) for E_o, eq. (6) for L, and simplifying, we obtain

$$E_s = \frac{V_o I_o \tau}{2(1 - f)} \tag{9}$$

We are now ready to evaluate these equations for

$$V_o = 10^5 V \qquad (100 \text{ kV})$$

$$I_o = 2 \times 10^4 \qquad (20 \text{ kA})$$

$$\tau = 2.5 \times 10^{-4} \text{ sec} \qquad (250 \ \mu\text{sec})$$

$$f = 0.7 \qquad (30\% \text{ droop})$$

$$\tau' = 2 \times 10^{-1} \text{ sec} \qquad (5 \text{ Hz})$$

The results are

$$E_o = 425 \text{ kJ}$$

$$L = 4.2 \text{ mH}$$

$$V_{pm} = 125 \text{ V}$$

$$E_s = 850 \text{ kJ}$$

The 4.2 mH storage inductor must be capable of withstanding the internal stresses due to the magnetic field and must have sufficient insulation to withstand the 100 kV which is generated. The electrical

generator must deliver a peak power of $V_{pm}I_o$ = 2.5 MW and an average power of 2.13 MW.

B. Modulator Size and Weight

The total size and weight of the complete modulator system determines the ultimate usefulness of inductive energy storage. The basic system configuration is as shown in Fig. V-1. Clearly, for a minimum total system size and weight, both the number of components and their individual sizes must be minimized. Initially there were some doubts that the small size of the inductive storage element could be successfully utilized in a system. These doubts concerned the availability of a suitable low voltage (125) high current (20 kA) power source. However, investigation showed that for this current level, it is technically possible to achieve a lightweight design.

The complete modulator has four essential elements: the fuel, the chemical-to-electrical energy converter, the continuous-to-high peak power converter, and the load. The load determines the pulse power required, but it is not part of this study. The fuel and tankage requirements will be assumed known and fixed. It is noted, however, that fuel consumption is a function of mission duty and could have a bearing on the choice of the chemical-to-electrical power converter. For example, if the mission duty were extensive, then it would be desirable to use a more efficient converter, even if the converter weight was greater in order to minimize the fuel weight. It is expected, however, that the fuel factor will not affect or be affected by the choice between capacitive and inductive storage systems. Thus only the chemical-to-electrical power converter and the continuous-to-peak power converter will be analyzed.

1. Chemical-to-Electrical Power Converter

The natural choice for an efficient converter is a gas turbine-generator set. Sufficient data are available on gas turbines to enable

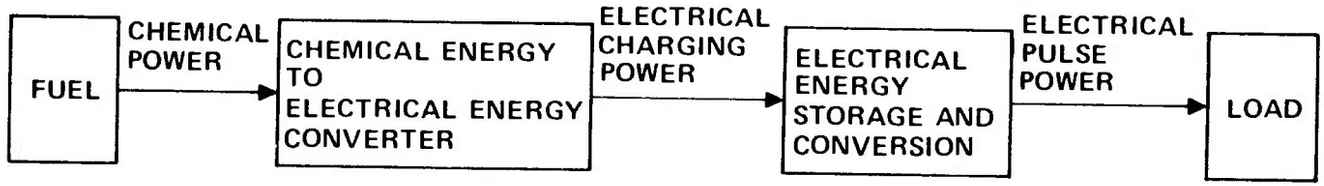

Fig. 53. Fundamental Power Conditioning Block Diagram

2159-7

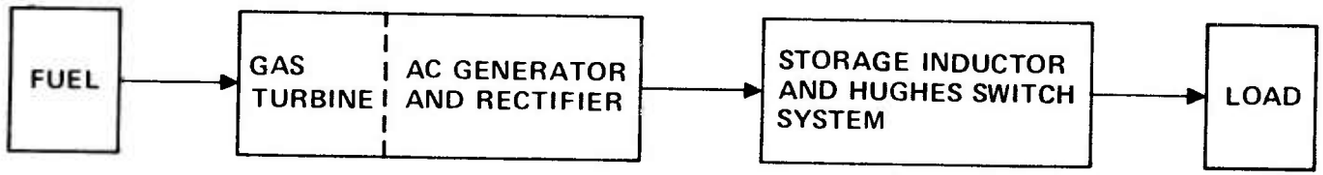

Fig. 54. Inductive Energy Storage Power Conditioning System

a weight and volume estimation to be made. A figure of $10^{-3}ft^3/kW$ and 0.1 lb/kW can be reasonably expected for the specific turbine size and weight. As mentioned above, data on a suitable low voltage high current generator are not available. Initially, it was thought that a homopolar type dc generator would be required. Analysis of this possibility revealed that the weight of such a machine was excessive. Investigators[6] feel that a figure of 1 lb/kW can be achieved but this would still be somewhat high. Inquiries to a manufacturer[7] of rotating aircraft generators, however, revealed that it was possible to build lightweight ac generators with rectifiers for the currents and power levels specified here. The figures given for the specific size and weight for an ac generator and rectifier is $4 \times 10^{-3}f^3/kW$ and 0.5 lb/kW. Combined with the turbine, this results in a specific size of $5 \times 10^{-3}ft^3/kW$ and specific weight of 0.6 lb/kW for the complete chemical to electric power converter. These figures are promising and unlikely to be bettered by a significant factor. Fuel cells and MHD generators can be considered, but for the power levels required, it is not certain that a significant system weight and size decrease would result.

2. Continuous to High Peak Power Converter

a. Inductor – As shown in Section V-A, the inductor must store 850 kJ for a current droop of 30%. This is twice the delivered energy. To determine the specific size and weight it is necessary to first determine the actual size and weight and then divide by the 2.13 MW average power level figure. Initially, the estimates were based on data reported in technical report AFAPL-TR-72-38, Vol. III, on superconducting coils pulsed at 5 Hz for 3000 pulses. These data were based on coil and dewar systems under 100 kJ and were extrapolated to the 850 kJ level. Later it was determined[8] that the extrapolation requires a downward correction because dewar size increases nonlinearly as the energy level is increased. Above the 100 kJ level the correction is quite substantial, and results in a volume

of 100 ft^3 and 1750 lb for a complete inductor and dewar, including enough cryogen (850 lb of LHe) for 3000 pulses. This results in a specific size and weight for our system of 0.05 ft^3/kW and 0.83 lb/kW. For a normal, LN_2 cooled system, these figures are increased by a factor of four.[9]

b. Switch – The Hughes IES switch is the model for calculation of the specific volume and weight for the IES modulator under consideration. From Section IV-C, we obtain the total size and weight of the Hughes switch, namely 40.5 ft^3 and 1057 lb. Dividing by the system power (2.1 MW) and rounding off slightly, we get a switch specific volume of 0.02 ft^3/kW and specific weight of 0.5 lb/kW.

3. Summary

The specific size and weight of the complete IES modulator (excluding fuel and load) is the sum of the specific sizes and weights of the components derived above, namely 0.075 ft^3/kW and 1.93 lb/kW. The total IES modular size and weight is 158 ft^3 and 4050 lb. This information is summarized in Table V-1.

TABLE V-1

Inductive Energy Storage Modulator System For 5 Hz

Average Power	2.13 MW
Pulse Repetition Frequency	5 Hz
Energy delivered per pulse	425 kJ
Energy stored (max)	850 kJ
Number of pulses	3000

Unit	Specific Vol, ft^3/kW	Specific Weight, lb/kW	Total Volume, ft^3	Total Weight, lb
Turbine[a]	1×10^{-3}	0.1	2.1	210
AC generator[b] and rectifier	4×10^{-3}	0.5	8.4	1050
Inductor,[c] cryogen, and dewar	50×10^{-3}	0.83	105.0	1740
Hughes Switch System	20×10^{-3}	0.5	42.0	1050
Total	75×10^{-3}	1.93	157.5	4050

[a]Mr. L. Allen, Communications and Radar Division, Hughes Aircraft Company, Fullerton, Calif. (714)-747-4000.

[b]Mr. E. Brown, Garrett Airesearch Corporation, Torrance, California, (213)-323-9500, ext. 2816.

[c]Mr. E. Lucas, Magnetic Corporation of America, Waltham, Mass. (617)-890-4247.

VI. CAPACITIVE VERSUS INDUCTIVE POWER CONDITIONING

This final major section of the report is devoted to answering three basic questions:

- For the set of specifications listed in the Statement of Work, does IES indeed possess a size and weight advantage over CES?
- Holding the system energy constant at the 2.13 MW level (derived from the Statement of Work), how does increased PRF influence the choice of energy storage system?
- If the entire power conditioning system is included in a tradeoff study, for what set of operating parameters is inductive storage preferred over capacitive storage?

Each of these questions is considered in turn below.

A. Energy Storage

The first comparison between the two power conditioning systems that is made is in the energy storage methods. This is of interest because it shows the basic difference between high voltage low current (capacitive), and low voltage high current (inductive) storage elements, for the fixed power and load current conditions specified in the Statement of Work. These conditions are:

Load voltage	=	100 kV
Load current	=	20 kA
Pulse repetition rate	=	5 Hz
Pulsewidth	=	250 μsec

To accommodate the inductive storage mode, a current droop of 30% was allowed. Thus, 850 kJ is initially stored in the inductor; 425 kJ is delivered at an average current of 17 kA from a 4.2 mH

superconducting inductor (Section V-A). From Table V-1, the inductor, dewar, and cryogen occupy 100 ft^3 and weigh 1750 lb. This inductor unit (cryogen for 3000 shots and dewar included) must be compared with a pulse forming network (PFN) to supply the 100 kV load with a square current pulse of 17 kA (to deliver the same energy).

For a capacitive system using a load matched to the PFN, a PFN voltage of 200 kV is required. The size and weight of such a PFN, with a lifetime of 10^5 shots, is 745 ft^3 and 8500 lb. This is based on state-of-the-art figures for capacitive storage of 50 J/lb and 3.3 J/in^3 at 5 Hz.[10] (This yields a specific weight of 4.1 lb/kW and a specific volume of 0.37 ft^3/kW). A comparison of IES and CES for the above set of system specifications yields a 645 ft^3 and 6750 lb reduction in size and weight for IES over CES. More dramatically stated, the IES is about 1/5 the weight and 1/7 the volume of CES.

B. Increased PRF

We now consider the system operating at the same 2.13 MW power level P with the same 100 kV load voltage V_o and the same 17 kA average current $\bar{I}$. Since

$$P = V_o \bar{I} \tau \nu$$

where τ is the load pulse width and ν is the PRF, we can write

$$\tau \nu = \frac{P}{V_o \bar{I}} = \text{const.}$$

Thus, τ and ν are directly related as indicated by the two abscissae of Fig. VI-1. This figure also shows the decreasing amount of stored energy required at higher PRF's (and correspondingly shorter pulse-widths). For example, at 250 Hz, the energy delivered per pulse is

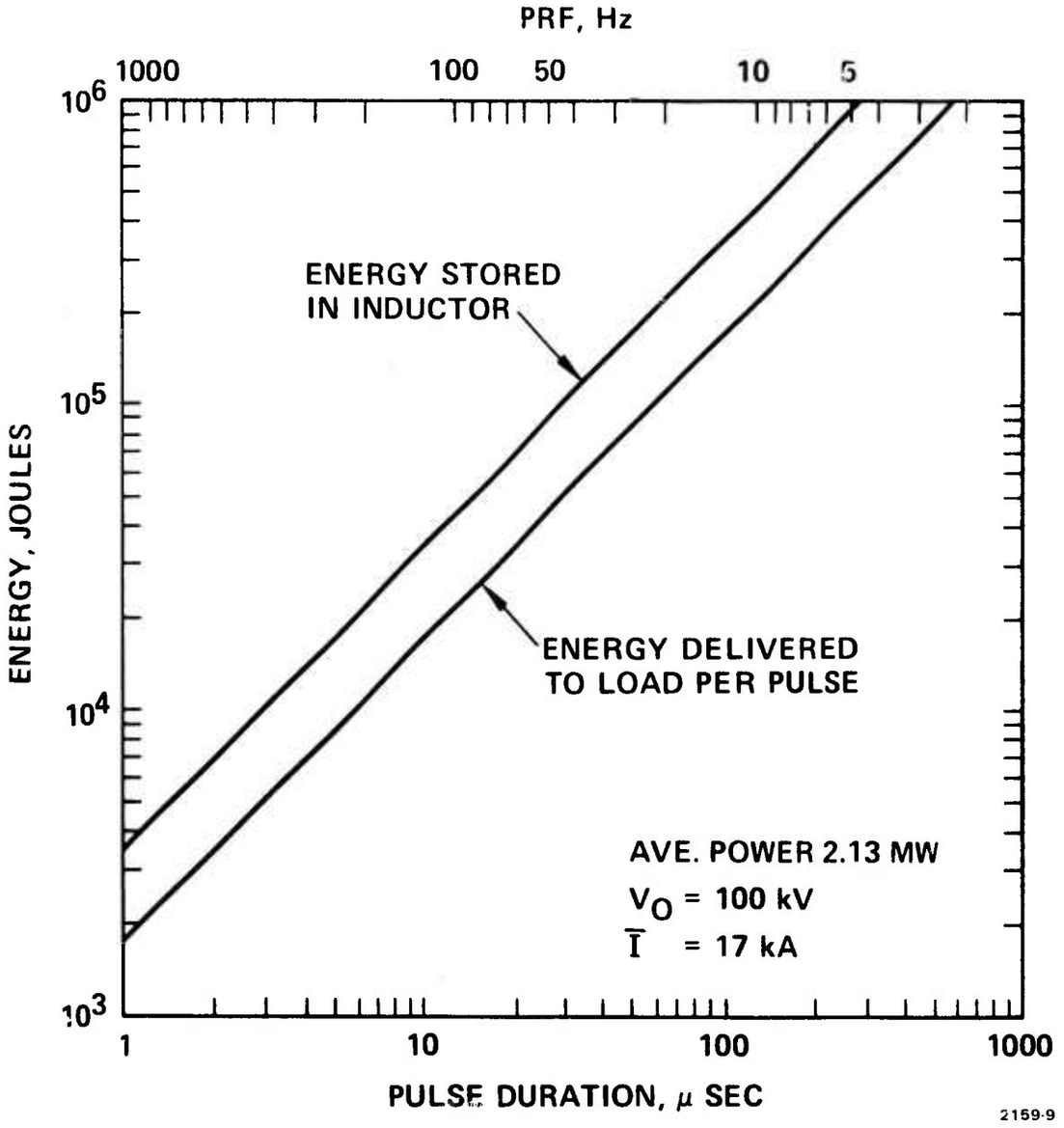

Fig. 55. Energy Stored and Delivered as a Function of PRF and Pulse Width for Fixed Average Power, Load current and Voltage.

only 8.5 kJ. Thus, the significant size and weight advantage of IES over CES which occurs for the large energy storage values at 5 Hz disappears at 250 Hz (at the same 2.1 MW power level).

Another consideration regarding the choice of energy storage system is the relation between the load pulsewidth and the characteristic switching time of the switch. In a capacitive pulser, the switch dissipates energy only during the load pulse. For a closing switch connecting a PFN to a load, nearly all the dissipation occurs during the turn-on time of the switch (anode fall time). Assuming a linear voltage collapse and a linear current rise in time τ_f^c, the energy dissipated

$$E_c = \frac{V_o I \tau_f^c}{6}$$

where V_o is the load voltage and I is the load current.

With an inductive pulser, most of the switch dissipation occurs when the switch opens and this dissipation is independent of the load pulse width. Thus,

$$E_I = V_o I \tau_f^I$$

where now τ_f^I is either the voltage rise time or current fall time in the Hughes interrupter. For simplicity, we neglect all other switch dissipation such as bypass switch arcing and ohmic losses.

The fractional efficiency of a modulator

$$\eta = 1 - \frac{E_{c,I}}{E_s}$$

where E_s is the stored energy. Since $E_s \approx E_o = V_o I\tau$ where E_o is the load energy and τ is the load pulsewidth, we have

$$\eta_c = 1 - \frac{E_c}{E_s} = 1 - \frac{\tau_f^c}{6\tau}$$

$$\eta_I = 1 - \frac{E_I}{E_s} = 1 - \frac{\tau_f^I}{\tau} \quad .$$

To achieve high efficiency, we want $\tau \gg \tau_f$. For closing switches, τ_f^c ~0.1 - 1 μsec so load pulse widths as short as 10 μsec yields high efficiency. For the Hughes interrupter, τ_f^I ~ 3-5 μsec. Thus, high efficiency is only achieved with IES systems when the pulse widths are greater than 30 to 50 μsec. At this power level of 2.1 MW, this requires $\nu < 25$ Hz.

C. Capacitive Versus Inductive Power Conditioning

We now consider the tradeoff between IES and CES for a complete system, using size and weight as the basis. The key parameter is PRF; we will consider 5 and 50 Hz. The reason for studying the tradeoff versus PRF is to attempt to answer the key question of whether it is reasonable to develop IES components for high PRF operation. Included in this calculation is the fact that the larger the inductor, the lower its weight-to-energy stored ratio. This ratio, of course, is constant for capacitors. Not included is the effect of lowered efficiency and therefore increased cooling requirements of IES at high PRF. The entire comparison is done for the one system power of 2.13 MW. The results are displayed in Table VI-1 and discussed below.

TABLE VI-1

Comparison Between Capacitive and Inductive Energy Storage Pulse Power Modulators

	5 Hz, 2.13 MW				50 Hz, 2.13 MW			
Capacitive Energy Storage Modulator	Specific Volume, ft^3/kW	Specific Weight, lb/kW	Total Volume, ft^3	Total Weight, lb	Specific Volume, ft^3/kW	Specific Weight, lb/kW	Total Volume, ft^3	Total Weight, lb
Turbine	1×10^{-3}	0.1	2.1	200	1×10^{-3}	0.1	2.1	200
AC Generator	3×10^{-3}	0.4	6.3	800	3×10^{-3}	0.4	6.3	800
Transformer-rectifier	2×10^{-3}	0.2	4.2	400	2×10^{-3}	0.2	4.2	400
Charging reactor	180×10^{-3}	6.0	360.0	12,000	22.5×10^{-3}	0.75	48.0	1600
Pulse forming network	370×10^{-3}	4.12	745.0	8,500	47×10^{-3}	0.52	98.0	1080
Thyratron switch	10×10^{-3}	0.06	20.0	125	15×10^{-3}	0.09	30.0	180
Total (Rounded off)	570×10^{-3}	11.0	1138.0	22,000	90×10^{-3}	2.0	190.0	4260
Inductive Energy Storage Modulator								
Turbine	1×10^{-3}	0.1	2.1	210	1×10^{-3}	0.1	2.1	210
AC Generator and rectifier	4×10^{-3}	0.5	8.4	1050	4×10^{-3}	0.5	8.4	1050
Inductor, dewar and LHe	50×10^{-3}	0.83	105.0	1740	24×10^{-3}	0.15	50.0	320
Hughes Switch System	20×10^{-3}	0.5	42.0	1050	40×10^{-3}	1.2	84.0	2500
Total (Rounded off)	75×10^{-3}	1.93	157.5	4050	69×10^{-3}	2.0	145.0	4080

1. 5 Hz

a. IES — These data are taken directly from table V-1.

b. CES — The size and weight of this system is based on using the following elements: A turbine-generator, a transformer-rectifier unit, a charging reactor, a high voltage pulse forming network, and a thyratron switch. The turbine-generator size and weight is based on 4×10^{-3} ft^3/kW and 0.5 lb/kW. The low weight of the transformer assumes that high frequency (up to 1200 Hz) is used and that the short one minute duty cycle will enable minimal conductor and iron weight to be used. A similar approach will be applied to the charging reactor weight and size estimation. The calculations leading to the data shown in Table VI-1 are as follows:

$$E = \frac{1}{2} C (2V_o)^2$$

where E is the load energy, C is the capacitor size, and V_o is the load voltage. For this 2.13 MW system at 5 Hz, E = 425 kJ. Using V_o = 100 kV, C = 21.2 μF. For resonant charging in 0.2 sec, the charging reactor inductance = 190 H. This is a large reactor and based on available data,[11] will result in a specific size and weight of 0.18 ft^3/kW and 6 lb/kW. Data for the PFN is based on size and weight given in Section VI-A, giving 0.37 ft^3/kW and 4.1 lb/kW. Thyratrons and auxiliaries give 10^{-2} ft^3/kW and 0.06 lb/kW.

c. Summary — A direct comparison between CES and IES for the set of specifications listed in the Statement of Work shows that an IES modulator using the Hughes switching system can reduce the size and weight of a CES modulator by 1000 ft^3 and 18,000 lb. It should be emphasized that the CES system circuit used for this comparison was of conventional design (HV PFN). The development of more exotic CES system designs (such as the Garrett approach with an LV PFN and SCR switch) would decrease, but by far, not eliminate the advantages of IES for this application.

2. 50 Hz

a. IES – No differences in the size and weight of the turbine-generator-rectifier unit is expected. The average power is the same and only the pulse current will change (decreas . The major change will be in the inductor and switch. The indu tor will need to store only 85 kJ. The size of an 85 kJ supercondu ng coil pulsed at 50 Hz is not definitively known. However, inter etation of the data obtained by Magnetic Corporation of America[1] shows that a storage capacity of 270 J/lb at 5 Hz for 3000 pulses is possible now, and assuming reasonable future development, a rate of 50 Hz for one minute at the same capacity level can be expected. The total size and weight of the inductor, dewar, and cryogen, based on this data, will be 50 ft^3 and 320 lb. The low density of 6.4 lb/ft^3 is accounted for by the large size of the LHe dewar. In comparing the energy storage density of this (85 kJ) unit with that of the 850 kJ inductor unit, it can be seen that the larger coil has nearly twice the energy density of the smaller coil. That is 500 J/lb versus 270 J/lb. The resulting specific volume and weight is $24 \times 10^{-3} ft^3/kW$ and 0.15 lb/kW.

The switch system increases in size and weight because the controls (motor drive and field coil pulsers) must now operate at 10 times the average power required at 5 Hz. The new specific switch figures are 0.04 ft^3/kW and 1.2 lb/kW compared with the old values of 0.02 ft^3/kW and 0.5 lb/kW.

b. CES – As in the case above, no significant change in the size of the turbine, generator or the transformer/rectifier is expected. However, the PFN and reactor will be reduced in size as follows: The PFN will need to store 42.5 kJ instead of 425 kJ in the 5 Hz case. Capacitor and reactor sizes, unlike superconducting inductors are generally proportional to the stored energy and a nominal 10:1 reduction in weight and size can thus be expected. However, at low energy levels some extra weight should be added

to take into account the bushings required for 200 kV holdoff. Also, in the reactor, the higher PRF will result in a higher RMS heat loss. For this estimation then it will be assumed that an 8:1 reduction can be assumed for both the PFN and the reactor. This is shown in Table VI-1.

The thyratron closing switch system and auxiliaries will be required to perform 10 times as many operations as before but at reduced current. The tubes may not be significantly increased in size by this requirement, but the auxiliary power supplies and cooling systems will be larger. A factor of 1.5 was chosen as a realistic expectation of the increase in size and weight of a 50 Hz switch system over a 5 Hz system. The switch contributes insignificantly to the overall size, however.

c. Summary – This direct comparison between an IES and a CES system operating at 2.1 MW at a PRF of 50 Hz has shown comparable sizes and weights. The uncertainty with regard to the IES switch capable of 50 Hz operation suggests that CES would be the more desirable approach. This conclusion holds for PRF's > 50 Hz, but may change as other system parameters change, especially the average power level.

VII. CONCLUSIONS AND RECOMMENDATIONS

A. Program Objectives and Accomplishments

The general objective of this program has been to design a switch suitable for use in IES power supplies. Within this general objective, there were six tasks. Each of these tasks and the principal accomplishments are listed below.

1. Task 1 – Evaluate Various Bypass Switch Mechanisms

A generalized study of contact ambients (vacuum, gas or oil) has revealed that high pressure SF_6 is most desirable for this application. Oil is too viscous to allow fast contact motion. Vacuum does not have sufficient voltage holdoff or recovery properties for the short gaps and deionization times required. High pressure SF_6 satisfies all the requirements for this application without the use of fragile bellows.

Two basic contact motions that have been considered are rotary and reciprocating. The rotary design, while capable of short opening and closing times with minimal contact accelerations, suffers from uncertainties in high current density brush design, inflexibility with respect to PRF, possible gyroforces and long start-up time. For these reasons, reciprocating contact motion was considered superior.

Two choices of reciprocating motion that were available were linear and torsional. Torsional motion has two distinct advantages over linear motion. First, there is lower inertia because only the contacts and not all the mass elements move. Second, coil springs used in linear drives have an upper speed limit less than torsion springs which does not permit contact opening in the short times required for this application. For these reasons, torsional motion was chosen.

2. Task 2 – Design the Bypass Switch

A conceptual design of a torsion bar switch yielded initial design information on the torsion bar, contact arm, drive motor and gas blast system. Two areas singled out for experimental verification were

electrodynamic drive motor torque and arc voltage generation. Apparatus was built and satisfactorily tested. The experimental data thus gained, along with existing analytical information, served as the basis for a detailed bypass switch design. This was completed and detailed design drawings have been produced.

3. Task 3 – Design the Interrupter Tube

At the outset of this program, it was not known whether high current density interrupter tubes could perform HVDC interruption without the aid of a shunt capacitor to limit the rate of voltage rise during the interruption process. If this capacitor were required and was of significant size, its weight could easily preclude the advantages of an IES system.

Extensive experimentation was performed to determine the current density/recovery rate limit. At 5 A/cm^2, recovery rates in the vicinity of 15 kV/μsec were observed. These rates were determined entirely by the circuit and tube; no shunt capacitor was used. This proved that compact tubes could be built to interrupt high currents without the use of recovery rate limiting capacitors.

Other experiments involving the ionizer (for reduced jitter), gas pressure control and magnetic field coil geometry as well as theoretical work on the interruption process contributed the data needed for the detailed design. This has been completed and a detailed design drawing has been produced.

4. Task 4 – Perform a Thermal Analysis

The detailed designs of the bypass switch and the interrupter tube contained a thermal analysis based on thermal inertia of the component parts. One minute of continuous operation was assumed with negligible cooling. During a ten-minute off period, cooldown is accomplished by liquid cooling. This simplified the cooling system requirements, requiring only a small liquid flowrate and a modest heat exchanger.

5. Task 5 – Determine the Range of Operating Parameters

Both current and voltage can range from essentially zero to the peak design values of 20 kA and 100 kV. Repetition rate can vary from single shot to 50 Hz, but the continuous operating time falls drastically at the higher rates. For the 2.1 MW system power under consideration, efficiency is high at 5 Hz, but falls rapidly at higher repetition rates. Interrupter tube recovery times (load voltage rise times) vary over the range of 3 to 10 μsec at 100 kV. Switch weight (without auxiliaries) varies over the range from 325 to 600 lb, depending on construction techniques and operating parameters.

6. Task 6 – Study Module Interconnections to Achieve Higher Power Levels and Study the Tradeoff Between Capacitive and Inductive Systems

At 20 kA and 100 kV, each switch handles a peak power of 2 GW. To achieve higher peak powers, several switch modules can be connected together in a variety of ways. The most promising circuit consists of a single high current prime power source with several parallel inductor, switch, and load branches. Current division between the switch modules is automatically achieved along with considerable flexibility.

At tradeoff study between a complete capacitive and inductive modulator system has been performed for the specifications given for this program. Considerable size and weight reductions are possible with the inductive system at 5 Hz. As the repetition rate approaches 50 Hz, these advantages disappear.

B. Conclusions

The use of a Hughes interrupter tube to accomplish HVDC interruption in an inductive energy storage modulator is more attractive than using forced commutation because of the significant size and weight contributed by the commutation capacitor bank. Furthermore, development of the mechanical switch is simplified when the interrupter tube is used because the switch has a relatively long (100 μsec) free recovery period available.

Interrupter tube development has advanced considerably during the course of this program. Routine operation is now performed at the 2.5 kA, 50 kV level without the use of recovery rate limiting capacitors. Current densities of 5 A/cm^2 and recovery rates in the 10 to 20 kV/μsec are routinely achieved. Operation at 5 Hz has also been demonstrated. Therefore, it is believed that interrupters such as the one designed for this program can be made to operate at the 100 kV, 20 kA levels required.

The mechanical, SF_6 torsion bar switch designed during this program has a great many advantages over other, more conventional switches. First, the use of high pressure SF_6 allows for shorter contact gap spacings and higher recovery rates than vacuum. Furthermore, bellows, responsible for limited life and limited contact parting speed, are not required. Second, the use of a torsional rather than a linear contact motion allows for faster contact parting and higher PRF operation. Maintenance, consisting of contact surface replacement, is easily performed.

The complete switch system designed herein is quite compact and lightweight, with components occupying only 40 ft^3 and weighing only 1000 lb. The auxiliary power requirement is about 7 kW for 5 Hz operation. When this switch is used in the calculation of the size and weight of a complete inductive energy storage modulator (excluding fuel and load) operating at the 2.1 MW level, we get a total component volume of 158 ft^3 and 4050 lb. This is a considerable savings over a capacitive system operating under the same conditions, being about one fifth the weight and one-seventh the size.

A tradeoff study comparing the size and weight of an inductive versus a capacitive system at the same 2.1 MW power level was also performed for 50 Hz operation. The result indicated approximately equal sizes and weights for both systems. Thus, inductive storage does not appear to offer significant advantages over capacitive storage at this power level for PRF's $\geq$ 50 Hz. The value of the tradeoff frequency for higher power levels will probably increase, but this has not been studied.

C. Recommendations

The switch which has been designed under this program has significant advantages over any other kind of IES switch for reasons which have been previously discussed. Furthermore, an IES system has significant size and weight advantages over a CES system for the set of operating parameters defined by this contract. Therefore, if the Air Force does indeed have a requirement for a modulator capable of operation at these levels, it is recommended that this hardware program be implemented.

In the absence of low repetition rate requirements, IES is not a high priority item. In this case, effort should be devoted to CES component development. This leads us to two specific recommendations in the switch area.

First, an improved gas discharge closing switch with a higher average current rating and lower dissipation than conventional hydrogen thyratrons needs to be developed. Present high power CES modulators require several such thyratrons in parallel which proves to be very cumbersome and unreliable. Hughes has recently submitted a proposal for an improved closing switch (72M-3124/C8955) to Weapons Laboratory, Kirtland AFB for consideration.

Second, the development of a relatively low impedance, higher switched power, on/off switch would make the use of a hard tube modulator possible. This would have several advantages over a line type pulser:

- Variable load impedance
- Variable pulsewidth
- Lower cost energy storage capacitors instead of pulse discharge units
- Capacitor voltage equals load voltage, not twice load voltage
- Simplicity

The Hughes interrupter tube designed in this contract has an on-off switching capability and with some modification would be an excellent candidate for such a switching function.

Finally, a study program is proposed to continue the comparisons between IES and CES systems begun under this program. This study would investigate the tradeoff between the two systems for various power levels and PRF's. It would investigate the relative merits of low voltage, high current ac generators and rectifiers and acyclic generators for IES. Further data on inductors would be obtained, including consideration of LN_2 versus LHe cooling, mission requirements, PRF, etc. A study of the use of a current fed network (to eliminate current droop) would be made to see if the required capacitors offset the advantages gained by eliminating current droop. Various CES systems would be studied, including full voltage PFN (Raytheon), low voltage PFN (Garret), and the hard tube modulator. All available component data and modulator configurations would be drawn together to give a comprehensive view of the options and tradeoffs available for high power airborne modulators.

APPENDIX A

DESIGN OF A ROTATING CYLINDER MECHANICAL SWITCH

The feasibility of a mechanical switch utilizing a rotating, slotted cylinder and stationary brushes was developed in Section II-B-1. A detailed evaluation of this concept led to a proposed design which was then compared to the torsion bar switch in a tradeoff study.

Carbon brushes have been found to operate satisfactorily in SF_6.[13] Copper-graphite brushes have been operated at high current densities, 300 to 1000 A/in.^{2}, for very short periods.[14] To extend the time to one minute, as required for the mechanical switch herein, would necessitate a design which emphasized means to limit brush temperature rise.[14] Based on a design objective of using the brushes at 1000 A/in.^{2} and the IES current of 17 kA average, the required brush contact surface area would be 16 in.^{2} per polarity. Expected brush performance is achieved only if this area is divided into many small individual brushes, for the same reasons as the metallic contacts of the torsion bar switch are divided into individual fingers. The brush manufacturer's recommendation[14] was for the individual brushes to have a contact surface area of 1 in.^{2} and be configured 1/2 x 2 in. but that the orientation of the brushes on the cylinder was optional. Orienting the brushes with the 2-in. dimension in the direction of travel of the cylinder enabled the design of a simple method to prevent the brushes from falling into the slots in the cylinder. This method offers important features unattainable in any other scheme conceived. The method is developed below.

The dimensions and features of the design given as an example in Section II-B-1 were adopted, viz:

Cylinder diameter = 12 in.

Number of brushes per brush track = 2

Number of slots per brush track = 2

Resultant number of gaps in IES circuit when in open position = 2 in series

Slot width = 3 in.

Brush width = 2 in.

Rotational speed of cylinder = 750 rpm (12-1/2 Hz)

Number of pulses produced per revolution = 2

PRF = 25 Hz

This design produces an apparent full open gap length at each gap of 1/2 in. However, after allowance is made for the effect of the wall thickness of the brush holder and the radius on the edges of the slots, the resultant gap length developed at each gap is the 1 cm (0.4 in.) quoted in Section II-B-1. From $v = r\omega$, tangential velocity equals radius times angular velocity, the surface of the cylinder would travel at 471 ips. The distance traveled to develop the 1 cm gap is 1/2 in. from the point where the brushes leave the cylinder surface and therefore the opening and closing times are $1/2 \div 471 \approx 1$ msec.
It is noted here that a surface speed of 471 ips is well within the range for satisfactory brush operation. Also, rotation of a cylinder 12 in. in diameter at 750 rpm is not unreasonable.

The brushes are spring loaded onto the surface of the cylinder and therefore would fall into the slots if a method was not developed to prevent it. The method adopted was the placement of brush guides in the slots as shown in Fig. A-1. The brush guides are of the same metal as the cylinder for the purpose of equal wear, compliance and surface finish but are insulated from the cylinder by virtue of being isolated islands in the slots and being supported by insulating material as shown in the figure. The 2-in. width of the brushes when compared with the 1/2 in. distance to be spanned, as measured at the surface of the cylinder, results in the fact that at least 3/4 of the brush contact surface is always supported. If less than 1/2 of the brush contact surface were supported at any instant, an instability of the brushes would develop.

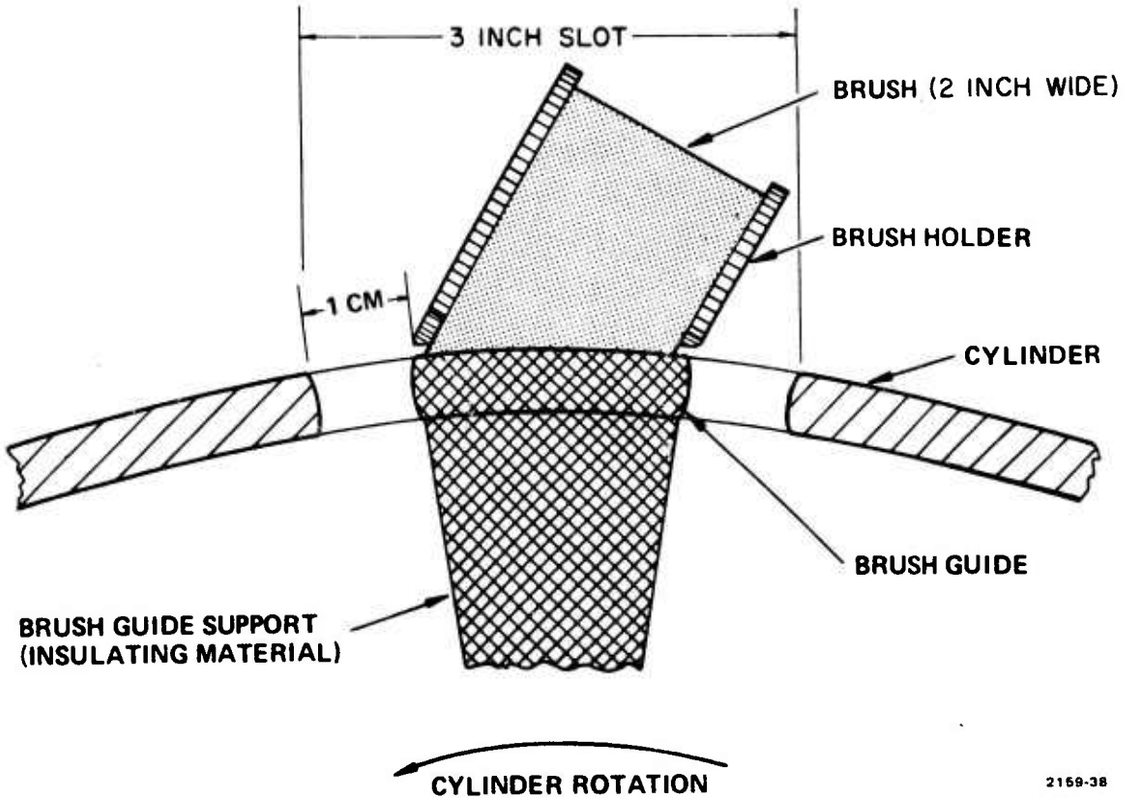

Fig. A1. Geometry of Slot in Cylinder, Brush, and Brush Guide.

Brush holders were designed to hold the brushes at an angle of 15° trailing.[14] This, together with a spring force with a component into the forward wall of the brush holder would result in a stable running brush.[15] The component of the spring force normal to the cylinder surface was to be 5 lb.[14] Brush wear was calculated to be less than 1/4 in. at the specified PRF = 5 Hz and life = 50,000 pulses. Brush wear is proportional to length of sliding and therefore would be less at higher PRF. The brush holder had 1/4 in. side walls for both rigidity and to provide a good heat conductance path to a massive (heat sinking) brush holder support. The cylinder was also to be relied on for heat sinking. Baffles were added to direct the circulating SF_6 gas (impelled by windage) onto the forward wall of the brush holder to help prevent a hot area that would develop otherwise. Beyond these measures there was the possibility of adding active cooling and/or precooling before each operating period, if found necessary.

The cylinder length was to be held to 20 in. in length by having four rows of slots, with one pair of diametrically opposite slots stagger along the cylinder length relative to the other pair of slots (see Fig. A-2). The brushes, therefore, would also be mounted in four rows so that all brushes would be over the midpoint of a slot at the same time. Duplex brush holders were to be used such that there would be two brush tracks per slot; hence the four slots per row.

Contacts other than the carbon brushes were provided to draw the arcs. These arcing contacts would be of the tulip finger type. The male contact (mounted to the cylinder) was to be able to pass through the fingers of the stationary female contacts. These contacts would engage ~1/4 msec (1/8 in. of cylinder surface travel) before the brushes separated and then separate ~1/8 msec after the brushes separated. Arc resistant copper-tungsten was to be used for the arcing contacts. There were provisions for blasting SF_6 radially outward through the arcs that would have been formed. The arcing contacts (2 diametrically opposite) were to be mounted close to the edge of the cylinder at one end.

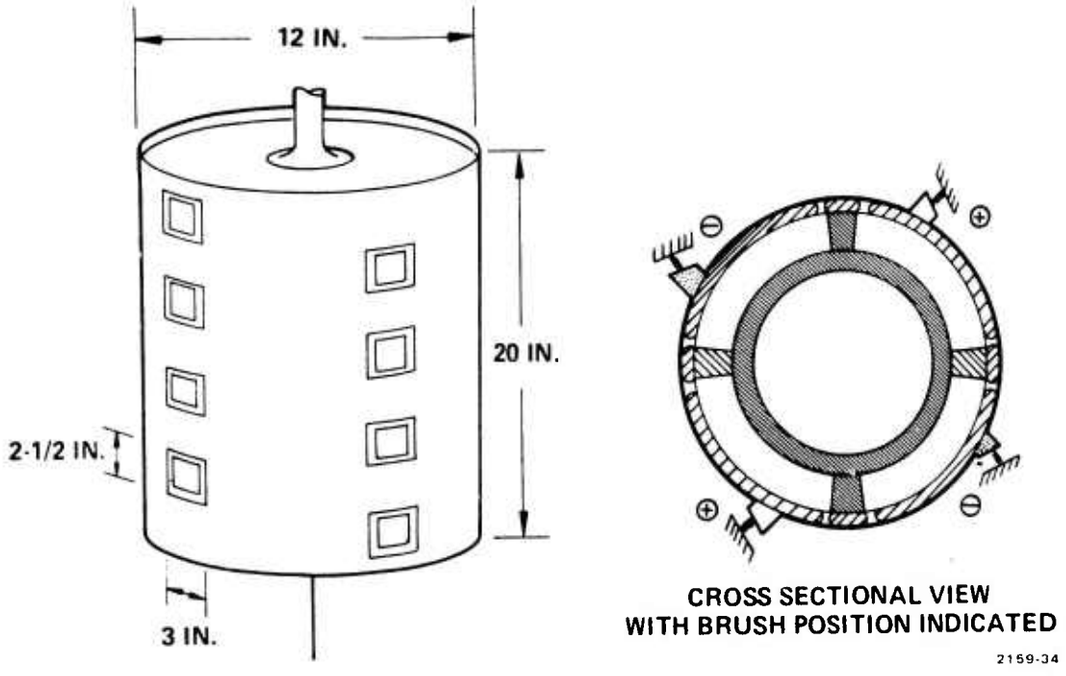

Fig. A-2. Slotted Cylinder for Rotating Switch.

PRF's of 12-1/2, 8-1/3, 6-1/4 or 5 Hz were to be produced by the addition of a gating switch in parallel with the rotary switch. The gating switch would not have the requirement for rapid opening and closing that the rotary switch has and therefore its design was not carried past the conceptual stage. The gating switch concept was introduced because (1) for PRF less than 25 Hz, the cylinder would have to be larger than 12 in. in diameter which was considered an upper limit, and (2) to offer some flexibility in PRF without an equipment exchange.

Size, weight, power, and maintainability considerations were not overwhelmingly against the rotating cylinder mechanical switch but the development program for satisfactory brush operation definitely involved a high risk.

REFERENCES

1. R. E. Voshall, "Current Interruption Ability of Vacuum Switches," Paper 71TP555, IEEE Summer Power Meeting 1971, Portland Oregon.

2. T. F. Perkins and L. S. Frost, "Current Interruption Properties of Gas-Blasted Air and SF_6 Arcs," Paper C72 530-4, IEEE Summer Power Meeting, San Francisco, 1972.

3. P. Brueckner and A. Erk, Elektrotechneschi Zeitschrift-A Vol. 82, 141 (1961).

4. Private communication with Mr. Robert Martin, Hughes Ground Systems, (714) 871-3232, X-3195.

5. T. H. Lee, D. R. Kurtz, and J. W. Porter, "Vacuum Arcs and Vacuum Circuit Interrupter," Conference Internationale Les Grands Reseaux Electriques a Haute Tension, June 8-18, 1966, Paris.

6. Dr. G. Rylander, Mechanical Engineering Department, University of Texas, Austin, Texas (512) 471-5136.

7. Mr. E. Brown, Garrett Airesearch Corporation, Torrance, California (213) 323-9500, X-2816.

8. Mr. E. Lucas, Magnetic Corporation of America, Waltham, Massachusetts (617) 890-4242.

9. Technical Report AFAPL-TR-69-101.

10. Mr. B. Hayworth, Capacitor Specialist Corporation, San Diego, California (714) 747-4000.

11. Mr. J. Romanelli, Communications and Radar Division, Hughes Aircraft Company, Fullerton, California (714) 871-3232.

12. Technical Report AFAPL-TR-72-38, Vol. 1.

13. J. L. Johnson and L. E. Moberly, "Brush Life and Commutation in Atmospheres of Air, SF_6 and CO_2," Proceedings of the Engineering Seminar on Electric Contact Phenomena, November, 1967.

14. Private communication with Dr. Erle I. Shobert, II, Manager of Research, Stockpole Carbon Company, St. Marys, Pennsylvania (814) 834-1521.

15. E. I. Shobert, II, Carbon Brushes, Chemical Publishing Company, 1965.

*U.S.Government Printing Office: 1975 — 657-021/582